

CHAPTER TWENTY SIX

HOMOGENEOUS AND HETEROGENEOUS CATALYTIC PROCESSES PROMOTED BY ORGANOACTINIDES

Carol J. Burns and Moris S. Eisen

- | | | | | | |
|------|--------------------------------------------------------------------------------------------------------------------------------|------|------------|--------------------------------------------------------------------------------------------------|------|
| 26.1 | Introduction | 2911 | 26.9 | Intramolecular hydroamination
by constrained-geometry
organoactinide
complexes | 2990 |
| 26.2 | Reactivity of organoactinide
complexes | 2912 | 26.10 | The catalytic reduction of
azides and hydrazines by
high-valent organouranium
complexes | 2994 |
| 26.3 | Oligomerization of
alkynes | 2923 | 26.11 | Hydrogenation of olefins
promoted by organoactinide
complexes | 2996 |
| 26.4 | Dimerization of terminal
alkynes | 2930 | 26.12 | Polymerization of α -olefins
by cationic organoactinide
complexes | 2997 |
| 26.5 | Cross dimerization of terminal
alkynes catalyzed by
[(Et ₂ N) ₃ U][BPh ₄] | 2947 | 26.13 | Heterogeneous supported
organoactinide
complexes | 2999 |
| 26.6 | Catalytic hydrosilylation of
olefins | 2953 | References | | 3006 |
| 26.7 | Dehydrocoupling reactions
of amines with silanes
catalyzed
by [(Et ₂ N) ₃ U][BPh ₄] | 2978 | | | |
| 26.8 | Intermolecular hydroamination of
terminal alkynes | 2981 | | | |

26.1 INTRODUCTION

During the last two decades, the chemistry of organoactinides has flourished, reaching a high level of sophistication. The use of organoactinide complexes as stoichiometric or catalytic compounds to promote synthetically important organic transformations has matured due to their rich, complex, and

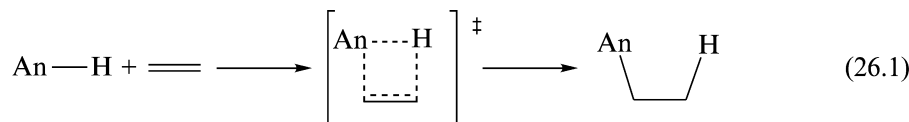
uniquely informative organometallic chemistry. Compared to early or late transition metal complexes, the actinides sometimes exhibit parallel and sometimes totally different reactivities for similar processes. In many instances the regiospecific and chemical selectivities displayed by organoactinide complexes are complementary to that observed for other transition metal complexes. Several recent review articles (Edelman *et al.*, 1995; Edelmann and Gun'ko, 1997; Ephritikhine, 1997; Hitchcock *et al.*, 1997; Berthet and Ephritikhine, 1998; Blake *et al.*, 1998; Edelmann and Lorenz, 2000), dealing mostly with the synthesis of new actinide complexes, confirm the broad and rapidly expanding scope of this field.

The aim of this chapter is to survey briefly and in a selective manner the catalytic chemistry of organoactinide complexes in homogeneous and heterogeneous catalytic reactions. A comprehensive review of the reactivities of actinide compounds has been published covering the literature until 1992 (Edelmann, 1995). This chapter reviews the new literature for the last decade. The treatment of this chapter is necessarily concise. We encourage the reader to seek the recent review articles and additional references given as an integral part of the sub-chapters for additional details and background material.

26.2 REACTIVITY OF ORGANOACTINIDE COMPLEXES

26.2.1 Modes of activation

Interest in the reactivity of organoactinide complexes is based on their ability to effect bond-breaking and bond-forming of distinctive moieties. The factors influencing these processes are both steric and electronic. A number of articles have been devoted to the steric control in organo-5f-complexes. Xing-Fu *et al.* (1986a) have proposed a model for steric saturation, suggesting that the stability of a complex is governed by the sum of the ligand cone angles (Xing-Fu *et al.*, 1986a,b; Xing-Fu and Ao-Ling, 1987). In this model, highly coordinated 'over-saturated' complexes will display low stability. An additional model concerning steric environments has been proposed by Pires de Matos (Marçalo and Pires de Matos, 1989). This model assumes pure ionic bonding, and is based on cone angles defining the 'steric coordination number'. A more important and unique approach to the reactivity of organo-5f-complexes regards the utilization of thermochemical studies. The knowledge of the metal–ligand bond enthalpies is of fundamental importance to allow the estimation of new reaction pathways (Marks *et al.*, 1989; Jemine *et al.*, 1992, 1993; King *et al.*, 1992; Leal *et al.*, 1992; Leal and Martinho Simões, 1994; King and Marks, 1995; Leal *et al.*, 2001). In addition, neutral organoactinides have been shown to follow a four-center transition state in insertion reactions [equation (26.1)], suggesting that prediction of new actinide patterns of reactivity is possible taking into account the negatives entropies of activation (Marks and Day, 1985).



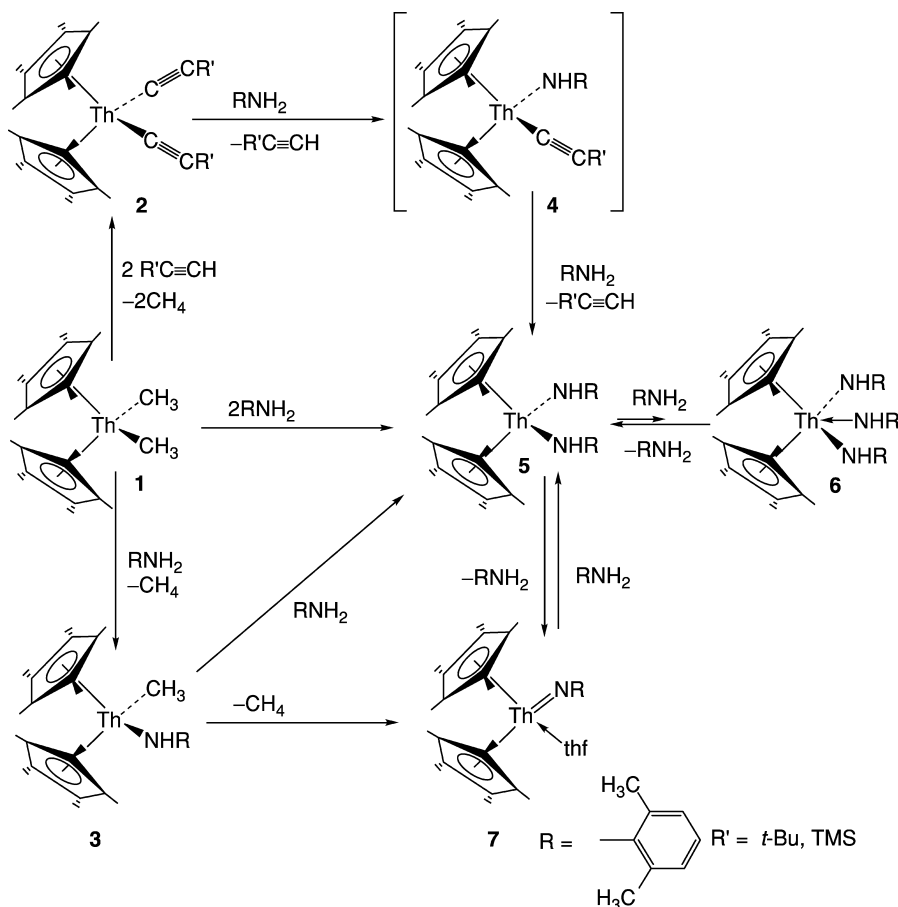
This chapter deals with the reactions of organoactinide complexes that comprise intermediate and key steps in catalytic processes, whereas the preceding chapter focuses in a more detailed and comprehensive fashion on the synthesis and characterization of similar complexes.

26.2.2 Stoichiometric reactions of organoactinide complexes of the type $(\text{C}_5\text{Me}_5)_2\text{AnMe}_2$

The different catalytic reactivity found for similar organoactinides, previously unprecedented in the chemistry of organoactinides, was the driving force for Haskel *et al.* (1999) to study the stoichiometric reactivity of organoactinide complexes of the type $(\text{C}_5\text{Me}_5)_2\text{AnMe}_2$ (An = Th, U). These complexes have been widely used for the hydrogenation of olefins under homogeneous conditions (Fagan *et al.*, 1981a; Fendrick *et al.*, 1988; Lin and Marks, 1990). The reactivity of the actinide complexes towards alkynes and/or amines is outlined in Schemes 26.1 and 26.2 for Th and U, respectively.

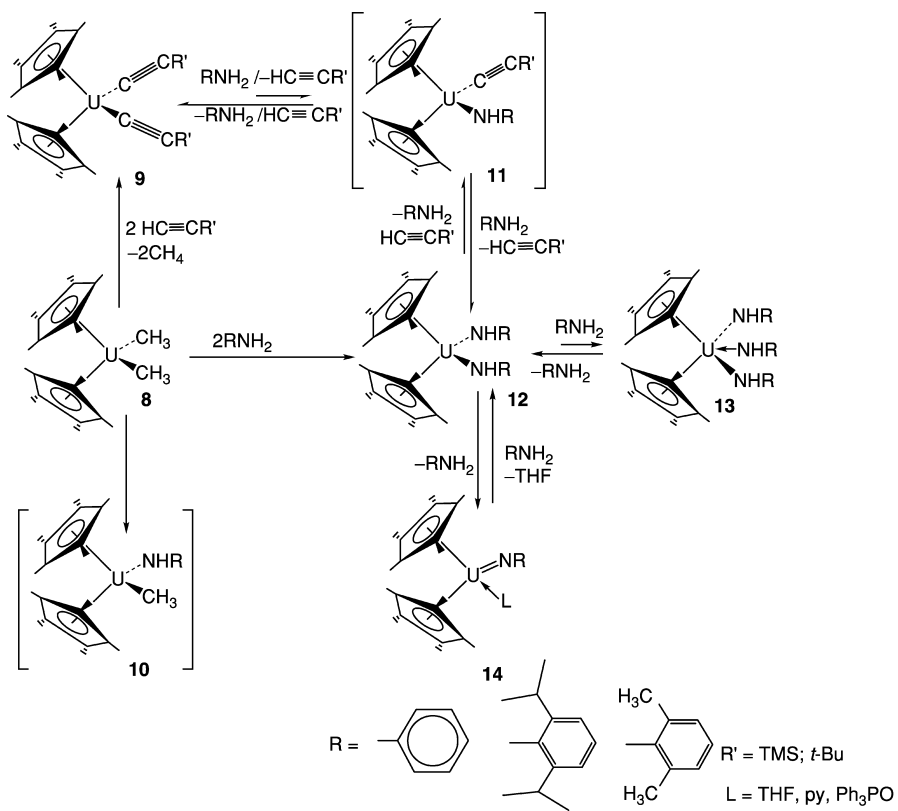
$(\text{C}_5\text{Me}_5)_2\text{ThMe}_2$ (**1**) was found to react with terminal alkynes producing the bisacetylide complexes $(\text{C}_5\text{Me}_5)_2\text{Th}(\text{C}\equiv\text{CR})_2$ (**2**) (R = *t*Bu, TMS). The reaction of these bisacetylide complexes **2** with equimolar amounts of amine yielded half of an equivalent of the corresponding bisamido complexes $(\text{C}_5\text{Me}_5)_2\text{Th}(\text{NHR})_2$ (**5**) and half of an equivalent of the starting bisacetylide complex, indicating that the second amine insertion into the thorium monoamido monoacetylide complex **4** was faster than the first insertion. The reaction of $(\text{C}_5\text{Me}_5)_2\text{Th}(\text{CH}_3)_2$ (**1**) with an equimolar amount of amine resulted in the formation of the monoamido thorium methyl complex **3**, which upon subsequent reaction with another equivalent of amine produced the bisamido complex **5**. Heating complex **5**, in THF, allowed the elimination of an amine molecule producing the formation of the thorium-imido complex **7**. This complex also was formed by eliminating methane by heating complex **3** (Haskel *et al.*, 1996). In the presence of an excess of amine, the bisamido complex **5**, was found to be in rapid equilibrium with the bisamido-amine complex **6** (Straub *et al.*, 1996), resembling lanthanide complexes (Gagné *et al.*, 1992a,b; Giardello *et al.*, 1994) though the equilibrium was investigated and found to lie towards the bisamido complex.

Similar reactivity has been found for the corresponding uranium complex, **8** (Scheme 26.2). The reaction with alkynes produced the bisacetylide complexes $(\text{C}_5\text{Me}_5)_2\text{U}(\text{C}\equiv\text{CR})_2$ (**9**) (R = Ph, TMS) but in contrast to the thorium species, these bisacetylide complexes are extremely stable and the bisamido complex **12** can be formed only by adding large excess of the amine, indicating that the

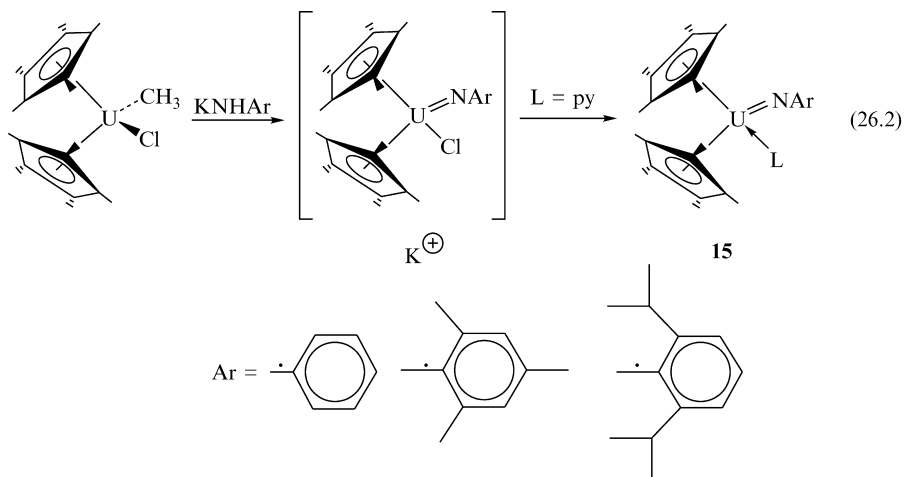


Scheme 26.1 Stoichiometric reactions of the complex $(C_5Me_5)_2ThMe_2$ with amines and terminal alkynes.

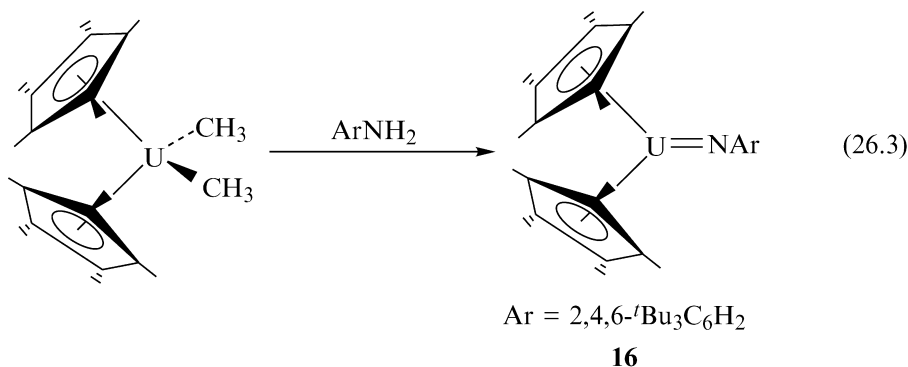
equilibrium between complexes **9** and **12** lies preferentially towards the bisacetylide complexes, instead of either the monoamido monoacetylide **11** or the bisamido complexes **12**. Attempts to isolate the monomethyl-amido complex **10**, by reacting one equivalent of amine with complex **8**, yielded only half of an equivalent of the bisamido complex **12**. Similar to the reactivity of the thorium complex, in the presence of an excess of amine, complex **12** was found to be in fast equilibrium with complex **13**, with the equilibrium favoring the bisamido complex. By heating the bisamido complex **12** in THF, elimination of an amine molecule was observed allowing the formation of the corresponding uranium-imido complex **14** (Eisen *et al.*, 1998). The U(IV) arene-imido complexes have also been prepared following a parallel pathway through a potassium salt [equation (26.2)] (Arney and Burns, 1995).



Scheme 26.2 Stoichiometric reactions of the complex $(C_5Me_5)_2UMe_2$ with amines and terminal alkynes.



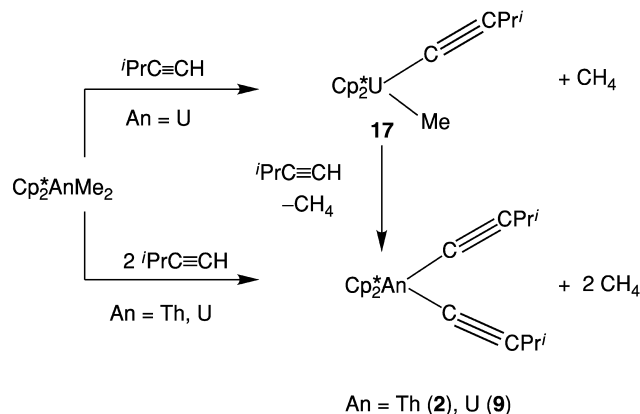
The only base-free monomeric organo-imido complex of U(IV) has been obtained for the bulky tris-*tert*-butyl phenyl amine derivative [equation (26.3)] [32].



The crystal structure of this coordinatively unsaturated organoimido uranium (iv) complex (**16**) exhibits almost a linear U–N-*ipso*-C linkage with and almost C₂ symmetry along the U–N bond. The U–N-*ipso*-C angle is 162.30(10), with the aryl substituent canted towards the uranium through the methyl group in the *ortho*- position of the aromatic ring. Interestingly, besides this close disposition, no chemical evidence was found regarding any agostic interactions. The remarkable feature in this complex was found to be the extremely short U–N bond length of 1.952(12) Å resembling the distance of aryl–imido complexes of U(v) and U(vi) (Brennan and Andersen, 1985; Burns *et al.*, 1990; Arney and Burns, 1993) when the differences in ionic radii due to the variation in the U oxidation states were taken into account (Shannon, 1976). Thus, it was suggested that in this aryl–imido uranium (iv) complex **16**, there is a high formal bond order presumably formed by donation of a lone pair of electrons from the nitrogen to the uranium center.

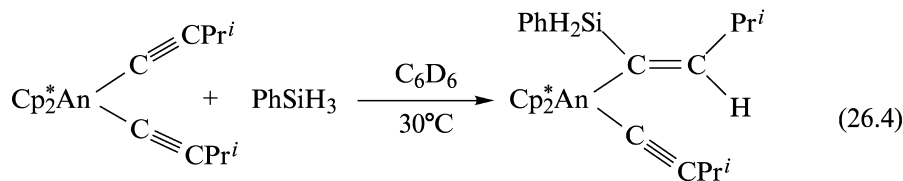
26.2.3 Stoichiometric reactions between (C₅Me₅)₂AnMe₂ (An = Th, U), alkynes and silanes

In order to detect the key organometallic intermediates in the hydrosilylation process (*vide infra*), a consecutive series of stoichiometric reactions were investigated, using the organoactinide precursor (C₅Me₅)₂AnMe₂ (An = Th, U), reacting with ⁱPrC≡CH and PhSiH₃. The stoichiometric reaction of PhSiH₃ with (C₅Me₅)₂UMe₂ induced the dehydrogenative coupling of the silane (PhSiH₃) to give oligomers, but the reaction PhSiH₃ with (C₅Me₅)₂ThMe₂ produced only the dimer and the corresponding [(C₅Me₅)₂ThH(μ-H)]₂, as described in the literature (Fagan *et al.*, 1981b; Aitken *et al.*, 1989). The reaction of the organoactinide complexes (C₅Me₅)₂AnMe₂ (An = Th, U) with alkynes in stoichiometric amounts allowed the preparation and characterization of monoacetylide and bisacetylide complexes of organoactinides as described in Scheme 26.3.



Scheme 26.3 Stoichiometric reactivity of the organoactinide complexes $(C_5Me_5)_2AnMe_2$ ($An = Th, U$) with terminal alkynes.

In stoichiometric reactions of $iPrC\equiv CH$ with $(C_5Me_5)_2U Me_2$, methane gas was evolved leading to the formation of the orange (mono)acetylide methyl complex, $(C_5Me_5)_2U(C\equiv CPr^i)(Me)$ (**17**). This transient species was found to be very reactive, and the addition of a second equivalent of $iPrC\equiv CH$ converted complex **17** rapidly into the deep red brown bisacetylide complex $(C_5Me_5)_2U(C\equiv CPr^i)_2$ (**9**). Addition of one equivalent of $PhSiH_3$ at room temperature to a benzene solution of any of the bisacetylide organoactinide complexes resulted in the quantitative formation of the silylalkenyl acetylide actinide complexes $(C_5Me_5)_2An(PhSiH_2C=CH^iPr)(C\equiv C^iPr)$ ($An = Th$ (**18**), U (**19**)), which were found to be intermediates in the catalytic cycle for the hydrosilylation reactions [equation (26.4)].

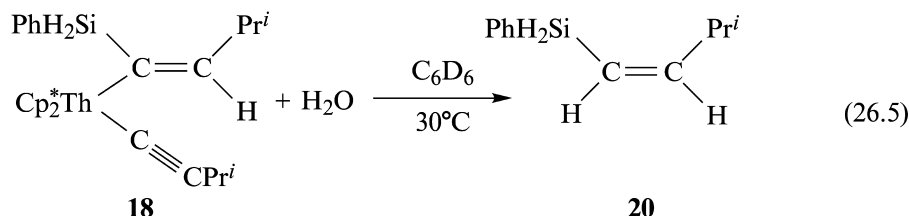


An = Th (**2**), U (**9**)

An = Th (**18**), U (**19**)

Formation of the intermediate was indicated by the change in color of the reaction from pale yellow to dark red for **18**, and orange to dark orange brown for complex **19**. The structure of **18** and **19** were unambiguously confirmed by 1H -, ^{13}C -, ^{29}Si -NMR spectroscopy as well as by nuclear overhauser effect (NOE) experiments. The silyl group was found to be in the *cis*-configuration with respect to the *iso*-propyl group in the organometallic

complex. Corroboration of this stereochemistry of the organometallic intermediate **18** was found by the quenching of **18** with H₂O producing the corresponding *cis*-vinylsilane product **20** [equation (26.5)].

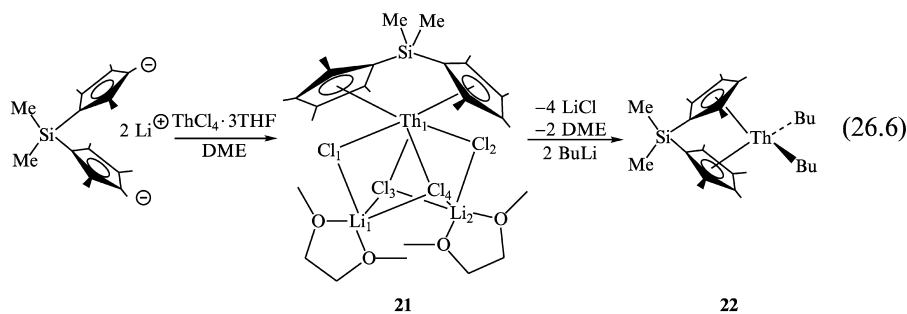


Intriguingly, no further reaction was observed with an excess of PhSiH₃ with complexes **18** or **19**, strongly suggesting that at room temperature, neither the silane nor the alkyne is able to induce the σ -bond metathesis or the protonolysis of the hydrosilylated alkene or the alkyne. The addition of an excess of alkyne at room temperature to complex **18** in the presence of PhSiH₃ yielded the unexpected *trans*-hydrosilylated alkyne, in addition to the corresponding alkene, silylalkyne, and the bis(acetylide) complex.

26.2.4 Synthesis of *ansa*-organoactinide complexes of the type Me₂Si(C₅Me₄)₂AnR₂

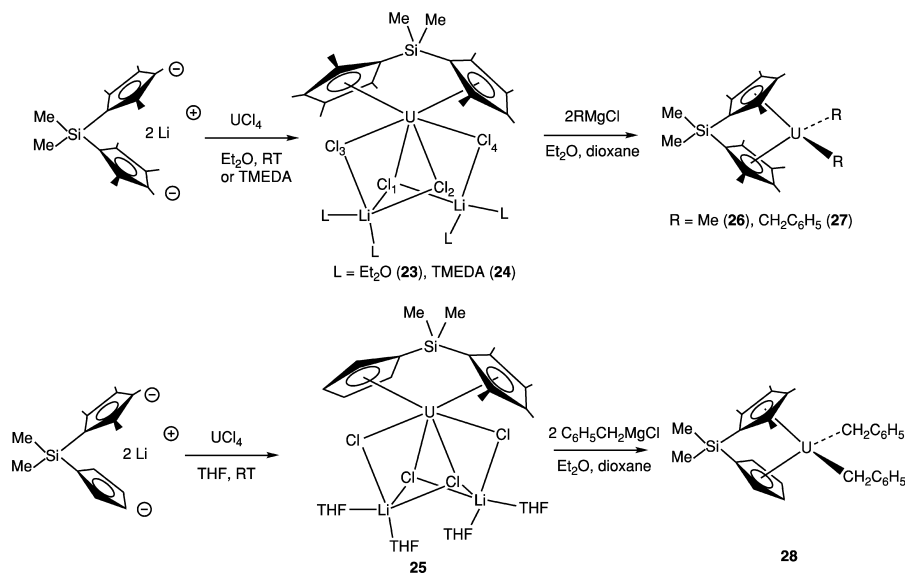
Stoichiometric and catalytic properties of organo-f-element complexes are profoundly influenced by the nature of the π ancillary ligands (Bursten and Strittmatter, 1991; Edelmann, 1995a,b; Anwander, 1996; Anwander and Herrmann, 1996; Edelmann, 1996; Molander, 1998). It has proven possible to generate a more open coordination sphere at the metal center by introducing a bridge metallocene ligation set as in the complex *ansa*-Me₂SiCp₂''MR₂ (Cp^{''} = C₅Me₄) (Fendrick *et al.*, 1984; Jeske *et al.*, 1985a,b; Fendrick *et al.*, 1988). The effect of opening the coordination sphere of organolanthanides in some catalytic processes resulted in an increase (10-fold to 100-fold) in rates for the olefin insertion into the M–R bond (Jeske *et al.*, 1985a,b; Gagné and Marks, 1989; Giardello *et al.*, 1994). In organoactinides, this modification was shown to cause an increase (10³-fold) in their catalytic activity for the hydrogenation of 1-hexene (Fendrick *et al.*, 1984). The syntheses of the complexes Me₂Si(C₅Me₄)₂ThCl₂ (**21**) and Me₂Si(C₅Me₄)₂ThⁿBu (**22**) have been reported as presented in equation (26.6) (Gagné and Marks, 1989; Dash *et al.*, 2001). The complex Me₂Si(C₅Me₄)₂ThCl₂ was isolated in 82% yield as a lithium chloride adduct. The single-crystal X-ray diffraction revealed a typical bent metallocene complex. The ring–centroid–Th–centroid angle (113.3°) is smaller than that observed in unbridged bis(pentamethylcyclopentadienyl) thorium complexes (130–138°) (Bruno *et al.*, 1986), and slightly smaller than the angle determined for the bridged thorium dialkyl complex Me₂Si(C₅Me₄)₂Th

($\text{CH}_2\text{Si}(\text{CH}_3)_2$)₂ (118.4°) (Fendrick *et al.*, 1984). The thorium–carbon (carbon = cyclopentadienyl ring carbons) bond lengths are not equidistant; the complex displays a shorter distance between the metal and the first carbon adjacent to the silicon bridge because of the strain generated by the Me_2Si -bridge, similar to that reported for other *ansa* types of complexes (Bajgur *et al.*, 1985).



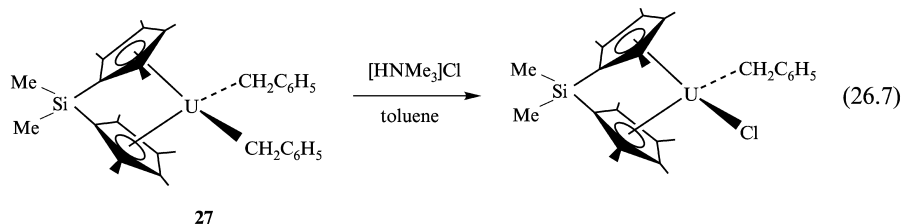
The X-ray analysis of complex **21** showed that two of the thorium–chloride bonds are shorter than the other two $\text{Th}(1) - \text{Cl}(1) = 2.770(2)\text{\AA}$, $\text{Th}(1) - \text{Cl}(2) = 2.661(2)\text{\AA}$, $\text{Th}(1) - \text{Cl}(3) = 2.950(2)\text{\AA}$, and $\text{Th}(1) - \text{Cl}(4) = 2.918(2)\text{\AA}$. The longer Th–Cl distances are those corresponding to the chlorine atoms disposed in the three-fold bridging positions and coordinated to both lithium atoms. Each of the other two chlorine atoms is coordinated only to one lithium atom. All the Th–Cl distances are longer than those observed for terminal Th–Cl distances ($\text{Th}-\text{Cl} = 2.601\text{\AA}$ for Cp^*ThCl_2 or 2.65\AA for $\text{Cp}^*\text{Th}(\text{Cl})\text{Me}$). *ansa*-Chelating bis(cyclopentadienyl) complexes of uranium have been prepared as presented in Scheme 26.4. Schnabel *et al.* (1999) have described an effective high yield procedure for these desired U(IV) complexes (Schnabel *et al.*, 1999).

The uranium complexes (**23–25**) were obtained as dark-red air- and moisture-sensitive materials. The complexes are soluble in aromatic solvents but insoluble in hexane. In solution, these complexes have shown no dynamic behavior. The molecular structure of complex **23** reveals a normal bent metallocene with an angle of 114.1° for the ring centroid–metal–ring centroid. This angle is smaller as compared to the non-bridged uranium complexes ($133\text{--}138^\circ$) (Fagan *et al.*, 1981b; Eigenbrot and Raymond, 1982; Duttera *et al.*, 1984; Cramer *et al.*, 1989a,b). The uranium atom is bound to four bridging chloride ligands; two bonds are much longer than the others $\text{U}-(\text{Cl}(1)) = 2.885(3)$, $\text{U}-(\text{Cl}(2)) = 2.853(3)$, $\text{U}-(\text{Cl}(3)) = 2.760(3)$, $\text{U}-(\text{Cl}(4)) = 2.746(3)\text{\AA}$, the longer U–Cl bonds are those associated with chlorides that bridge to one lithium atom. For the preparation of the dialkyl complexes, the corresponding chloride–TMEDA complex **24** was used as a precursor. The alkylation of the halide precursors with Grignard reagents produced the corresponding alkyl complexes using a large excess of dioxane as the precipitating solvent for the magnesium salts.



Scheme 26.4 Synthetic pathway for the preparation of ansa-organouranium complexes.

Interestingly, complex **28** is very stable in comparison to the corresponding dimethyl thorium complex (Fendrick *et al.*, 1984). The dimethyl complex of the mixed cyclopentadienyl precursor **25** could not be isolated. Instead, the precipitation of insoluble material and the evolution of gas were observed. In contrast, the dibenzyl complexes **27** and **28** were obtained in high yields. The mixed benzyl–chloride complex was obtained by protonation of the dibenzyl complex **27** with $[\text{HNMe}_3]\text{Cl}$ as described in equation (26.7).

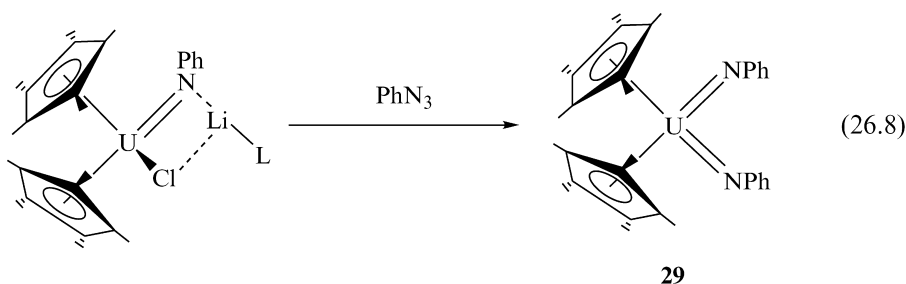


26.2.5 Synthesis of high-valent organouranium complexes

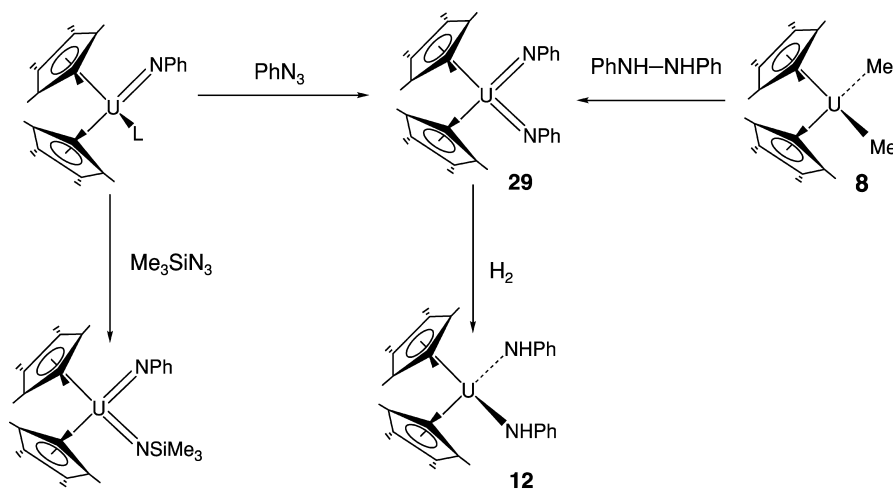
The reactivity of organoactinide (iv) alkyl, amido, or imido complexes towards unsaturated organic substrates such as olefin, alkynes, and nitriles follows a four-center transition state as described in equation (26.1). These complexes

display this type of reactivity due to the high-energy orbital impediment to oxidative addition and reductive elimination. Consequently, the synthesis, characterization, and reactivity studies of high-valent organouranium complexes are of primary importance. The ability to transform U(IV) to U(VI) and vice versa can create complementary modes of activation inducing unique and novel reactivities.

The first high-valent organouranium(VI) bis(imido) complex **29** was prepared by Arney *et al.* (1992) by the oxidation of a lithium salt of an organoimido uranium chloride complex with phenylazide [equation (26.8)] (Arney *et al.*, 1992).



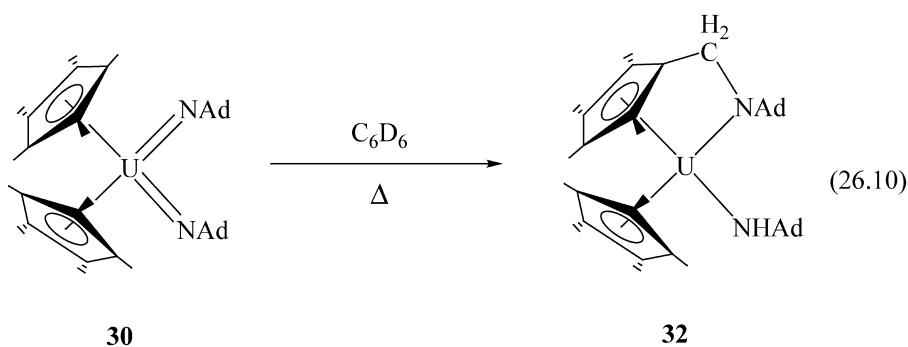
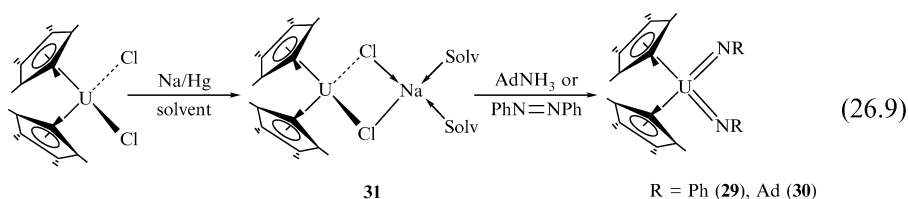
Other bis(imido) organouranium (VI) complexes have been prepared as described in Scheme 26.5. The reactions involve the oxidation of uranium (IV)



Scheme 26.5 Alternative synthetic pathways for the preparation of high-valent organouranium-imido complexes and their reactivity with dihydrogen.

bis(alkyl) or uranium (iv) imido complexes with the two-electron atom transfer reagents in high yield (Brennan and Andersen, 1985).

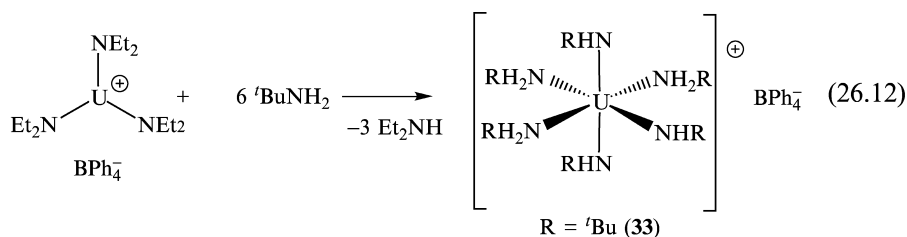
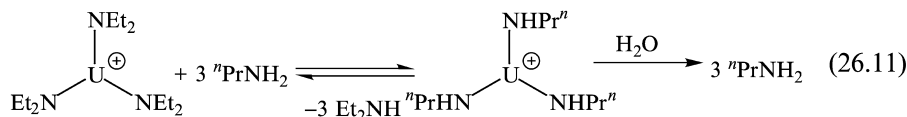
A very elegant and simple procedure for the generation of high-valent bis(imido) organouranium (vi) complexes has been described starting from an organometallic uranium (iii) species. The reaction involves the direct reduction of diazenes or azides [equation (26.9)] (Warner *et al.*, 1998). Complex **30** was found to react at elevated temperature activating one methyl of the cyclopentadienyl ring (Peters *et al.*, 1999a) [equation (26.10)].



26.2.6 Reactivity of the cationic complex [(Et₂N)₃U][BPh₄] with primary amines

As will be presented in the course of this chapter, a large amount of work has been dedicated towards catalytic reactions using the cationic complex [(Et₂N)₃U][BPh₄] (Berthet *et al.*, 1995). In order to tailor the possibilities of such cationic complexes, stoichiometric reactions with amines have been studied. Under mild conditions (room temperature in benzene), the amido ligands of [(Et₂N)₃U][BPh₄] were straightforwardly activated. The reaction of [(Et₂N)₃U][BPh₄] with *n*-propylamine yielded an organoactinide intermediate that upon consecutive quenching reaction with water, after all volatiles were removed, yielded *n*-propylamine with no traces of Et₂NH. This result indicated that all three amido groups were easily transaminated [equation (26.11)] (Wang *et al.*, 2000). NMR spectroscopy has indicated that complexes

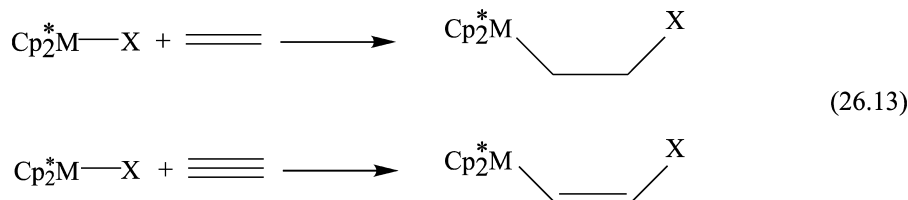
of the type $[(R_2N)_3U][BPh_4]$ normally adopts a zwitterionic structure in non-coordinating solvents, with two phenyl groups of BPh_4 coordinated to the metal center (Wang *et al.*, 2002a).



Similarly reaction of $[(Et_2N)_3U][BPh_4]$ with *t*butylamine allowed the formation of the complex $[(tBuNH_2)_3(tBuNH)_3U][BPh_4]$ (**33**) [equation (26.12)]. The X-ray diffraction analysis of **33** revealed a uranium atom in a slightly distorted octahedral environment, with the three amido and three amine ligands arranged in a *mer* geometry. The U–N(amido) bond lengths average 2.20(2) Å and were similar to those determined in the distorted facial octahedral cation $[(Et_2N)_3(THF)_3U]^+$ (mean value of 2.18(1) Å) (Wang *et al.*, 2002a). The complex $[(tBuNH_2)_3(tBuNH)_3U][BPh_4]$ is a unique uranium(IV) complex with primary amine ligands that have been crystallographically characterized (Wang *et al.*, 2002a). The mean U–N(amino) bond distance of 2.67(3) Å can be compared with the average U–N bond length of 2.79(2) Å in $[UCl_4(Me_2NCH_2CH_2NMe_2)_2]$ (Zalkin *et al.*, 1986). The shorter U–N(amido) bond length (U–N = 2.185(7) Å) and the longer U–N(amine) bond length (U–N = 2.705(8) Å) were found to be those which are in *trans* positions. The small octahedral distortion was manifested in the different angles between the amine–amido, amine–amine, and amido–amido groups.

26.3 OLIGOMERIZATION OF ALKYNES

The last decade has witnessed an intense investigation of the chemistry of electrophilic d⁰/f lanthanide and actinide metallocenes (Edelmann, 1995a,b). A substantial impact was encountered in diverse catalytic areas, where the key step is an insertion of an olefinic (alkene or alkyne) functionality into a metal–alkyl, metal–hydride, or metal–heteroatom moiety [equation 26.13; Cp* = η⁵-C₅Me₅; X = alkyl, H, NR₂].



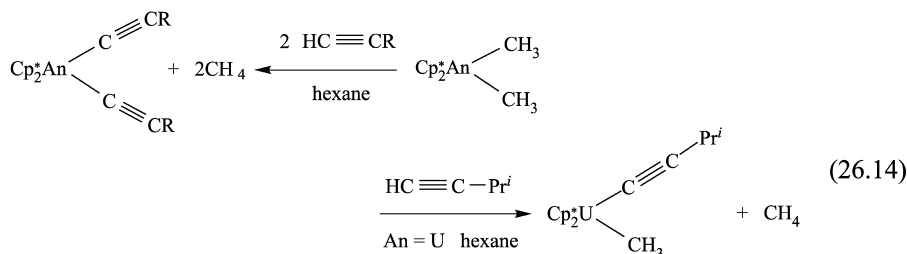
For organolanthanides, such processes include hydrogenation (Molander and Hoberg, 1992; Giardello *et al.*, 1994; Haar *et al.*, 1996; Molander and Winterfeld, 1996; Roesky *et al.*, 1997a,b), dimerization (Heeres *et al.*, 1990), oligomerization/polymerization (Jeske *et al.*, 1985c; Watson and Parshall, 1985; Heeres and Teuben, 1991; Schaverien, 1994; Fu and Marks, 1995; Ihara *et al.*, 1996; Mitchell *et al.*, 1996), and other related reactions that will be discussed later in this chapter, whereas for organoactinides, until 1991 C–H activation (Smith *et al.*, 1986a; Fendrick *et al.*, 1988) and hydrogenation (Fagan *et al.*, 1981a,b; Fendrick *et al.*, 1988; Lin and Marks, 1990) comprised all such processes. Mechanistically, these insertion reactions are not in general well understood and are certainly more efficient in very different metal–ligand environments than the more extensively studied analogs of the middle- and late-transition metals (Collman *et al.*, 1987; Elschenbroich and Salzer, 1989; Hegedus, 1995). Hence, the d^0/f metal ions are likely to be in a high formal oxidation state, and in neutral complexes are expected to be electronically unsuitable for π -back-donation. In addition, these types of complexes are unlikely to form stable olefin/alkyne complexes, due to the relatively polar metal–ligand bonding with strong affinity for ‘hard’ ligands, and to feature startling M–C/M–H bond disruption enthalpy patterns as compared with those of the late transition elements (Marthino Simões and Beauchamp, 1990; Nolan *et al.*, 1990; King and Marks, 1995).

26.3.1 Bisacetylide organoactinide complexes

Organometallic complexes containing an acetylide moiety have played an important role in the development of organolanthanide chemistry (Evans *et al.*, 1983, 1989; Den Haan *et al.*, 1987; Shen *et al.*, 1990). A number of synthetic routes applicable to the preparation of this class of compounds have been developed, examples of which include the salt metatheses between lanthanide halides with main group acetylides, and the σ -bond metatheses between lanthanide alkyl or hydrides and terminal alkynes.

Bisacetylide organoactinide complexes can be synthesized at room temperature by the reaction of $(\text{C}_5\text{Me}_5)_2\text{AnMe}_2$ (An = Th, U) with either stoichiometric or excess amounts of the corresponding terminal alkynes (Schemes 26.1 and 26.2). The reaction is faster for the organoactinide uranium complex than for the corresponding thorium complex. In all cases, the bisacetylide complexes

were obtained instead of the uranium methyl acetylide complex (**34**) [equation (26.14)], indicating that the metathesis substitution of the second methyl ligand by the terminal alkyne is normally much faster than the first σ -bond metathesis.



An = Th (**2**), U (**9**)

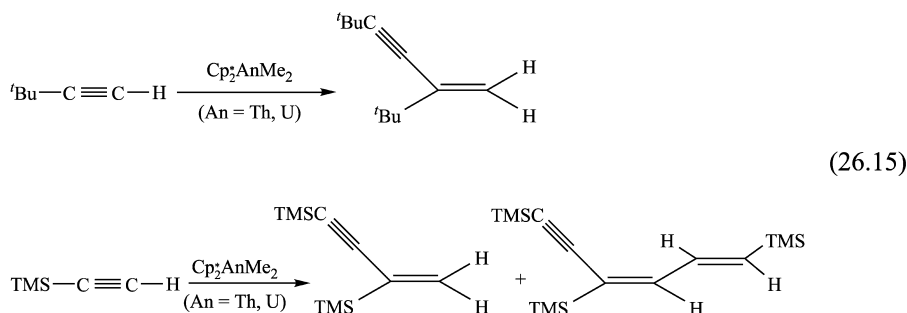
34

An = Th, R = TMS, ^iPr ; An = U, R = Ph, ^tBu , ^iPr

Due to the paramagnetism of the $5f^2$ uranium (IV) center and its rapid electron spin-lattice relaxation times, the chemical shifts of the magnetically non-equivalent ligand protons were found to be generally sharp, well-separated, and readily resolved in the ^1H -NMR spectra.

26.3.2 Oligomerization of terminal alkynes catalyzed by neutral organoactinide complexes of the type $(\text{C}_5\text{Me}_5)_2\text{AnMe}_2$

The reaction of $(\text{C}_5\text{Me}_5)_2\text{AnMe}_2$ (An = Th, U) with an excess of *tert*-butylacetylene yielded the regioselective catalytic formation of the head-to-tail dimer, 2,4-di-*tert*-butyl-1-butene-3-yne (Th = 99%; U = 95%), whereas with trimethylsilylacetylene the head-to-tail geminal dimer, 2,4-bis(trimethylsilyl)-1-butene-3-yne (Th = 10%; U = 5%), and the head-to-tail-to-head trimer, (*E,E*)-1,4,6-tris(trimethylsilyl)-1-3-hexadiene-5-yne (Th = 90%; U = 95%), were the exclusive products [equation (26.15)] (Straub *et al.*, 1995):



For other terminal alkynes such as $\text{HC} \equiv \text{CPh}$, $\text{HC} \equiv \text{CPr}^i$, $\text{HC} \equiv \text{CC}_3\text{H}_9$, the $(\text{C}_5\text{Me}_5)_2\text{AnMe}_2$ complexes also produced mixtures of the head-to-head and

head-to-tail dimers and the formation of higher oligomers with no specific regioselectivity and chemo-selectivity. For the bulky 4-Me-PhC≡CH, a different reactivity was found for the different organoactinide complexes. Whereas $(C_5Me_5)_2ThMe_2$ generated a mixture of dimers and trimers, the corresponding $(C_5Me_5)_2UMe_2$ afforded *only* the head-to-head *trans*-dimer. In contrast to the reactivity of lanthanide complexes, the organoactinides did not induce the formation of allenic compounds. Although the turnover frequencies for both of the organoactinide complexes were in the range of the 1–10 h⁻¹, the turnover numbers were found to be higher, in the range of 200–400.

26.3.3 Key intermediate complex in the oligomerization of terminal alkynes promoted by neutral $(C_5Me_5)_2AnMe_2$ organoactinides

When the reaction of TMS-C≡CH with $(C_5Me_5)_2ThMe_2$ was followed spectroscopically, two different compounds were observed. The first compound observed at room temperature was the bisacetylide complex. The oligomerization reaction started only upon heating the reaction mixture to 70°C, whereupon the bisacetylide complex disappeared and the new complex **35** (Fig. 26.1) was spectroscopically characterized, indicating that both acetylide positions at the metal center were active sites.

26.3.4 Kinetic, thermodynamic, and thermochemical data in the oligomerization of terminal alkynes promoted by neutral $(C_5Me_5)_2AnMe_2$ organoactinides

A kinetic study of the trimerization of TMS-C≡CH with $Cp_2^*UMe_2$ was monitored *in situ* by ¹H-NMR spectroscopy. From the kinetic data, the empirical rate law for the organoactinide-catalyzed oligomerization of TMS-C≡CH is given by equation (26.16). The derived rate constant at 70°C for the production

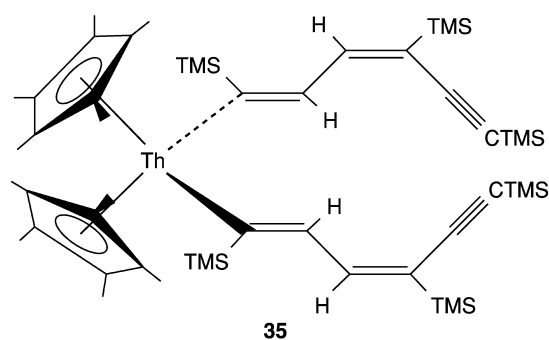


Fig. 26.1 Bis(dienyne) organoactinide complex **35** found in the linear oligomerization of terminal alkynes.

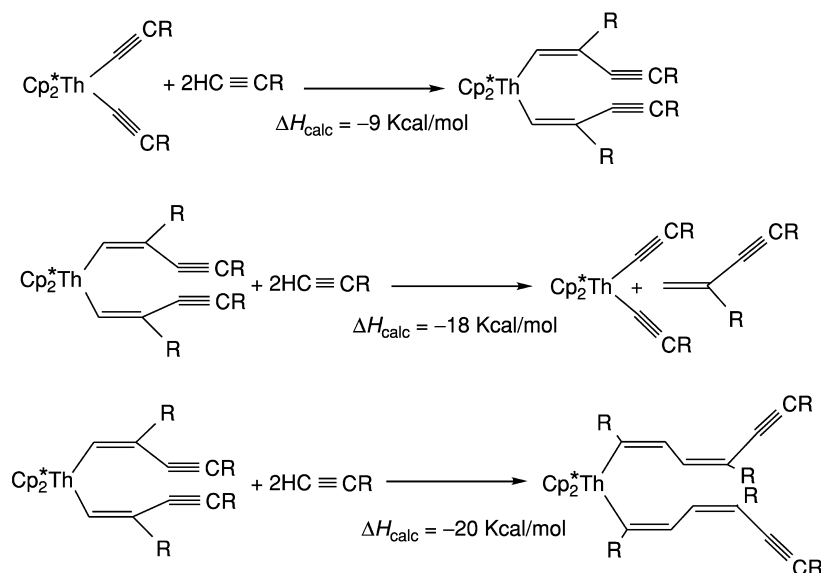
of the corresponding trimer was found to be $k = 7.6 \times 10^{-4} (6) \text{ s}^{-1}$.

$$v = k[\text{alkyne}]^1[\text{U}]^1 \quad (26.16)$$

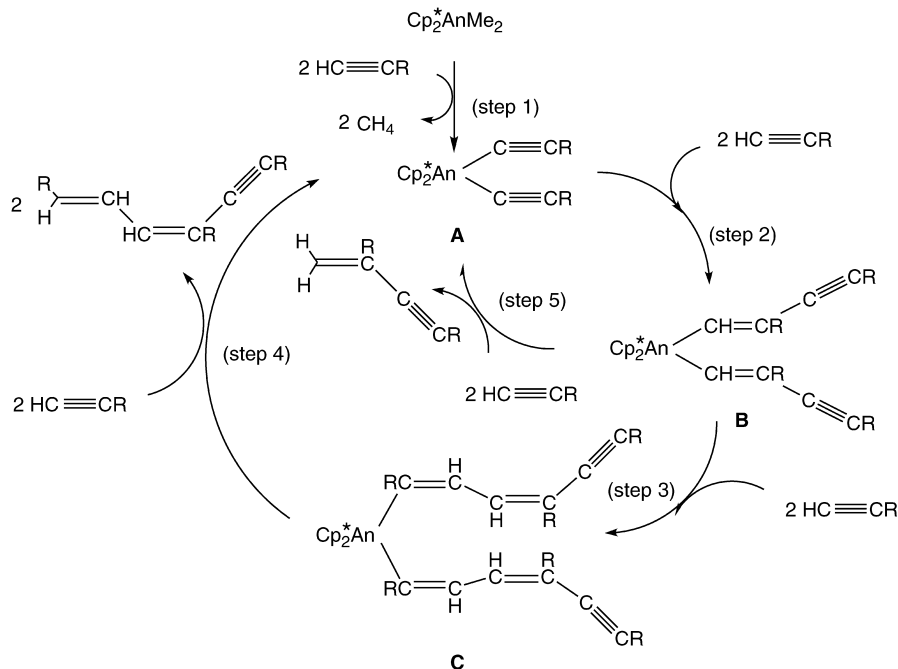
A similar kinetic dependence on alkyne and catalyst concentration was observed over a range of temperatures permitting the derivation of the activation parameters from the corresponding Eyring analysis. The values measured were $E_a = 11.8(3) \text{ kcal mol}^{-1}$, $\Delta H^\ddagger = 11.1(3) \text{ kcal mol}^{-1}$, and $\Delta S^\ddagger = -45.2(6) \text{ eu}$, respectively (Straub *et al.*, 1999).

Thermodynamically, higher oligomers and even polymers were expected (Ohff *et al.*, 1996; Wang and Eisen, 2003). The reaction of either the Th or U organoactinide complex with acetylene ($\text{HC}\equiv\text{CH}$) resulted in the precipitation of black *cis*-polyacetylene. The *cis*-polyacetylene was thermally converted to the corresponding *trans*-polyacetylenes at 80°C . The enthalpies of reaction may be calculated for the addition of triple bonds in a conjugated manner (Scheme 26.6). The ΔH_{calc} for the dimer formation is exothermic by 27 kcal mol^{-1} , whereas additional insertions are calculated to be exothermic by an additional 20 kcal mol^{-1} . Thus, ΔH_{calc} for the trimer formation is exothermic by 47 kcal mol^{-1} , supporting the results in which non-bulky terminal alkynes were oligomerized with no chemoselectivity.

A plausible pathway was proposed for the organoactinide-oligomerization of terminal alkynes, presented in Scheme 26.7. The mechanism is a sequence of well-established reactions such as insertion of an alkyne into a M–C σ -bond and



Scheme 26.6 Calculated enthalpies of reaction for the oligomerization of terminal alkynes.

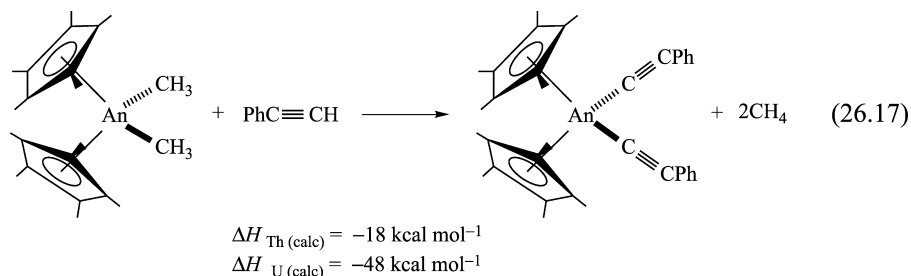


Scheme 26.7 Proposed mechanism for the linear oligomerization of terminal alkynes catalyzed by organoactinide bisacetylide complexes.

σ -bond metathesis. The first step in the catalytic cycle involves the protonation of the alkyl groups in the organoactinide precatalyst at room temperature, yielding the bisacetylide complexes $(\text{C}_5\text{Me}_5)_2\text{An}(\text{C}\equiv\text{CR})_2$ (**A**), with the concomitant elimination of methane (step 1). In general, this is a very rapid reaction extremely exothermic as calculated for the reaction of the organoactinides with $\text{PhC}\equiv\text{CH}$ [equation (26.17)]

The 1,2-head-to-tail-insertion of the alkyne into the actinide-carbon σ -bond was proposed to yield the plausible bisalkenyl actinide complex **B** (step 2). Complex **B** may undergo either a σ -bond metathesis with the C-H bond of another alkyne producing the corresponding geminal dimer and **A** (step 5), or an additional 2,1-tail-to-head-insertion of an alkyne, with the expected regioselectivity (for $\text{TMSC}\equiv\text{CH}$), into the organoactinide alkenyl complex **B**, yielding the bis(dienyl)organoactinide complex **C** (step 3). The reaction of complex **C** with an incoming alkyne was proposed to yield the corresponding trimer and regenerating the active actinide bisacetylide complex **A** (step 4). The turnover-limiting step for the catalytic trimerization was identified to be the elimination of the organic trimer from the organometallic complex **C**. This result indicated that the rate for σ -bond metathesis between the actinide-carbyl and the alkyne and the rate of insertion of the alkyne into the metal-acetylide (steps 1 and 2)

were much faster than the rate for σ -bond metathesis of the alkyne with the metal–dialkenyl bond in the catalytic cycle (step 4).



26.3.5 Cross oligomerization of ${}^t\text{BuC}\equiv\text{CH}$ and $\text{TMSC}\equiv\text{CH}$ promoted by $(\text{C}_5\text{Me}_5)_2\text{UMe}_2$

In the oligomerization of ${}^t\text{BuC}\equiv\text{CH}$ with $(\text{C}_5\text{Me}_5)_2\text{UMe}_2$, the geminal dimer was found to be the major product, indicating that the addition of the alkyne to the metal acetylide was regioselective with the bulky group pointing away from the cyclopentadienyl groups (Fig. 26.2).

The reaction of equimolar amounts of ${}^t\text{BuC}\equiv\text{CH}$ and $\text{TMSC}\equiv\text{CH}$ with $(\text{C}_5\text{Me}_5)_2\text{UMe}_2$ produced two dimers (14%) and three specific trimers (86%). The dimers generated in the reaction were characterized to be the geminal dimer **36** (10%) and the cross geminal dimer **37** (4%), resulting from the insertion of a ${}^t\text{BuC}\equiv\text{CH}$ with the same regioselectivity as observed in Fig. 26.2 into the uranium bis(trimethylsilylacetylide) complex. The trimers obtained were the head-to-tail-to-head trimer, (*E,E*)-1,4,6-tris(trimethylsilyl)-1-3-hexadiene-5-yne (**38**), as the major product (43%), the trimer **39** (15%), resulting from the insertions of two $\text{TMSC}\equiv\text{CH}$ into the *tert*-butylacetylide complex, and the unexpected trimer **40** (27%) [equation (26.18)]. Trimer **40** was

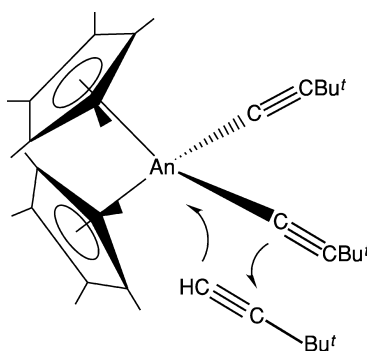
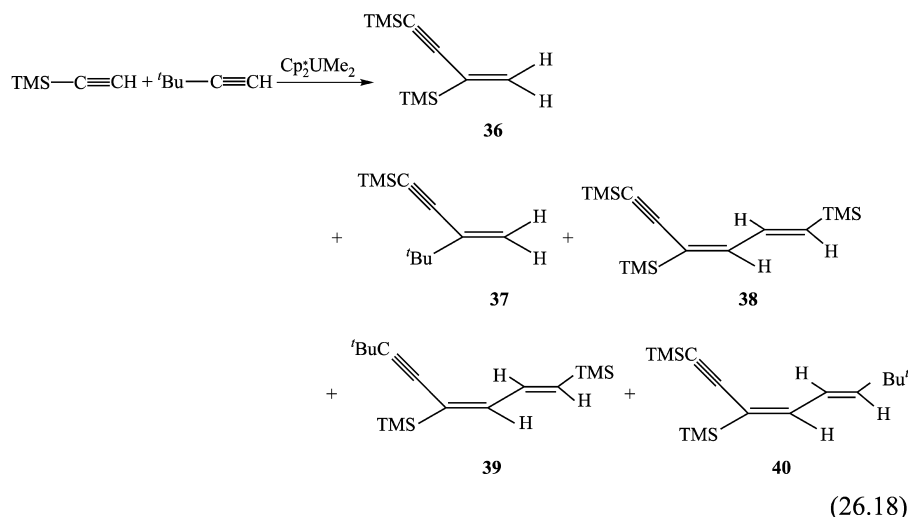


Fig. 26.2 Regioselectivity of the insertion of ${}^t\text{BuC}\equiv\text{CH}$ into an organoactinide acetylide bond.

formed by the consecutive insertion of ${}^t\text{BuC}\equiv\text{CH}$ after the $\text{TMSC}\equiv\text{CH}$ insertion. These results indicated that in the formation of trimers, the last insertion rate must be fast and competitive for both alkynes, and that the metathesis of the free alkyne is the rate-determining step.



26.4 DIMERIZATION OF TERMINAL ALKYNES

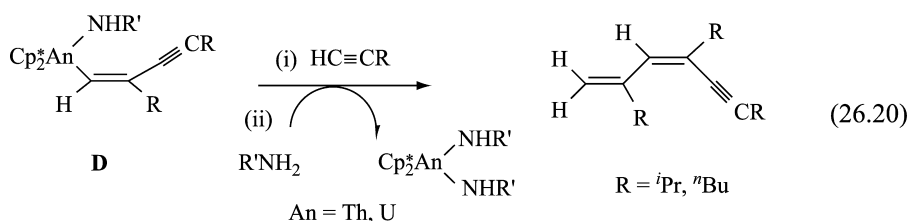
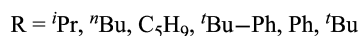
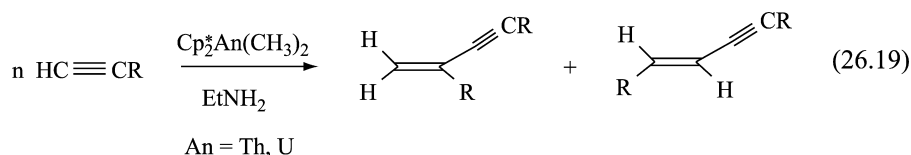
Due to the different reactivities displayed in the selective dimerization of terminal alkynes by different neutral and cationic organo-5f-complexes, this topic will be divided based on the nature of the catalytic species.

26.4.1 Dimerization of terminal alkynes promoted by neutral $(\text{C}_5\text{Me}_5)_2\text{AnMe}_2$ complexes in the presence of amines

An interesting rationale has been presented in connection with the proposed mechanism, suggesting the means to permit the formation of a specific dimer while limiting the formation of higher oligomers. This would, in effect block steps 3 and 4 in Scheme 26.7 and restrict the reaction to follow steps 2 and 5. Haskel *et al.* (1999) have reported a principle for the selective control over the extent of the oligomerization of terminal alkynes by using an acidic chain-transfer agent. The basic approach employs a chain transfer reagent not ending up in the product and not involving subsequent elimination from the product to release the unsaturated oligomer (in contrast to e.g. ethene oligomerization by metallocene catalysts or magnesium reagents) (Samsel, 1993; Pelletier *et al.*, 1996). The dimerization was performed in the presence of an amine (primary or

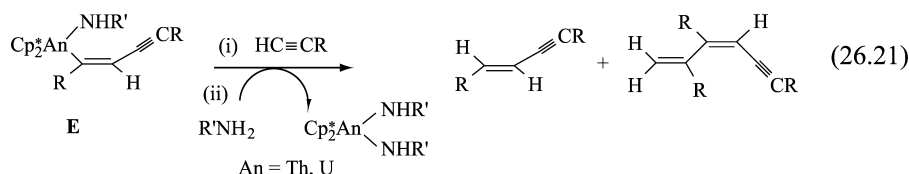
secondary); this resulted in minimal alteration of the turnover frequencies compared with the non-controlled process. The selectivity control (i.e. the amount of the different oligomers obtained by the different complexes (Th, U)) of the new catalytic cycle is explained by considering the difference in the calculated bond-disruption energies between an actinide–alkenyl- and an actinide–amido-bond, and combining non-selective catalytic pathways with individual stoichiometric reactions.

Organoactinide complexes of the type $(C_5Me_5)_2AnMe_2$ ($An = Th, U$) reacted with terminal alkynes in the presence of primary amines yielding preferentially alkyne dimers [equation (26.19)] and for certain alkynes small amounts of regioselective trimers [equation (26.20)]. This selectivity was opposite to that found in the oligomerization of alkynes under the same conditions in the absence of amines. In general, the initial reaction of $(C_5Me_5)_2AnMe_2$ ($An = Th, U$) with an alkyne yielded the bisacetylide complex, though in the presence of amines, for the thorium complex, the corresponding $(C_5Me_5)_2Th(NHR)_2$ (**5**) was formed. For the uranium complex, no bisamido complex is observed unless large excess of the amine was used.

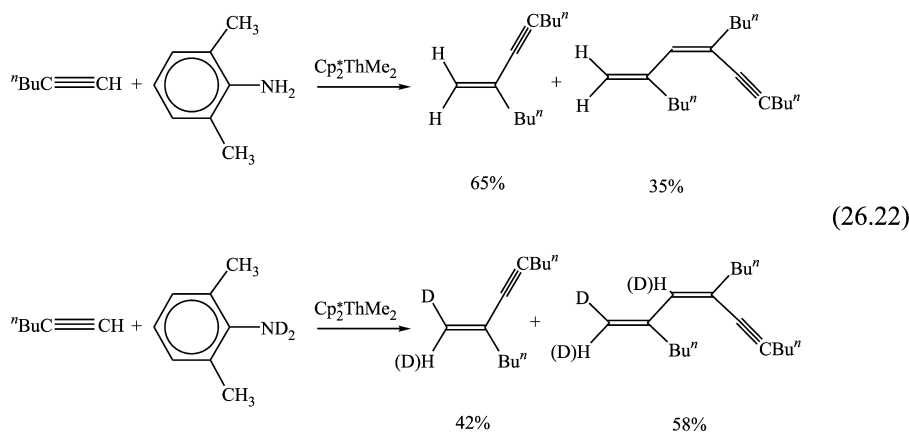


When comparing the oligomerization of terminal alkynes promoted by the thorium complex in the presence of amines as to the results obtained without amines, a dramatic reduction in the extent of oligomerization was observed. When EtNH_2 or other primary amines were used with aliphatic alkynes, mixtures of the corresponding *geminal* and *trans* dimer were produced, while for aromatic alkynes, just the *trans* dimer was formed. Increasing the bulkiness of the primary amine for aliphatic alkynes allowed only the formation of the *geminal* dimer, and the specific trimer as represented in equation (26.20). These results indicated that the insertion of the second alkyne into the metalla–ene-yne **D** complex and the trimer elimination [equation (26.20)] are faster than either the insertion of an alkyne into the intermediate complex **E**,

and/or the protonolysis of **E** by either the alkyne or the amine, eliminating the corresponding isomeric trimer and/or dimer, respectively [equation (26.21)]. Reactions of the thorium precursor with secondary amines allowed the formation of higher oligomers (up to pentamers), however in lower yields, as compared with the results obtained in the reactions in the absence of amines. It was proposed that for secondary amines, the protonolysis of the growing oligomer from the metal was much slower as compared to the insertion of the alkynes and cutting the oligomer chain by the alkyne itself.



For uranium, the oligomerization of non-bulky alkynes with secondary amines showed no control whereas for primary amines ($\text{R}'\text{NH}_2$), the intermolecular hydroamination product obtained was exclusively ($\text{RCH}_2\text{CHN}=\text{R}'$) (Haskel *et al.*, 1996). While the dimerization of ${}^t\text{BuC}\equiv\text{CH}$ produced the *geminal* dimer, in the presence of ${}^t\text{BuNH}_2$, a mixture of both dimers were obtained, which suggested the attachment of the amine to the metal center at the time of the alkyne insertion allowing different regioselectivities. Previously, for the non-controlled oligomerization reactions, the actinide-bisacetylide complex was proposed as the active species in the catalytic cycle. In the controlled oligomerization reaction, the formation of the organoactinide bisamido complex, which was the predominant species, provided strong evidence that the amine was the major protonolytic agent. A novel strategy was implemented in support of the protonolytic theory to increase the selectivity towards the trimeric isomer. Enhanced selectivity was attained by providing a kinetic delay for the fast protonolysis using deuterated amine. The kinetic effect allowed more trimer formation, in a reaction producing both dimer and trimer [equation (26.22)]. The strategy biased the chemoselectivity of the oligomerization increasing the trimer:dimer ratio.



When the product formation was followed as a function of time, the first deuterium was observed at the geminal position, but at higher conversions, more olefinic positions were deuterated, suggesting that the alkyne and the deuterated amine were in equilibrium through a metal complex only exchanging hydrogen/deuterium atoms.

(a) Kinetic, thermodynamic, and mechanistic studies of the controlled oligomerization of terminal alkynes

Kinetic measurements of the controlled oligomerization reaction of ${}^n\text{BuC}\equiv\text{CH}$ with ${}^i\text{BuNH}_2$ promoted by $(\text{C}_5\text{Me}_5)_2\text{ThMe}_2$ revealed a first-order dependence of the catalytic rate on substrate concentration, an inverse first-order in amine and first-order dependence in precatalyst. Thus, the rate law for the controlled oligomerization of terminal alkynes promoted by organoactinides can be written as presented in equation (26.23).

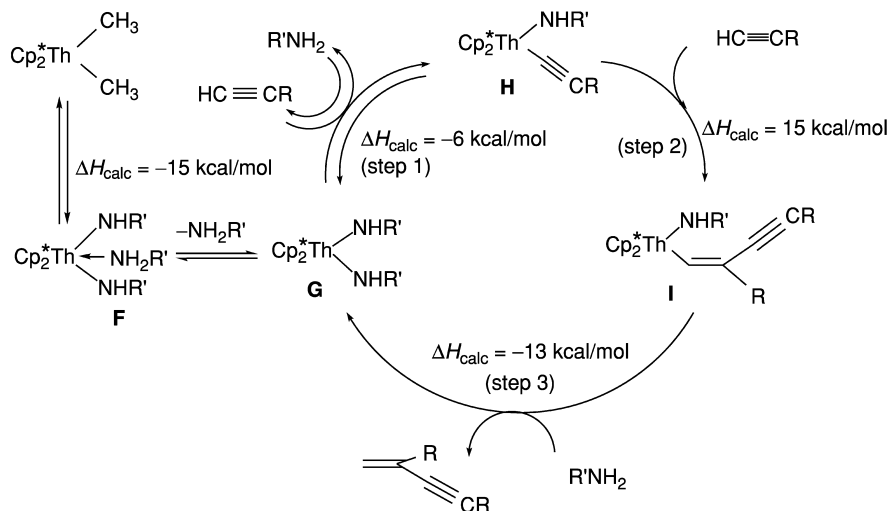
$$v = k [\text{Th}]^1 [\text{alkyne}]^1 [\text{amine}]^{-1} \quad (26.23)$$

The derived ΔH^\ddagger and ΔS^\ddagger values from an Eyring analysis were measured to be 15.1(3) kcal mol⁻¹ and -41.2(6) eu, respectively.

An inverse proportionality in catalytic systems is consistent with a rapid equilibrium before the rate-limiting step. For this reaction, it was consistent with the equilibrium between the bisamido complex and a bisamido-amine complex, as found in the hydroamination of terminal alkynes promoted by early transition complexes (Walsh *et al.*, 1992; Baranger *et al.*, 1993) and in the hydroamination of olefins promoted by organolanthanide complexes (Gagné *et al.*, 1992a,b; Molander and Hoberg, 1992).

A reasonable mechanism for the controlled oligomerization of terminal alkynes is described in Scheme 26.8.

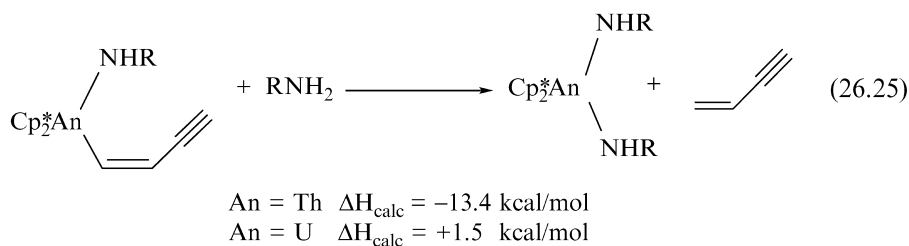
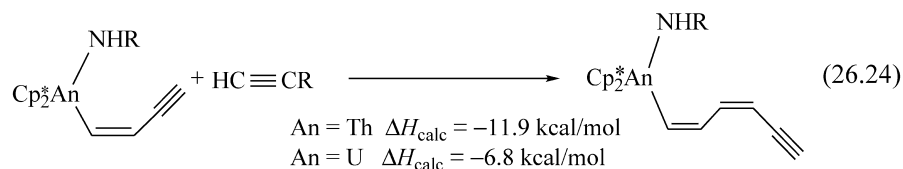
The mechanism presented in Scheme 26.8 consists of a sequence of simple reactions, such as insertion of acetylene into an M-C σ -bond, and σ -bond metathesis. The starting complex $(\text{C}_5\text{Me}_5)_2\text{ThMe}_2$ reacts fast with amines to the bisamido complex **G** and the bisamido-amine complex **F**. These complexes were found to be in rapid equilibrium and responsible for the inverse proportionality in the kinetic dependence of the amine (Straub *et al.*, 1996). Complex **G**, which was found to be the resting state for the catalytic species, reacted with one equivalent of alkyne in the rate-limiting step, producing complex **H** (step 1). Comparison of the results obtained for the oligomerization of phenylacetylene in the absence of amines (with amines only a dimer was obtained), in which both dimers and higher oligomers were obtained, indicated that an amido acetylide and not the bisacetylide complex was responsible for the regio-differentiation. Complex **H** reacts with an alkyne, yielding the actinide-alkenyl amido complex **I** (step 2), which may undergo either a σ -bond protonolysis with the amine to yield the corresponding dimer and the bisamido complex **G** (step 3), or another



Scheme 26.8 Plausible mechanism for the oligomerization of terminal alkynes, in the presence of amines, promoted by organothorium complexes.

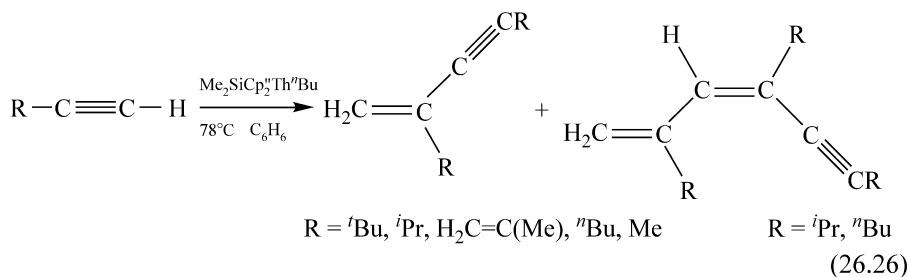
insertion of an alkyne and concomitant σ -bond protonolysis by the amine, yielding the oligomeric trimer and the bisamido complex **G**. Thus the reaction rate law presented in equation (26.23) was compatible with rapid, irreversible alkyne insertion (step 2), rapid σ -bond protonolysis of the oligomer by the amine (step 3), a slow pre-equilibration involving the bis-amido **G** and the mono amido-acetylide complex (**H**) (step 1), and a rapid equilibrium between the bisamido complex **G** and the bisamido-amine complex **F**.

Control over the oligomerization was accomplished by a kinetic competition between the insertion reaction of a new alkyne molecule into the metal-alkenyl bond [equation (26.24)] and the protonolysis by the amine [equation (26.25)]. The insertion reaction produces a larger metallaligomer complex, whereas the competing protonolysis produces the organic product and the bisamido organometallic complex. The difference in selectivity found for the thorium and uranium complexes was corroborated using bond disruption energy data (Bruno *et al.*, 1983; Smith *et al.*, 1986b; Marthino Simões and Beauchamp, 1990; Giardello *et al.*, 1992). For thorium, both reactions [equations (26.24) and (26.25)] were calculated to be exothermic by almost equal amounts generating control over the extent of oligomerization. For the corresponding uranium complex, where no control over chain length was observed, the formation of the bisamido complex was calculated to be endothermic, limiting the control over the degree of oligomerization.

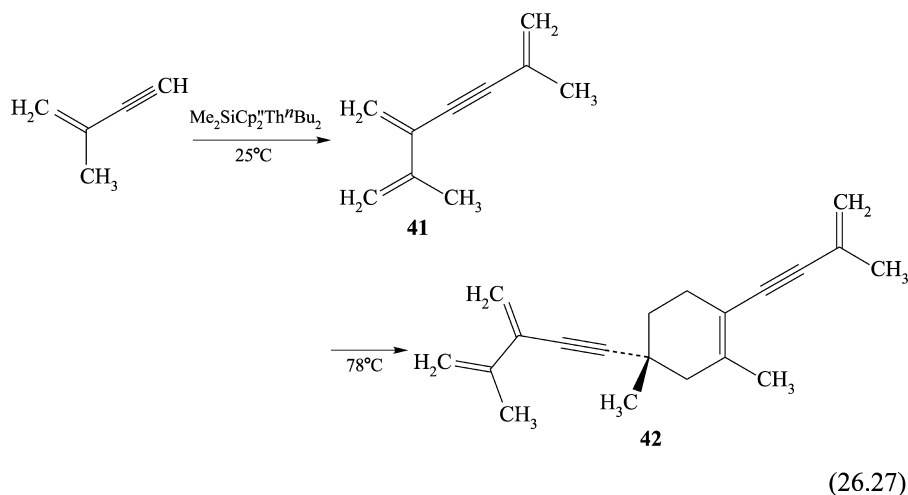


26.4.2 Dimerization of terminal alkynes promoted by the *ansa*-organothorium complex $\text{Me}_2\text{Si}(\text{C}_5\text{Me}_4)_2\text{Th}^n\text{Bu}_2$

The *ansa*-bridged organoactinide complex $\text{Me}_2\text{Si}(\text{C}_5\text{Me}_4)_2\text{Th}^n\text{Bu}_2$ was found to be an excellent precatalyst for the chemo- and regio-selective dimerization of terminal alkynes. At room temperature, head-to-tail geminal dimers were obtained, whereas at higher temperature (78°C), the geminal dimer and some minor amounts of the specific head-to-tail-to-tail trimer (up to 5%) were also observed particularly for the specific alkynes ${}^i\text{PrC}\equiv\text{CH}$ and ${}^n\text{BuC}\equiv\text{CH}$ [equation (26.26)] (Dash *et al.*, 2001). Although no large difference was observed among similar alkyne substituents, the dimerization reaction of either ${}^i\text{PrC}\equiv\text{CH}$ or ${}^n\text{BuC}\equiv\text{CH}$ with $\text{Me}_2\text{Si}(\text{C}_5\text{Me}_4)_2\text{Th}^n\text{Bu}_2$ was much faster and more selective than the dimerization with $\text{Cp}_2^*\text{ThMe}_2$. The most striking result regarding the dimerization/oligomerization of terminal alkynes was found for $\text{TMSC}\equiv\text{CH}$ ($\text{TMS} = \text{Me}_3\text{Si}$). No catalytic reaction was observed by using the *ansa*-bridged complex (butane was evolved), in contrast to the results obtained in the reaction of $\text{TMSC}\equiv\text{CH}$ with $\text{Cp}_2^*\text{ThMe}_2$, in which the geminal dimer (10%) and the head-to-tail-to-head trimer (90%) were obtained with high regioselectivity (Straub *et al.*, 1995).



A domino reaction was observed in the dimerization of the alkene-functionalized alkyne producing dimer **41**, which undergoes a quantitative intermolecular Diels–Alder cyclization to produce compound **42** [equation (26.27)].



(a) Kinetic studies of the dimerization of terminal alkynes promoted by $\text{Me}_2\text{Si}(\text{C}_5\text{Me}_4)_2\text{Th}''\text{Bu}_2$

The kinetics for the dimerization of ${}^i\text{PrC}\equiv\text{CH}$ promoted by $\text{Me}_2\text{Si}(\text{C}_5\text{Me}_4)_2\text{Th}''\text{Bu}_2$ were studied. The reaction displayed a first-order dependence in precatalyst, and two different kinetic domains were observed, with differing alkyne dependence (Fig. 26.3). At low concentrations of alkyne, an inverse proportionality was observed indicating that the reaction is in an inverse first-order, but at higher concentrations, the reaction exhibited a zero order in alkyne (Eisen *et al.*, 1998). The change from an inverse rate to a zero rate was rationalized by invoking two equilibrium processes. In one of these equilibrium processes, the complex was removed from the catalytic cycle (inverse order), whereas the second equilibrium was found to be the rate-determining step in the dimer formation. The latter was measured only at high alkyne concentrations. The derived activation parameters E_a , ΔH^\ddagger , and ΔS^\ddagger from an Eyring analysis were $11.7(3) \text{ kcal mol}^{-1}$, $11.0(3) \text{ kcal mol}^{-1}$, and $22.6(5) \text{ eu}$, respectively.

Given that the stereochemical approach of the alkyne to the organometallic moiety is likely side-on, the highly regioselective production of the geminal dimers was rationalized by suggesting that the insertion of the alkyne occurs with the substituent away from the metal center. The methyl groups of the cyclopentadienyl spectator ligand also disfavor the disposition of the alkyne substituent facing the metal center.

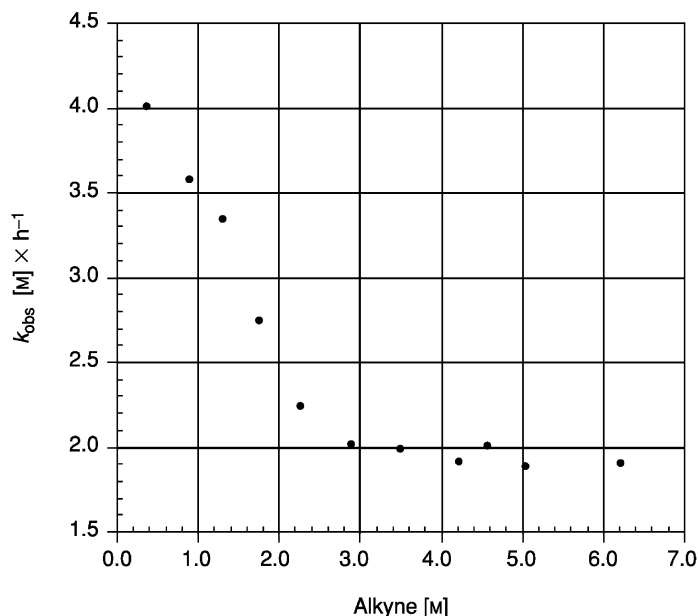
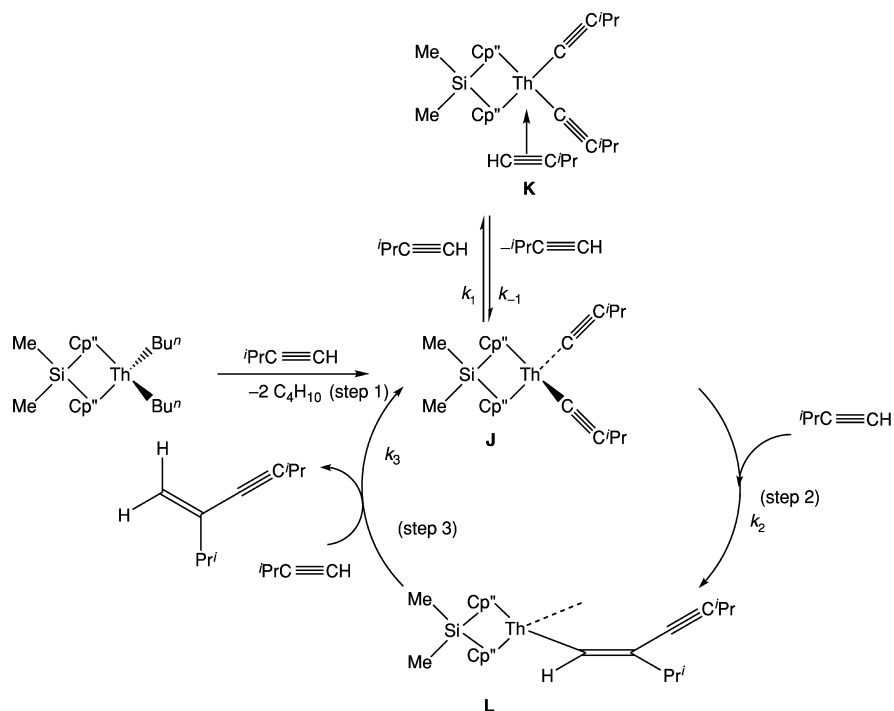


Fig. 26.3 Alkyne dependence in the dimerization of ${}^i\text{PrC}\equiv\text{CH}$ promoted by $\text{Me}_2\text{Si}(\text{C}_5\text{Me}_4)_2\text{Th}^n\text{Bu}_2$.

A plausible mechanism for the selective dimerization of ${}^i\text{PrC}\equiv\text{CH}$ promoted by $\text{Me}_2\text{Si}(\text{C}_5\text{Me}_4)_2\text{Th}^n\text{Bu}_2$ is presented in Scheme 26.9. The initial step in the catalytic cycle is the alkyne C–H activation by the complex $\text{Me}_2\text{Si}(\text{C}_5\text{Me}_4)_2\text{Th}^n\text{Bu}_2$ and the formation of the bisacetylide complex **J** together with butane (step 1). Complex **J** is proposed to be in equilibrium with an alkyne, forming the proposed π -alkyne acetylide complex **K**, which removes the active species from the catalytic cycle (inverse rate dependence). Alternatively, **J** undergoes a head-to-tail insertion with another alkyne into the thorium–carbon σ -bond, producing the substituted alkenyl complex **L** (step 2). Complex **L** goes through a σ -bond protonolysis with an additional alkyne (step 3), yielding the corresponding dimer and regenerating the active acetylide complex **J**. In contrast to the general expectations for organoactinides, complex **K** was the first π -olefin intermediate complex (*vide infra*) exhibiting new rich and versatile reactivity for actinide complexes.

The turnover-limiting step for the catalytic dimerization was measured to be the insertion of the alkyne into the thorium–acetylide complex **J** (step 2). Thus, the derived rate law based on the mechanism proposed in Scheme 26.9 for the oligomerization of terminal alkynes promoted by the complex $\text{Me}_2\text{SiCp}_2''\text{Th}^n\text{Bu}_2$ is given by equation (26.28), fitting the kinetic performances of the alkyne and catalysts.



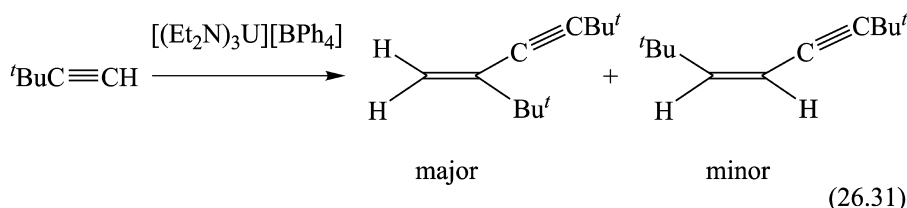
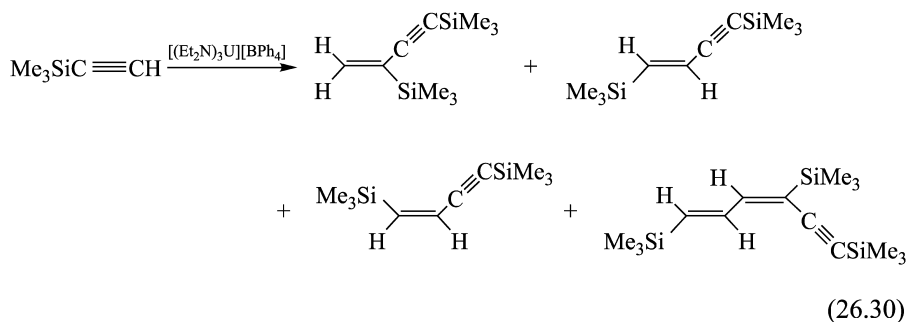
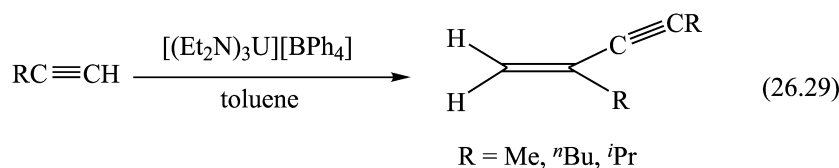
Scheme 26.9 Proposed mechanism for the dimerization of terminal alkynes promoted by $\text{Me}_2\text{SiCp}''_2\text{Th}''\text{Bu}_2$.

$$v = \frac{k_{-1}k_2[\text{Cat}]}{k_1 + k_2 - \frac{k_2k_{-2}}{k_3[\text{alkyne}]}} \quad (26.28)$$

26.4.3 Catalytic dimerization of terminal alkynes promoted by the cationic actinide complex $[(\text{Et}_2\text{N})_3\text{U}][\text{BPh}_4]$. First f-element alkyne π -complex $[(\text{Et}_2\text{N})_2\text{U}(\text{C}\equiv\text{C}^i\text{Bu})(\eta^2\text{-HC}\equiv\text{C}^i\text{Bu})][\text{BPh}_4]$

Unlike neutral organoactinide complexes, homogeneous cationic d^0/f^n actinide complexes have been used as catalysts for the polymerization of α -olefins (Jia *et al.*, 1997; Chen *et al.*, 1998), as have their isolobal group 4 complexes. The alkyne oligomerization reaction has been mentioned as a useful probe for the insertion and σ -bond metathesis reactivity of organoactinide complexes. For the corresponding cationic actinide complexes, little was known regarding their reactivity with terminal alkynes (Wang *et al.*, 1999). Reaction of the cationic complex $[(\text{Et}_2\text{N})_3\text{U}][\text{BPh}_4]$ (Berthet *et al.*, 1995) with the terminal alkynes $\text{RC}\equiv\text{CH}$, ($\text{R} = \text{Me}$, ^iBu , ^iPr) resulted in the chemo- and regio-selective catalytic formation of the head-to-tail *gem*-dimers without the formation of the *trans* dimer or any other major oligomers [equation (26.29)]. For $\text{PhC}\equiv\text{CH}$, the

reaction was less chemoselective, allowing the formation of some trimers (dimer:trimer ratio = 32:58). For $\text{TMSC}\equiv\text{CH}$, besides the formation of the geminal head-to-tail dimer, the *trans*-head-to-head dimer, and the regioselective head-to-tail-to-head-trimer (*E,E*)-1,4,6-tris(trimethylsilyl)1-3-hexadien-5-yne, the unexpected head-to-head *cis* dimer was also formed [equation (26.30)]. For ${}^t\text{BuC}\equiv\text{CH}$, besides the geminal dimer also the unexpected *cis*-dimer was formed [equation (26.31)].



As already mentioned, mechanistically, the relatively polar metal–ligand bonds, the absence of energetically accessible metal oxidation states for oxidative addition/reductive elimination processes and the presence of relatively low-lying empty σ -bonding orbitals, implicate a ‘four-center’ heterolytic transition state in the metal–carbon bond cleavage (Marks and Day, 1985; Marks, 1986a,b). The reaction of the metal acetylide with a terminal alkyne occurs in a *syn* mode and the σ -bond protonolysis of the resulting alkenyl complex will be expected to maintain the *cis*-stereochemistry at the product (Fig. 26.4).

Hence, the formation of the *trans* dimers [equations (26.30) and (26.31)] argued for an isomerization pathway before the products were released from the metal center. For comparison, in the oligomerization of terminal alkynes promoted by the cationic complexes $[\text{Cp}_2^*\text{AnMe}][\text{B}(\text{C}_6\text{F}_5)_4]$ (An = Th, U), the

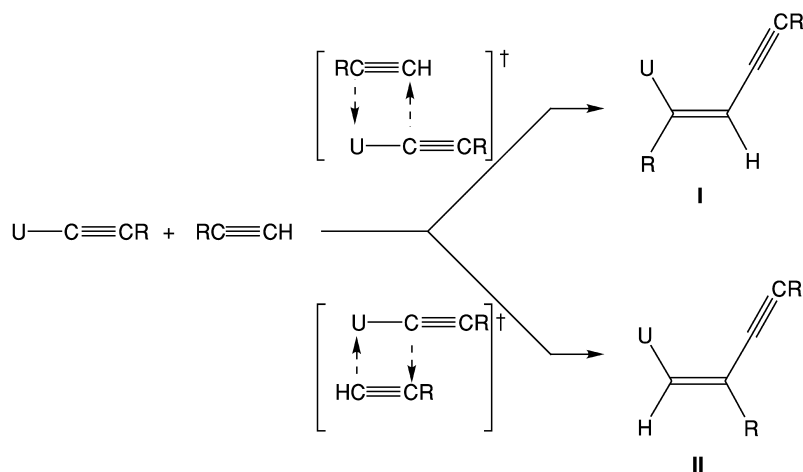
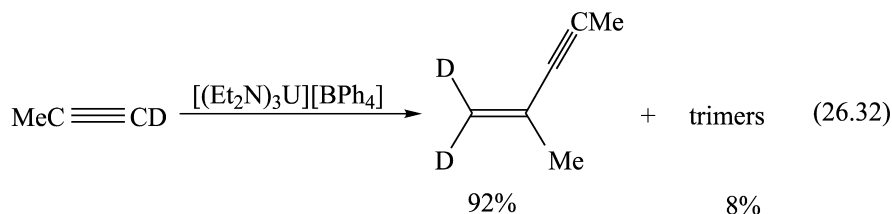


Fig. 26.4 Modes of activation of an actinide-acetylide complex with an alkyne through a syn four-centered transition state pathway towards the formation of the intermediates I or/and II.

geminal dimer was chemoselectively formed with no trace formation of either *cis* or *trans* dimers (Haskel *et al.*, 1999).

Mechanistically, in the reaction of $[(\text{Et}_2\text{N})_3\text{U}][\text{BPh}_4]$ with terminal alkynes, one equivalent of the Et_2NH amine was released in solution, forming the bisamido acetylide cationic complex $[(\text{Et}_2\text{N})_2\text{U}-\text{C}\equiv\text{CR}][\text{BPh}_4]$. This reaction was shown to be a slow equilibrium, and the addition of different equimolar amounts of external Et_2NH to the reaction mixture led to a linear lowering of the reaction rate (Fig. 26.5).

Considering that in the reactions with alkynes, the amount of the released free amine was stoichiometric, it was deduced that the free terminal alkyne was also the major protonolytic agent. The confirmation of this protonolytic hypothesis was obtained by generating a kinetic delay for the presumed fast protonolysis by the alkyne to allow trimer formation, through replacement of the terminal hydrogen with deuterium [equation (26.32)]. By using that strategy, the chemoselectivity of the oligomerization was altered allowing formation of the deuterated geminal dimer, and some trimer (Dash *et al.*, 2000).



The kinetics of the dimerization reaction of $^n\text{BuC}\equiv\text{CH}$ was studied, indicating that the reaction behaved with a first-order dependence in precatalyst, and as

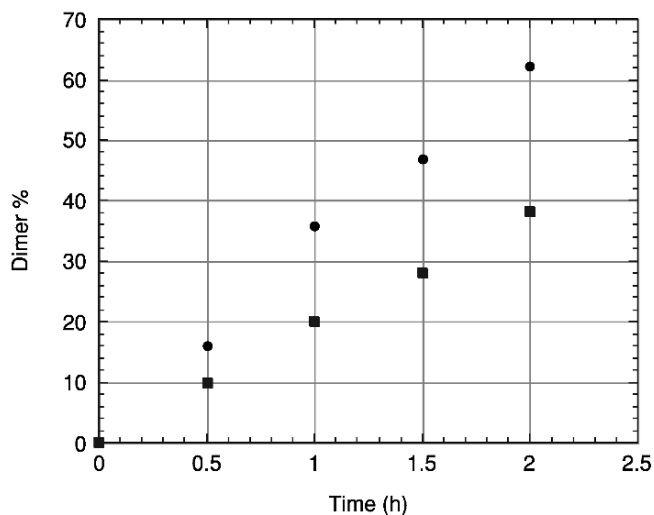


Fig. 26.5 Following the dimer formation as a function of time in the reaction of ${}^i\text{PrC}\equiv\text{CH}$ catalyzed by $[(\text{Et}_2\text{N})_2\text{U}-\text{C}\equiv\text{CR}][\text{BPh}_4]$. Absence of external amine (●), presence of one equivalent of external Et_2NH (■).

a function of alkyne, the kinetic plots showed two domains (Fig. 26.6). At low alkyne concentrations, an inverse proportionality was observed, indicating that the reaction was inverse first-order, and at higher concentrations, the reaction exhibits a zero-order in alkyne, similar to the behavior displayed in Fig. 26.3.

The activation parameters derived for the dimerization of ${}^n\text{BuC}\equiv\text{CH}$ were characterized by a small enthalpy of activation ($\Delta H^\ddagger = 15.6(3) \text{ kcal mol}^{-1}$) and a negative entropy of activation ($\Delta S^\ddagger = -11.4(6) \text{ eu}$). The proposed mechanism for the dimerization of ${}^n\text{BuC}\equiv\text{CH}$ is presented in Scheme 26.10. The initial step in the catalytic cycle is the alkyne C–H activation by the cationic uranium amide complex and the formation of the bisamido carbyl complex $[(\text{Et}_2\text{N})_2\text{U}-\text{C}\equiv\text{C}{}^n\text{Bu}][\text{BPh}_4]$ (**M**) together with Et_2NH . Complex **M** can be in equilibrium with an alkyne forming the π -alkyne acetylide uranium complex **N**, which drives the active species out of the catalytic cycle (inverse rate dependence), or undergoes with an alkyne a head-to-tail insertion into the uranium–carbon σ -bond, yielding the substituted uranium alkenyl complex **O**. Complex **O** may undergo a σ -bond metathesis with an additional alkyne, leading to the corresponding dimer and regenerating the active carbyl complex **M**.

Complex **N** (for $\text{R} = {}^t\text{Bu}$) was trapped and its structure spectroscopically determined. The ${}^1\text{H}$ - and ${}^{13}\text{C}$ -NMR spectra of complex **N** showed sharp lines as found for other actinide-IV type of complexes. The ${}^1\text{H}$ -NMR spectrum exhibited the acetylide signal ($\equiv\text{C}-\text{H}$) at $\delta = -2.14$ which correlated in the distortionless enhancement by polarization transfer (DEPT) and in the 2D C–H correlation NMR experiments to the carbon having the signal at $\delta = -19.85$

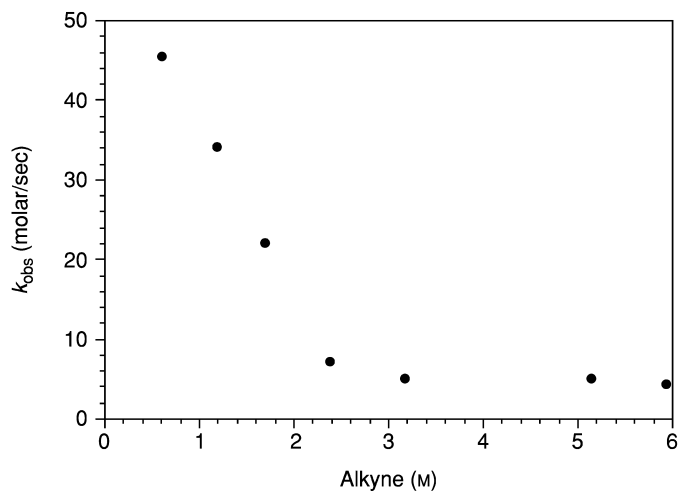
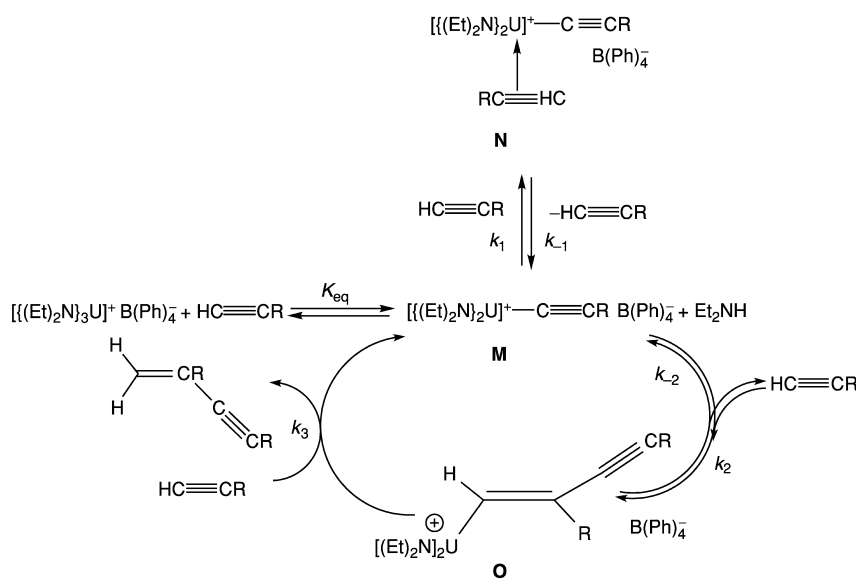


Fig. 26.6 Alkyne dependence in the dimerization of ${}^n\text{BuC}\equiv\text{CH}$ promoted by $[(\text{Et}_2\text{N})_3\text{U}][\text{BPh}_4]$.

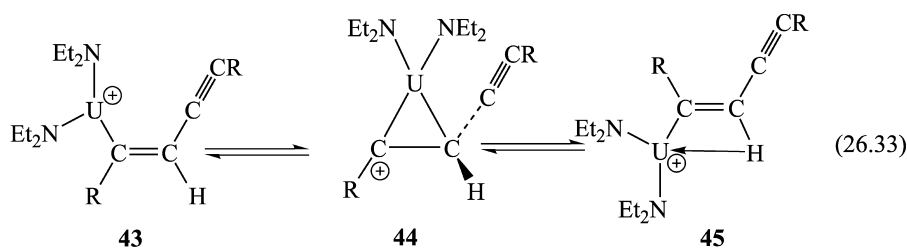


Scheme 26.10 Proposed mechanism for the dimerization of terminal alkynes promoted by $[(\text{Et}_2\text{N})_3\text{U}][\text{BPh}_4]$.

ppm, with a coupling constant of ${}^1J = 250$ Hz. A confirmation of the formation of an alkyne η^2 -complex, as compared to an acetylide complex or to a free alkyne was also obtained by FT-IR spectroscopy. The $\text{C}\equiv\text{C}$ stretching of the free alkyne (2108 cm^{-1}) disappeared, giving rise to two signals at lower

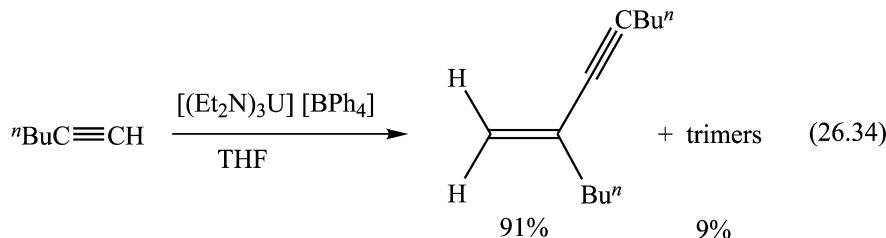
frequencies, as expected for η^2 -transition metal complexes, one at 2032 cm^{-1} similar to acetylide lanthanides, and the second one at 2059 cm^{-1} . The turnover-limiting step for the catalytic dimerization was found to be the insertion of the alkyne into the uranium–carbyl complex **M**. The proposed mechanism also agreed with the formation of trimer oligomers, which are only expected if a kinetic delay in the protonolysis was operative [equation (26.32)].

For sterically demanding alkyne substituents (TMS, ^tBu), it was proposed that the rate of the protonolysis step is lower than that of the isomerization of the metalla–alkenyl complex **43**, producing the unexpected *cis*-dimer **45**, probably through the metalla–cyclopropyl cation (**44**), via the ‘envelope isomerization’ [equation (26.33)] (Faller and Rosan, 1977). The preference for the *cis*-isomer was suggested to arise from an agostic β -hydrogen interaction to the metal center (Wang *et al.*, 1999; Dash *et al.*, 2000).

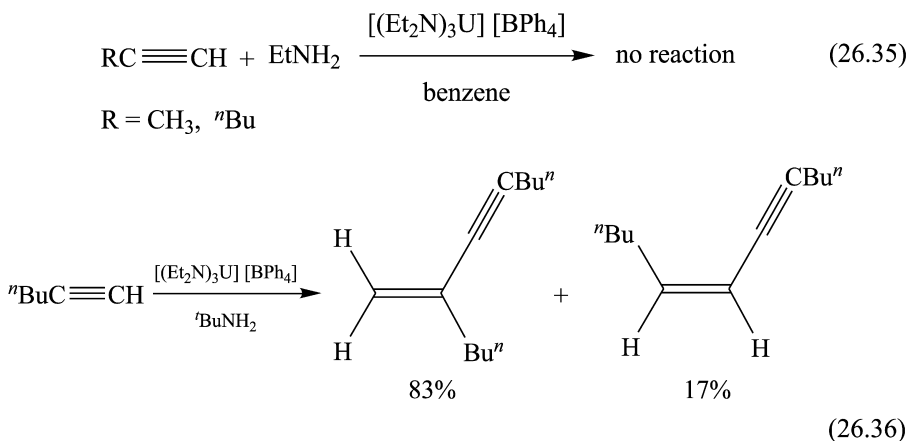


(a) Effect of external amines in the dimerization of alkynes promoted by the cationic complex [(Et₂N)₃U][BPh₄]

Since the formation of the cationic complex **M** is an equilibrium reaction (Scheme 26.10), it was possible to tailor the regiochemistry of the dimerization by using external amines. The expectation was that the amine would be bonded to the cationic metal center, causing a kinetic delay, but also allowing unique regiochemistry. As presented above in the reaction of 1-hexyne with a catalytic amount of the cationic complex [(Et₂N)₃U][BPh₄] [equation (26.29)] the geminal dimer was chemoselectively obtained. However, when the reaction was carried out in a polar solvent like THF, the reaction was much slower, yielding besides the dimer a mixture of trimers [equation (26.34)]. The result was rationalized by the lower reactivity of the THF adduct [(Et₂N)₃(THF)₃U]⁺ resulting in slower protonolysis of the corresponding alkenyl intermediate [(Et₂N)₂(THF)₃U(C=C(H)C≡CR)]⁺ (R = ⁿBu), and allowing further alkyne insertion with the formation of trimers, but with a total lack of regioselectivity.

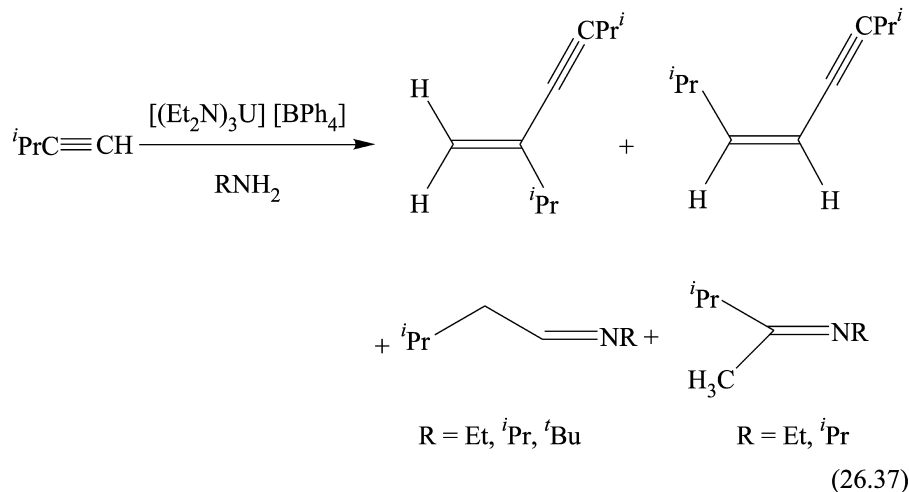


For 1-hexyne, the addition of equimolar amounts of the external amine EtNH_2 (alkyne:amine = 1:1) to the reaction mixture impeded the occurrence of the dimerization process. The same behavior was found for propyne [equation (26.35)]. This lack of reactivity for these alkynes was proposed to be a consequence of either their inability to engage in the equilibrium reaction (Scheme 26.10), resulting in the formation of the acetylide complex **M** in the presence of external EtNH_2 , or the formation of an inactive π -alkyne complex, similar to **N** in Scheme 26.10. When 1-hexyne was reacted in the presence of an equimolar amount of the bulkier amine ${}^t\text{BuNH}_2$, the *gem* dimer and the unexpected *cis* dimer were obtained [equation (26.36)], indicating that the bulky amine probably allowed the formation of the acetylide intermediate $[({}^t\text{BuNH}_2)_x({}^t\text{BuNH})_2\text{U}(\text{C}\equiv\text{C}^n\text{Bu})]^+$ by the reaction of ${}^n\text{BuC}\equiv\text{CH}$ with the trisamido cation $[({}^t\text{BuNH}_2)_3({}^t\text{BuNH})_3\text{U}]^+$. This acetylide would then undergo insertion of an alkyne molecule to give the corresponding alkenyl species and dimerization products.



(b) Dimerization and hydroamination of ${}^i\text{PrC}\equiv\text{CH}$ and ${}^t\text{BuC}\equiv\text{CH}$ catalyzed by $[(\text{Et}_2\text{N})_3\text{U}][\text{BPh}_4]$ in the presence of amines

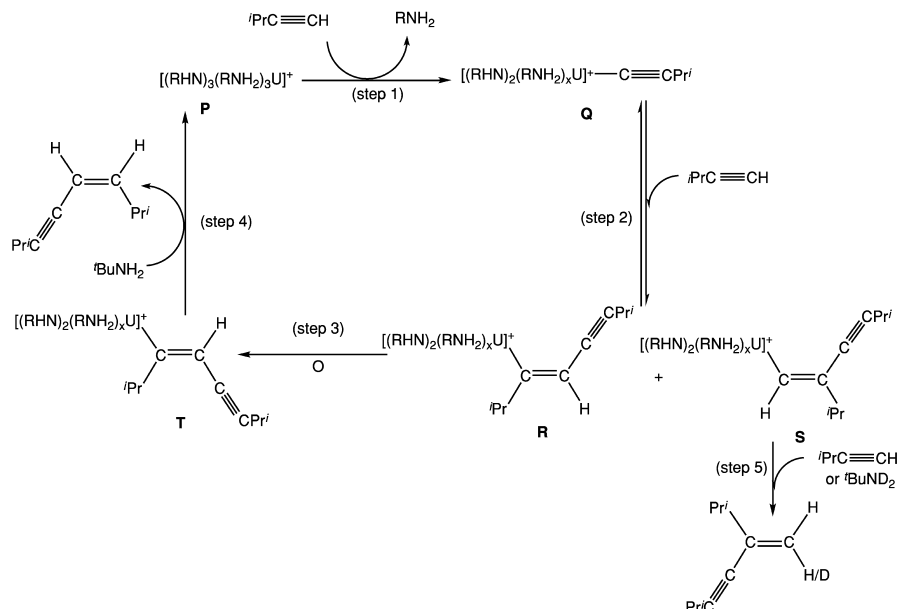
Unpredictably, the reactions of ${}^i\text{PrC}\equiv\text{CH}$ and ${}^t\text{BuC}\equiv\text{CH}$ followed a quite distinct course. These alkynes were found to be more reactive than 1-hexyne or propyne in the presence of different amines. The nature of the diverse products were found to be strongly dependent on the size or steric encumbrance of the amine. The reaction of ${}^i\text{PrC}\equiv\text{CH}$ with $[(\text{Et}_2\text{N})_3\text{U}][\text{BPh}_4]$ in the presence of EtNH_2 or ${}^i\text{PrNH}_2$ afforded the *cis* dimer, trace amounts of the *gem* dimer, and depending on the amine, one or both of the two corresponding hydroamination products were generated. By using the bulkier amine ${}^t\text{BuNH}_2$ both dimers and only one hydroamination product were observed [equation (26.37)] (Wang *et al.*, 2002a).



The rather large effect of alkyne concentration on the distribution of the products was revealed by the relative proportions of the dimers (*gem* to *cis*), which vary from 40:24 in the reaction of ${}^t\text{BuND}_2$ with two equivalents of ${}^i\text{PrC}\equiv\text{CH}$ to 70:8 in the reaction of ${}^t\text{BuNH}_2$ with one equivalent of ${}^i\text{PrC}\equiv\text{CH}$. The results agreed with a dimerization mechanism such as that in Scheme 26.11. The mechanism consists of the formation of complex **Q** by the reaction of the cationic complex **P** with the alkyne (step 1). The acetylide complex reacts with an additional alkyne, producing the mixture of alkenyl compounds **R** and **S** (step 2). Isomerization of complex **R** through an envelope mechanism [equation (26.33)] allowed the formation of complex **T** (step 3) that by protonolysis yielded the unexpected *cis*-dimer (step 4). The addition of a large amount of alkyne in combination with a source of deuterium (as ${}^t\text{BuND}_2$) removed complex **S** from the catalytic cycle as the *geminal* product (step 5). This latter species was found partially deuterated since the alkyne served also as a protonolytic reagent. The rate-determining step in the reaction was proposed to be the isomerization reaction (step 3).

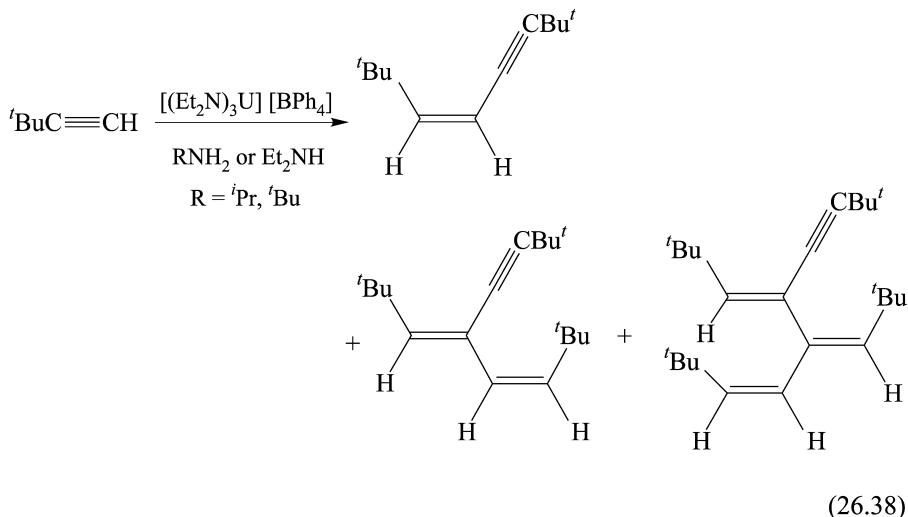
(c) Regioselective oligomerization of ${}^t\text{BuC}\equiv\text{CH}$ promoted by $[(\text{Et}_2\text{N})_3\text{U}][\text{BPh}_4]$ in the presence of amines

Reaction of the bulkier alkyne ${}^t\text{BuC}\equiv\text{CH}$ with the cationic uranium complex $[(\text{Et}_2\text{N})_3\text{U}][\text{BPh}_4]$ in the presence of ethylamine gave mainly the *cis* dimer and small amounts of the *gem* isomer (up to 2%), showing the remarkable influence of the nature of the amine on the dimerization reaction, by transposing the regioselectivity [see equation (26.31)]. With other primary or secondary amines, the *cis* dimer was the major product although the concomitant formation of one regiospecific trimer and one regiospecific tetramer were also observed.



Scheme 26.11 Proposed mechanisms for the formation of the gem- and cis-dimers, promoted by the cationic complex $[(\text{Et}_2\text{N})_3\text{U}][\text{BPh}_4]$ in the reaction of $i\text{PrC}\equiv\text{CH}$ with primary amines.

The most remarkable result, aside from the formation of only one trimer and one tetramer, was the fact that the regiochemistry of these oligomers was unpredictable, regardless of amine [equation (26.38)]. The trimer and the tetramer corresponded to the consecutive insertions of an alkyne molecule into the vinylic CH bond *trans* to the bulky *tert*-butyl group.

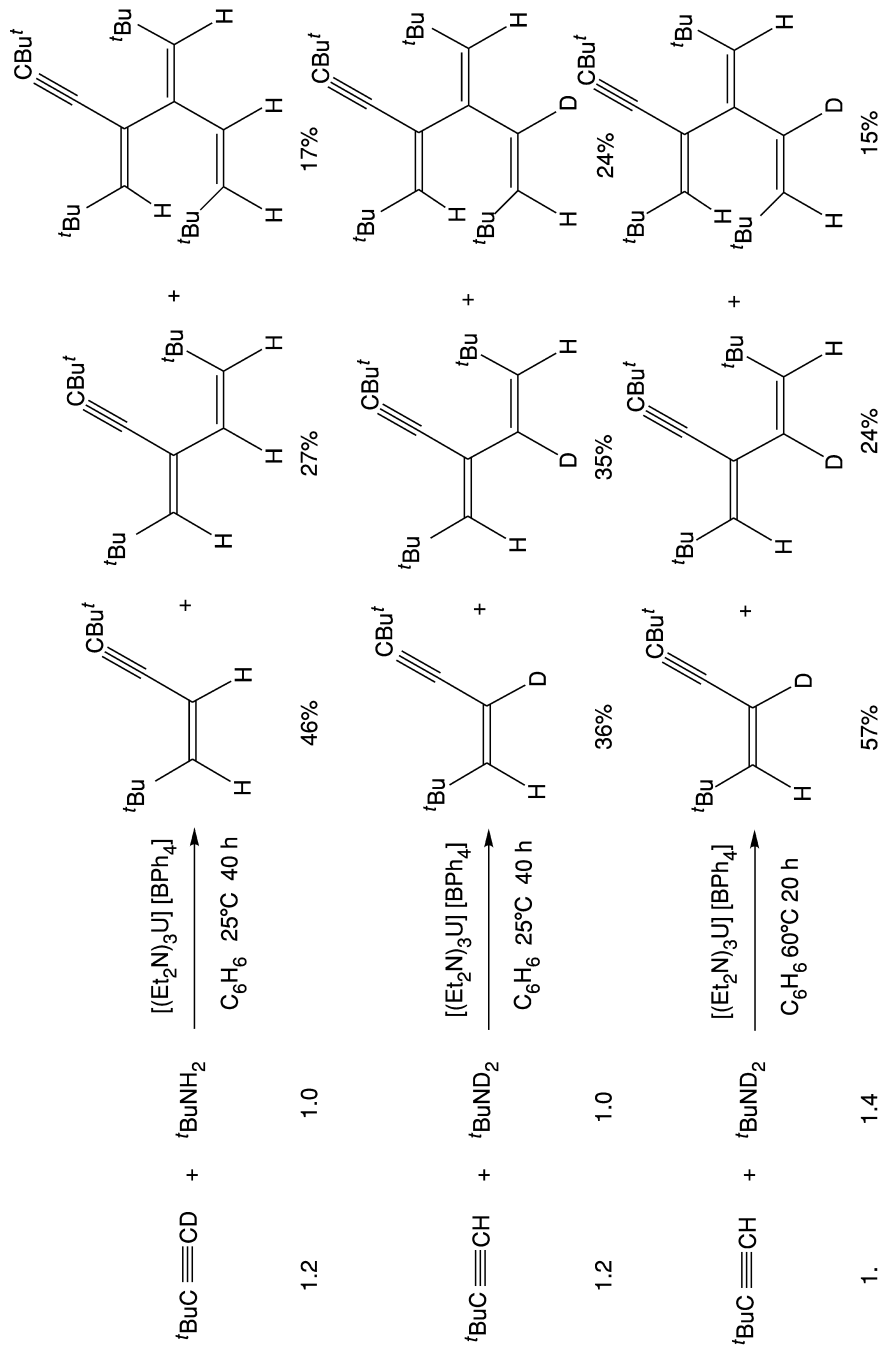


To reveal the role of the amine, and to examine the possibility that the initially *cis* isomer was reactivated to yield the regioselective trimer and tetramer, the reactions with deuterated amine ¹BuND₂ and deuterated alkyne ¹BuC≡CD were performed (Scheme 26.12). The reaction of ¹BuC≡CD with ¹BuNH₂ gave the products with *no* deuterium, indicating that ¹BuC≡CD was transformed into ¹BuC≡CH. The reaction for the H/D exchange between ¹BuC≡CH and ¹BuND₂ was found to be active in the presence of the catalyst, to give ¹BuC≡CD and ¹BuNHD. These compounds were also observed at early stages of the catalytic oligomerization of ¹BuC≡CH in the presence of ¹BuND₂, which afforded the *cis* dimer as a mixture of mono- and non-deuterated compounds. The amount of the non-deuterated dimer was always larger than that of the mono-deuterated dimer. The deuterium atom in the dimer was found only in the *trans* position relative to the ¹Bu group. Mixtures of non- and mono-deuterated compounds were also obtained for the trimer and tetramer having the deuterium atom always in the internal position, *trans* to the ¹Bu group. The presence of only one deuterium atom in the oligomers, in unique positions, strongly suggested that this D atom was introduced during the protonolysis steps of the catalytic cycle. In agreement with this hypothesis was the increasing proportion of the trimer and dimer, which likely results from the slower cleavage of the alkenyl intermediate by the deuterated amine or alkyne, permitting further insertion of an alkyne molecule into the U–C bond.

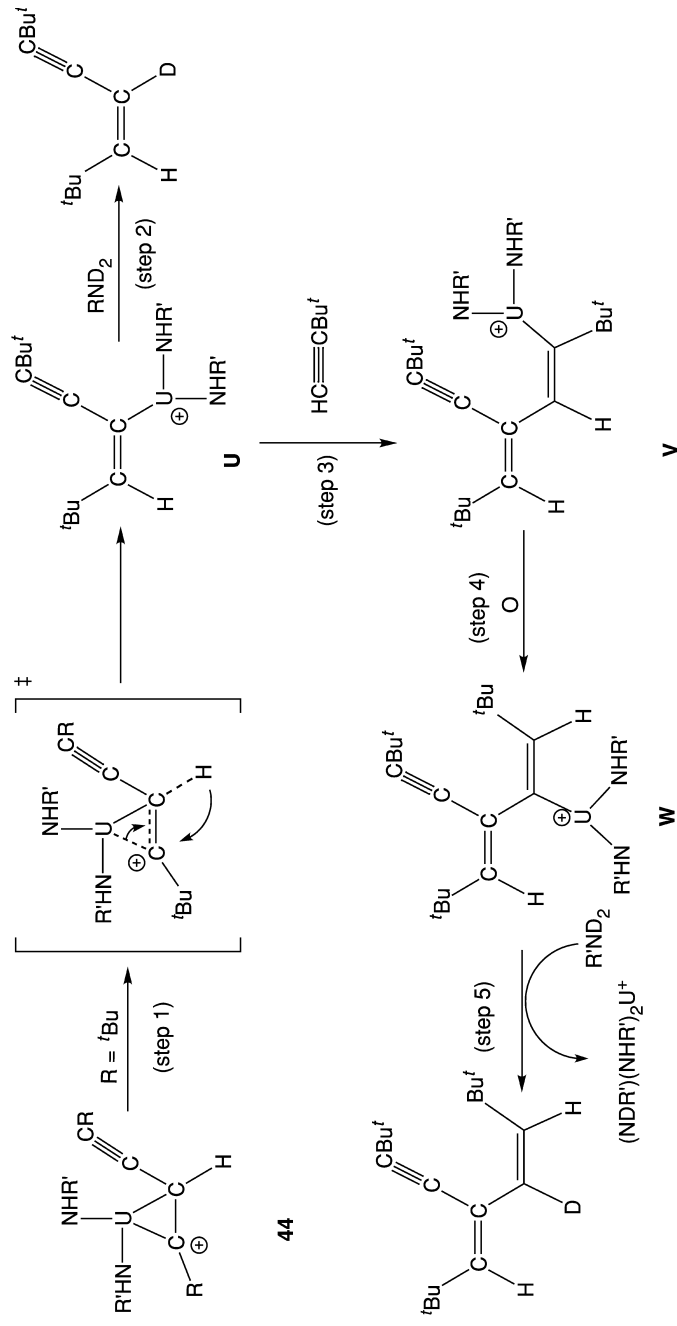
The proposed mechanism for the regiospecific formation of the trimer and tetramer is described in Scheme 26.13. The same intermediate **44**, which was proposed to explain the *trans*–*cis* isomerization of the alkenyl intermediate by the envelope mechanism [equation (26.33)] was proposed to explain conceptually the regiospecific formation of one trimer and one tetramer. The mechanism is based on the 1,2-hydride shift isomerization of the metal–alkenyl complex **44**, leading to the isomeric compound **U** (step 1). Deuterolysis at this stage liberates the deuterated dimer regioselectively (step 2). Insertion of an alkyne molecule into the U–C bond of **U** leads to the formation of complex **V**. The regioselectivity of this insertion (step 3) results from the steric hindrance between the alkyne substituent at the α-position of the metal–alkenyl chain and the incoming alkyne. The same isomerization process as before converts complex **V** into the *syn* complex **W** (step 4). Protonolysis of **W** regenerates the catalyst and produces the specific trimer (step 5), whereas the additional insertion of the alkyne, envelope isomerization, and protonolysis yielded the specific tetramer.

26.5 CROSS DIMERIZATION OF TERMINAL ALKYNES CATALYZED BY [(Et₂N)₃U][BPh₄]

Based on the different regioselectivities observed for the cationic complex [(Et₂N)₃U][BPh₄], it was proposed that selective cross dimerization of alkynes could be induced. In the reaction of an equimolar mixture of ¹BuC≡CH

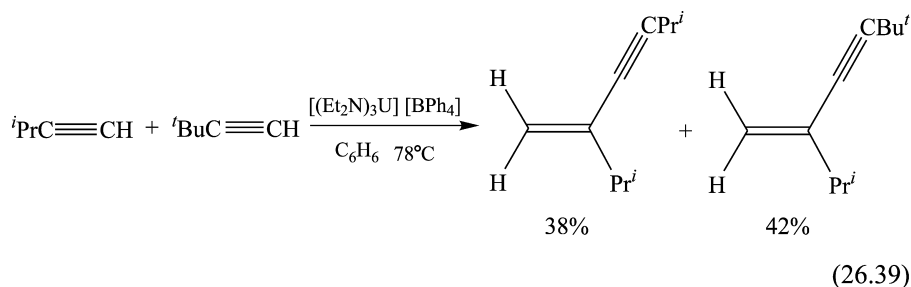


Scheme 26.12 Deuterium labeling experiments in the oligomerization of ${}^t\text{BuC}\equiv\text{CH}$ with ${}^t\text{BuNH}_2$ and ${}^t\text{BuC}\equiv\text{CD}$ with ${}^t\text{BuNH}_2$ promoted by $[(\text{Et}_2\text{N})_3\text{U}][\text{BPh}_4]$.



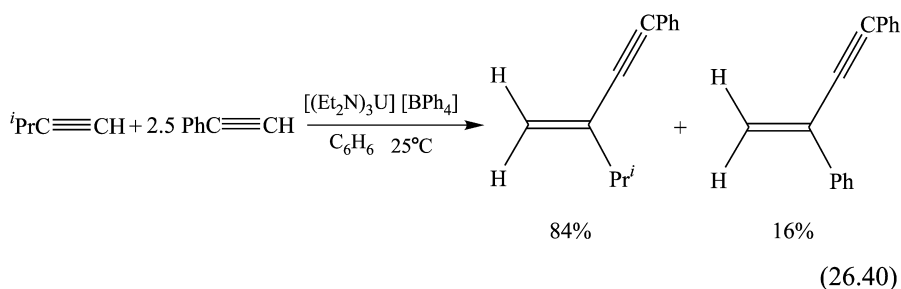
Scheme 26.13 Proposed mechanism for the regioselective dimerization and trimerization of $t\text{-BuC}\equiv\text{CH}$ promoted by $[(\text{Et}_2\text{N})_3\text{U}][\text{BPh}_4]$ in the presence of $t\text{-BuNH}_2$.

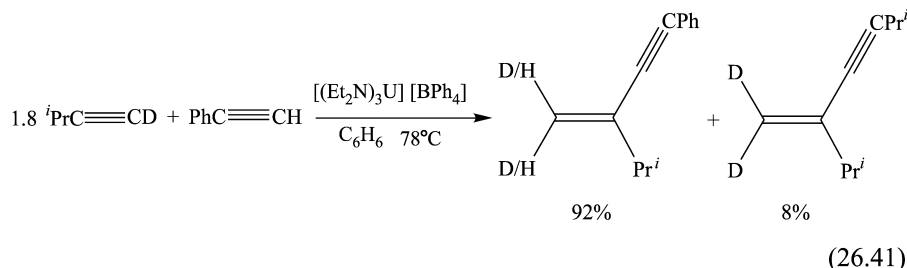
and ${}^i\text{PrC}\equiv\text{CH}$ with $[(\text{Et}_2\text{N})_3\text{U}][\text{BPh}_4]$, the *gem*-dimer of ${}^i\text{PrC}\equiv\text{CH}$ and the *gem*-codimer were obtained [equation (26.39)] (Wang *et al.*, 2002b).



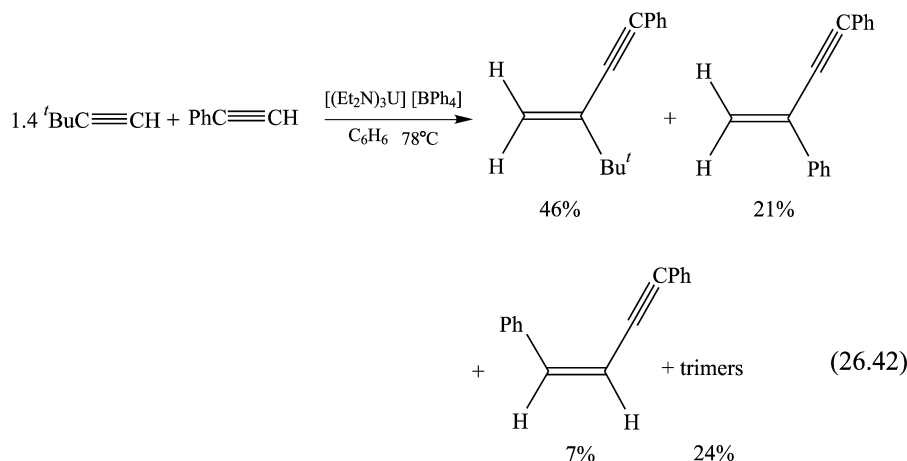
This result was extremely important, since it pointed out that the formation of both metal–acetylide complexes, $\text{M}-\text{C}\equiv\text{CR}$ ($\text{R} = {}^i\text{Pr}, {}^t\text{Bu}$), was rapid and of comparable rates, although the insertion of ${}^i\text{PrC}\equiv\text{CH}$ into both $\text{M}-\text{C}\equiv\text{CR}$ ($\text{R} = {}^i\text{Pr}, {}^t\text{Bu}$) moieties was much faster than that of ${}^t\text{BuC}\equiv\text{CH}$. The lack of any trimer formation implied that the protonolysis of the metal–alkenyl fragments by either one of the terminal alkynes was faster than any additional alkyne insertion.

When a mixture of ${}^i\text{PrC}\equiv\text{CH}$ and $\text{PhC}\equiv\text{CH}$ was reacted at room temperature (to avoid trimers), the *gem*-codimer was obtained. This codimer was the result of the protonolysis of the metal–alkenyl fragment produced from the insertion of ${}^i\text{PrC}\equiv\text{CH}$ into the $\text{M}-\text{C}\equiv\text{CPh}$ moiety. Along with the codimer, a small amount of the *gem*-dimer of $\text{PhC}\equiv\text{CH}$ was also produced by the insertion of $\text{PhC}\equiv\text{CH}$ into the $\text{M}-\text{C}\equiv\text{CPh}$ moiety before the protonolysis [equation (26.40)]. This result showed that $\text{PhC}\equiv\text{CH}$ preferentially reacted with the precatalyst $[(\text{Et}_2\text{N})_3\text{U}][\text{BPh}_4]$ forming the acetylide complex $\text{U}-\text{C}\equiv\text{CPh}$ into which ${}^i\text{PrC}\equiv\text{CH}$ inserted faster as compared with the aromatic alkyne. To shed light on which of the alkynes is the major protonolytic reagent the reaction of a mixture of ${}^i\text{PrC}\equiv\text{CD}$ and $\text{PhC}\equiv\text{CH}$ was performed [equation (26.41)].



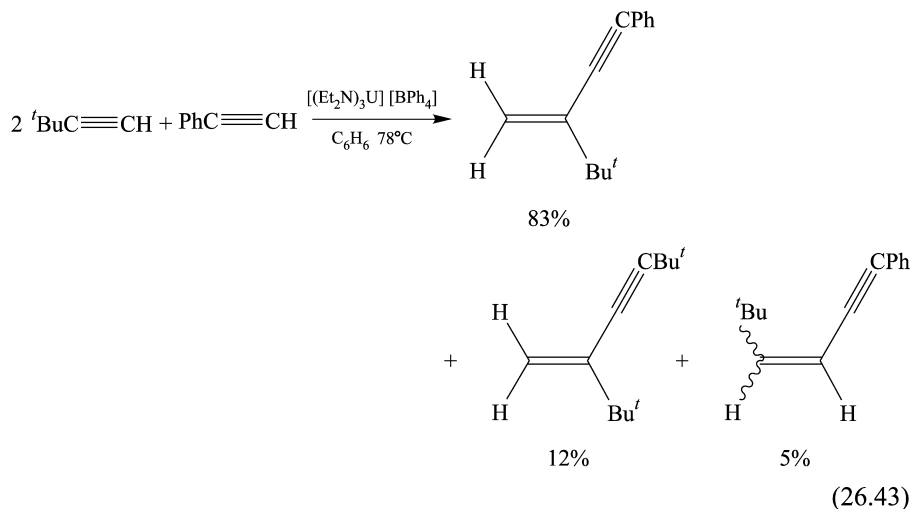


The favored formation of the codimer was substantiated with the following observations: (i) the aromatic metal-acetylide moiety was initially formed; (ii) $^i\text{PrC}\equiv\text{CD}$ inserted faster than the corresponding aromatic alkyne; (iii) the protonolysis by $\text{PhC}\equiv\text{CH}$ was faster than that of the aliphatic alkyne; (iv) the formation of the deuterated *gem*-dimer was obtained due to some excess of the aliphatic alkyne that was present in the reaction. The scrambling of the deuterium atom at the geminal position (only one deuterium at each dimer) was the result of the exchange of acidic H/D atoms between the two aliphatic and aromatic alkynes through the metal center. With an excess of the aliphatic alkyne, the deuterolysis of the most stable $\text{U}-\text{C}\equiv\text{CPh}$ by $^i\text{PrC}\equiv\text{CD}$ produced $\text{PhC}\equiv\text{CD}$ and $\text{U}-\text{C}\equiv\text{CPr}^i$ that reacted again with the aromatic alkyne yielding back $\text{U}-\text{C}\equiv\text{CPh}$ and $^i\text{PrC}\equiv\text{CH}$. The intermediate $\text{U}-\text{C}\equiv\text{CPr}^i$ was the fragment responsible for the formation of the *gem* unlabelled dimer when the aliphatic alkyne was present in excess. The absence of trimers was an indication that the protonolysis by the $\text{PhC}\equiv\text{CH/D}$ was much faster than any alkyne insertion, aromatic or aliphatic, into the metal-alkenyl complex.



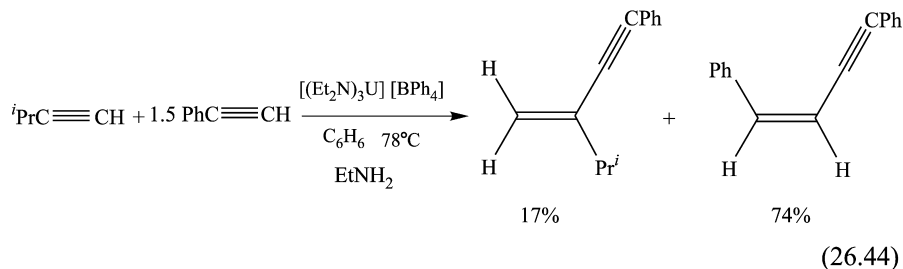
As mentioned above, when the bulkier alkyne $^t\text{Bu}\equiv\text{CH}$ was dimerized, the *cis* product was formed in addition to the *geminal* dimer [equation (26.31)]. Thus, in the codimerization of $^t\text{Bu}\equiv\text{CH}$ with $\text{PhC}\equiv\text{CH}$ [equation (26.42)], the

gem-codimer and the two dimers (*gem* and *cis*) of the aromatic alkyne were characterized as products. This result argued once more for the preferred formation of the aromatic metal–acetylide $U-C\equiv CPh$ into which both $tBuC\equiv CH$ or $PhC\equiv CH$ are able to insert. $PhC\equiv CH$ inserted in this codimerization with low regioselectivity and the protonolysis was found to be not as fast as the insertion, since mixtures of trimers of $PhC\equiv CH$ were also found in trace quantities.



To avoid the trimers and to allow a better regioselectivity a larger excess (two equivalent) of $tBuC\equiv CH$ and one equivalent of $PhC\equiv CH$ were used in the cross dimerization [equation (26.43)] producing the *gem*-codimer as the major isomer (83%), the *gem*-dimer of the aliphatic alkyne (12%), and small amounts of the codimer (5%). This result indicated again that the $U-C\equiv CPh$ moiety was the first intermediate formed. To this acetylide intermediate, $tBuC\equiv CH$ inserts preferentially in the head-to-tail manner to obtain the precursor of the codimer.

The effect of external amines in the cross dimerization of terminal alkynes with the cationic complex $[(\text{Et}_2\text{N})_3\text{U}][\text{BPh}_4]$ was investigated by the reaction of an excess of $PhC\equiv CH$ with $iPrC\equiv CH$ in the presence of EtNH_2 . The reaction generated low yields of the codimer $\text{CH}_2=\text{C}(iPr)\text{C}\equiv\text{CPh}$ (17%), as compared with the reaction without external amine, and remarkably the *cis* aromatic dimer, was the major product [equation (26.44)].

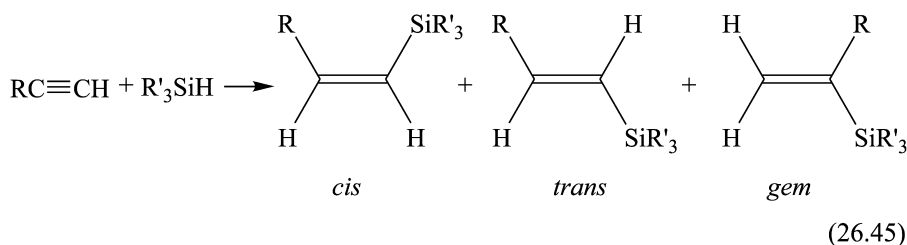


26.6 CATALYTIC HYDROSILYLATION OF OLEFINS

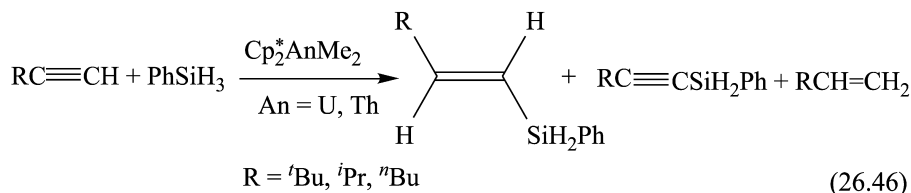
26.6.1 Catalytic hydrosilylation of terminal alkynes promoted by neutral organoactinides

The metal-catalyzed hydrosilylation reaction, which is the addition of a Si–H bond across a carbon–carbon multiple bond, is one of the most important reactions in organosilicon chemistry and has been studied extensively for half a century. The hydrosilylation reaction is used in the industrial production of organosilicon compounds (adhesives, binders, and coupling agents), and in research laboratories, as an efficient route for the syntheses of a variety of organosilicon compounds, silicon-based polymers, and new type of dendrimeric materials. The versatile and rich chemistry of vinylsilanes has attracted considerable attention in recent years as they are considered important building blocks in organic synthesis (Chan, 1977; Colvin, 1988; Fleming *et al.*, 1989).

The syntheses of vinylsilanes have been extensively studied and one of the most convenient and straightforward methods is the hydrosilylation of alkynes (Esteruelas *et al.*, 1993; Takeuchi and Tanouchi, 1994; Asao *et al.*, 1996). In general, hydrosilylation of terminal alkynes produces the three different isomers, *cis*, *trans*, and *geminal*, as a result of both 1,2 (*syn* and *anti*) and 2,1 additions, respectively, as shown in equation (26.45). The distribution of the products is found to vary considerably with the nature of the catalyst, substrates, and the specific reaction conditions.

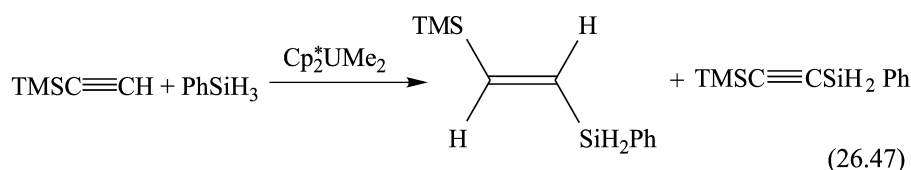
(a) Hydrosilylation of terminal alkynes: scope at room temperature by (C₅Me₅)₂AnMe₂ complexes

The room temperature reaction of (C₅Me₅)₂AnMe₂ (An = Th, U) with an excess of terminal alkynes RC≡CH (R = ^tBu, ⁱPr, ⁿBu) and PhSiH₃ resulted in the catalytic formation of the corresponding *trans*-vinylsilanes RCH = CHSiH₂Ph, the dehydrogenative silylalkyne RC≡CSiH₂Ph and alkenes RCH=CH₂ (R = ^tBu, ⁱPr, ⁿBu) [equation (26.46)] (Dash *et al.*, 1999).



Irrespective of the alkyl substituents and the metal center, the major product in the hydrosilylation reaction was the regio- and stereoselective *trans*-vinylsilane without any trace formation of the other two hydrosilylation isomers (*geminal* or *cis*). For bulky alkynes ($\text{'BuC}\equiv\text{CH}$), the product distribution was nearly the same for both catalytic systems, whereas for other terminal alkynes, it varies from one catalytic system to another. In the hydrosilylation reaction of the alkynes with $(\text{C}_5\text{Me}_5)_2\text{ThMe}_2$ and PhSiH_3 , similar amounts of the alkene and the silylalkyne were obtained. This result suggested a mechanistic pathway involving two organometallic complexes formed possibly in a consecutive manner, each species being responsible for each one of the products.

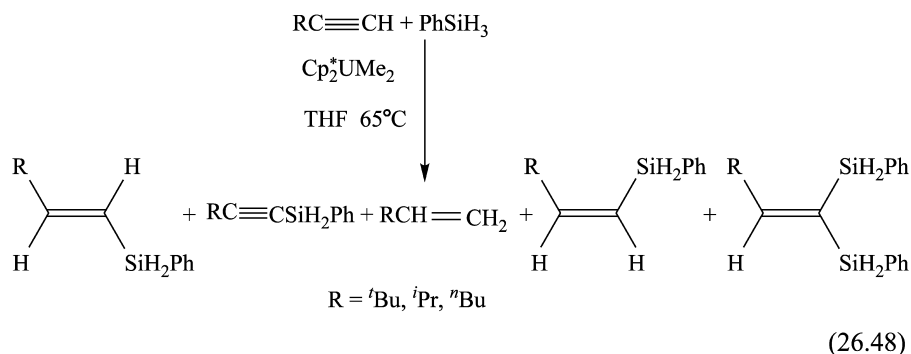
The reaction of $(\text{C}_5\text{Me}_5)_2\text{UMe}_2$ with $\text{TMSC}\equiv\text{CH}$ ($\text{TMS} = \text{Me}_3\text{Si}$) and PhSiH_3 was slow producing the *trans*- $\text{TMSCH} = \text{CHSiH}_2\text{Ph}$ and the silylalkyne $\text{TMSC}\equiv\text{CSiH}_2\text{Ph}$ respectively, whereas for the analogous $(\text{C}_5\text{Me}_5)_2\text{ThMe}_2$, no hydrosilylation or dehydrogenative coupling products were observed [equation (26.47)].



(b) Hydrosilylation of terminal alkynes: scope of catalysis at high temperature by $(\text{C}_5\text{Me}_5)_2\text{AnMe}_2$ complexes

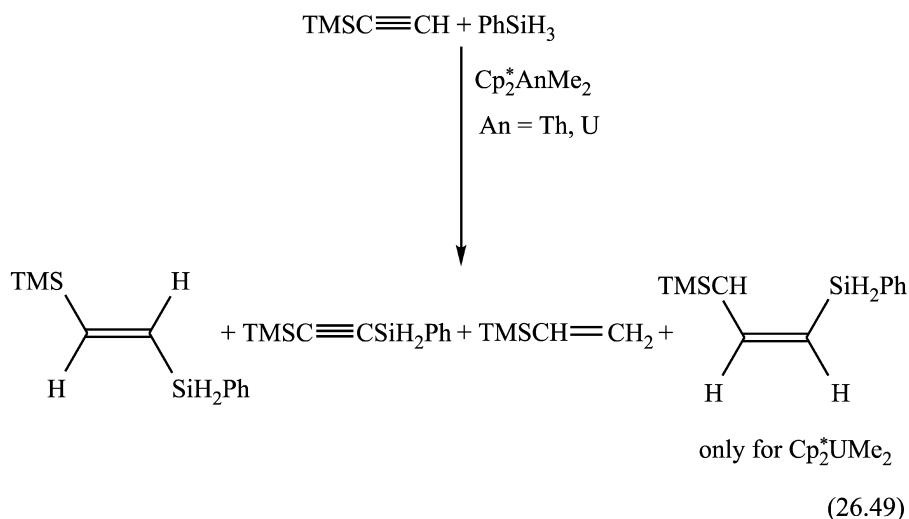
The chemoselectivity and the regioselectivity of the vinylsilanes formed in the organoactinide-catalyzed hydrosilylation of terminal alkynes with PhSiH_3 at high temperature ($65\text{--}78^\circ\text{C}$) were found to be diverse, as compared to the hydrosilylation results obtained at room temperature. The hydrosilylation of $\text{RC}\equiv\text{CH}$ ($\text{R} = \text{'Bu, 'Pr, "Bu}$) with PhSiH_3 catalyzed by $(\text{C}_5\text{Me}_5)_2\text{UMe}_2$, produced in addition to the hydrosilylation products at room temperature [equation (26.46)] the corresponding *cis*-hydrosilylated compounds, *cis*- $\text{RCH}=\text{CHSiH}_2\text{Ph}$, and small to moderate yields of the *unexpected* double hydrosilylation products $\text{RCH}=\text{C}(\text{SiH}_2\text{Ph})_2$ ($\text{R} = \text{'Bu, 'Pr, "Bu}$), in which the

two silyl moieties are attached to the same carbon atom [equation (26.48)] (Dash *et al.*, 1999).



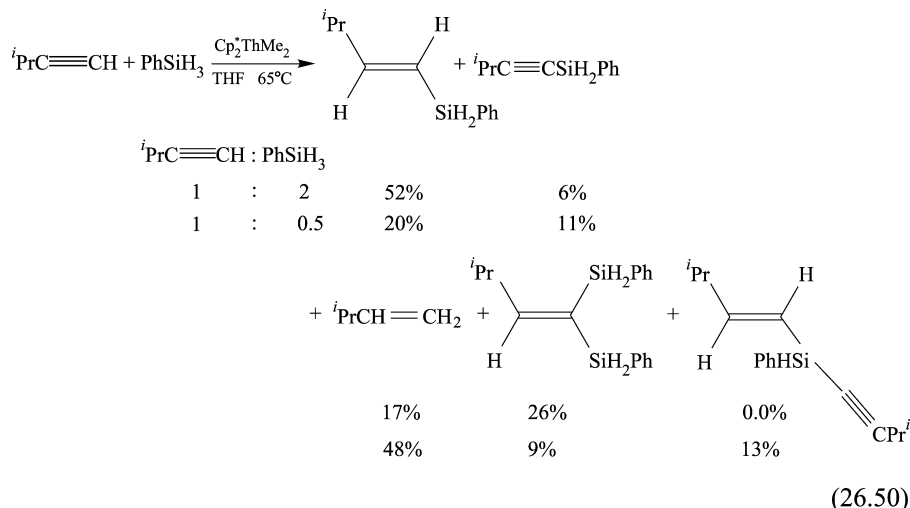
Whereas $(\text{C}_5\text{Me}_5)_2\text{UMe}_2$ catalyzed the hydrosilylation yielding a mixture of both *cis*- and *trans*-vinylsilane, remarkably, $(\text{C}_5\text{Me}_5)_2\text{ThMe}_2$ afforded only the *trans*-vinylsilane.

In the hydrosilylation reaction of $\text{TMSCH}\equiv\text{CH}$ with PhSiH_3 catalyzed by $(\text{C}_5\text{Me}_5)_2\text{UMe}_2$, besides the *trans*-vinylsilane and the silylalkyne products, which were also obtained at room temperature [equation (26.47)], the *cis*-vinylsilane and the olefin $\text{TMSCH}=\text{CH}_2$ were also observed [equation (26.49)]. For $(\text{C}_5\text{Me}_5)_2\text{ThMe}_2$, the same products as in the hydrosilylation reaction promoted by $(\text{C}_5\text{Me}_5)_2\text{UMe}_2$ were formed except for the *cis*-vinylsilane, in contrast to the room temperature reaction, in which no products were found.



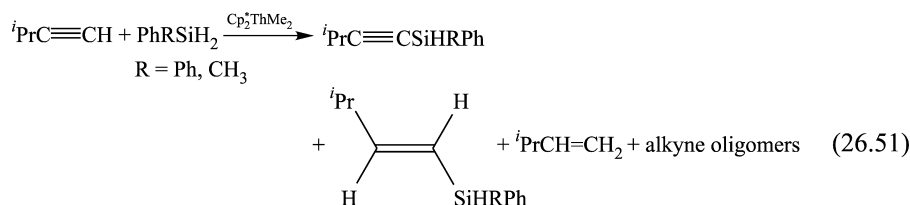
(c) Effect of the Ratio Alkyne:Silane and the Silane Substituent in the Hydrosilylation Reaction

The effect of PhSiH_3 on the formation of the different products was studied by performing comparative experiments. Large chemoselectivity and regioselectivity dependence of the products on the silane concentrations was observed [equation (26.50)].



When the hydrosilylation reaction was carried out using a 1:2 ratio of $\text{}^i\text{PrC}\equiv\text{CH}:\text{PhSiH}_3$ with $(\text{C}_5\text{Me}_5)_2\text{ThMe}_2$, the *trans*-vinylsilane was found to be the major product. When the reaction was conducted with the opposite ratio between the substrates ($\text{}^i\text{PrC}\equiv\text{CH}:\text{PhSiH}_3 = 0.5$), the olefin $\text{}^i\text{PrCH}=\text{CH}_2$ was found to be the major product, in addition to the other products (*trans*- $\text{}^i\text{PrCH}=\text{CHSiH}_2\text{Ph}$, $\text{}^i\text{PrC}\equiv\text{CSiH}_2\text{Ph}$, the double hydrosilylated olefin, and the tertiary silane *trans*- $\text{}^i\text{PrCH}=\text{CHSiH}(\text{Ph})(\text{C}\equiv\text{C}^i\text{Pr})$). The tertiary silane was obtained by the dehydrocoupling metathesis between the *trans*-alkenylsilane and the metal acetylide complex.

The replacement of a hydrogen atom on PhSiH_3 by either an alkyl or a phenyl group generated a reduction in the hydrosilylation reaction rate when compared to the rate obtained utilizing phenylsilane. The selectivities of the products were appreciably different when compared to those obtained using PhSiH_3 as the hydrosilylating agent [equation (26.51)].



(d) Kinetic studies on the hydrosilylation of $i\text{PrC}\equiv\text{CH}$ with PhSiH_3 catalyzed by $(\text{C}_5\text{Me}_5)_2\text{ThMe}_2$

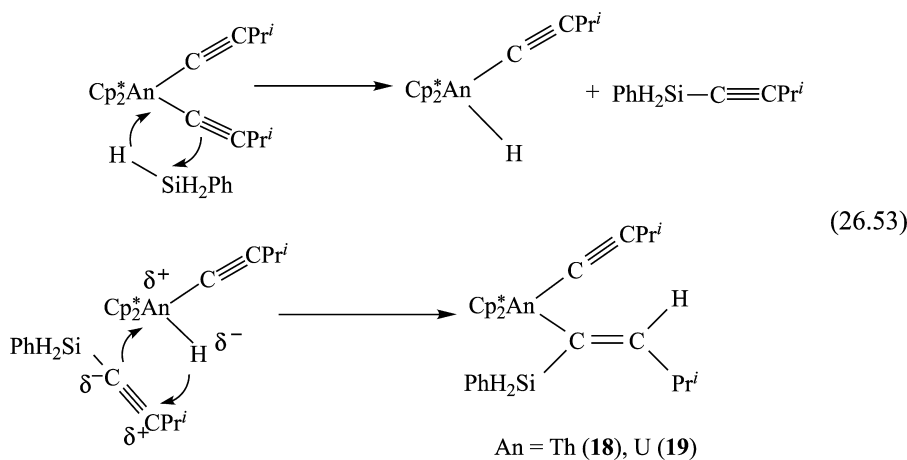
The kinetic study of the hydrosilylation of $i\text{PrC}\equiv\text{CH}$ with PhSiH_3 catalyzed by $(\text{C}_5\text{Me}_5)_2\text{ThMe}_2$ shows a first-order dependence in alkyne, silane, and catalyst. The empirical rate law expression for the $(\text{C}_5\text{Me}_5)_2\text{ThMe}_2$ catalyzed hydrosilylation of $i\text{PrC}\equiv\text{CH}$ with PhSiH_3 is given by equation 26.52.

$$v = k[i\text{PrC}\equiv\text{CH}][\text{PhSiH}_3][(C_5\text{Me}_5)_2\text{ThMe}_2] \quad (26.52)$$

From the Eyring analysis, the derived activation parameters, E_a , ΔH^\ddagger , and ΔS^\ddagger values are 6.9 (3) kcal mol⁻¹, 6.3(3) kcal mol⁻¹, and 51.1(5) eu, respectively.

(e) Formation of active species, mechanism, and thermodynamics in the hydrosilylation of alkynes

We have already seen that in the reaction of either bisacetylide organoactinide complex with PhSiH_3 the quantitative isolation of complexes **18** and **19**, for thorium and uranium, respectively, was observed [equation (26.4)]. These complexes were formed by the σ -bond metathesis with the silane forming the corresponding actinide hydrides and the silylalkyne, which rapidly reinsert producing **18** or **19** [equation (26.53)].



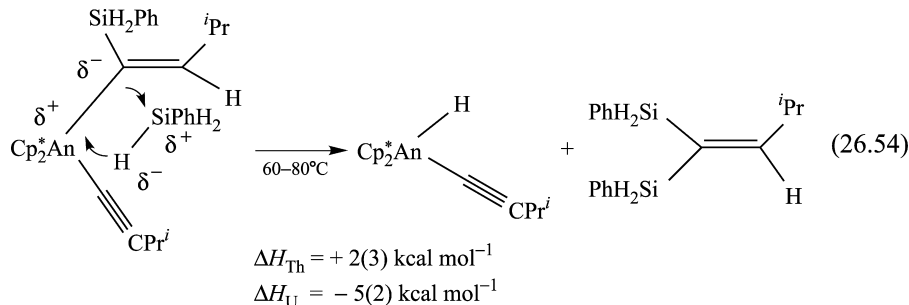
The regioselectivity of the insertion of $\text{PhSiH}_2\text{C}\equiv\text{CPr}^i$ into the actinide hydride bond is electronically favored, driven by the polarity of the organoactinides and the π^* orbital of the alkyne (Apeioig, 1989). In addition, since the insertion occurs through a four-center transition state mechanism, the *cis*-stereochemistry is expected, as corroborated by the H_2O poisoning experiment and the high-temperature reactions with alkyne or silane [equation (26.5)]. The same regioselective insertion of $\text{TMSC}\equiv\text{CH}$ into an organothorium

alkenyl complex Th–C bond was observed in the organoactinide-catalyzed oligomerization of alkynes (Straub *et al.*, 1995, 1999).

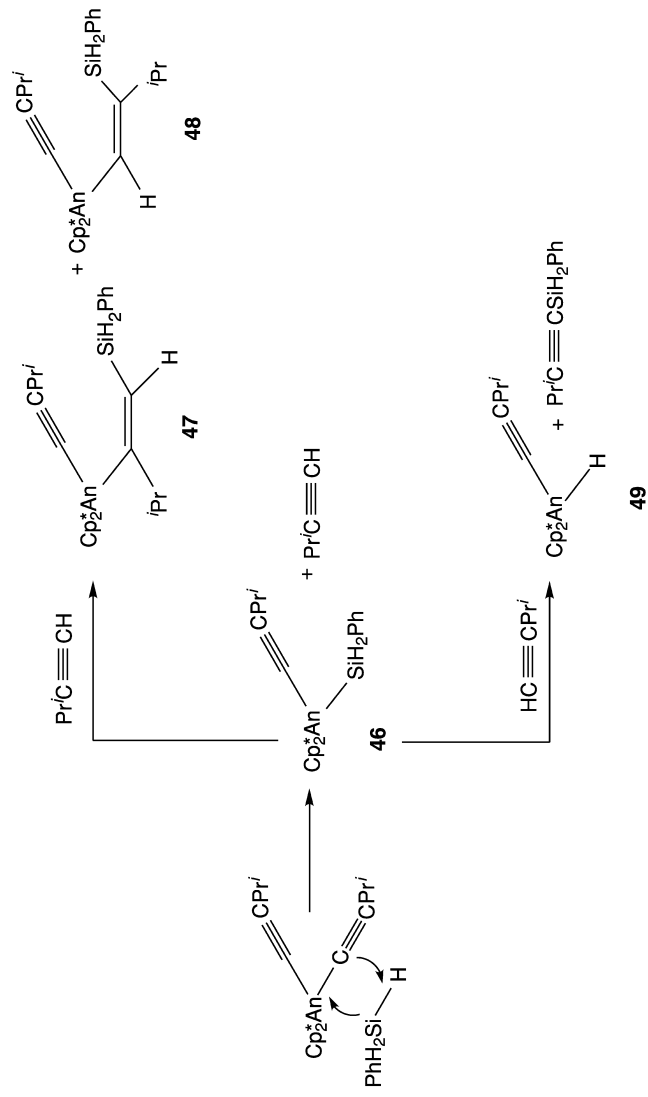
The formation of an organoactinide–silane intermediate **46** as described in Scheme 26.14 was shown to be not operative by the following experiments: (1) quenching experiments with water gave exclusively the *cis* vinylsilane; (2) under stoichiometric conditions, the addition of silane did not induce the protonolysis of the acetylide–alkenylsilane complex (**18** or **19**), to yield complex **46**; (3) no geminal hydrosilylated products were obtained (as would be expected were complex **48** an intermediate); (4) no *cis* hydrosilylated products can be obtained from complex **46**, and (5) no *cis* double hydrosilylated product was observed (if σ -bond metathesis occurred from complex **47** or **48**) (Dash *et al.*, 1999).

The reactions of complexes **18** or **19** yielding the double hydrosilylated product [equation (26.54)] were proposed to be stereoselectively favored, due to the assumed polarization of the PhSiH_3 towards the metal center, as well as the preferred thermodynamics, as compared to the protonolysis by the silane producing complex **46** and the *cis* hydrosilylated product ($\Delta H_{\text{Th}} = +15$ (4) kcal mol^{-1} ; $\Delta H_{\text{U}} = -3$ (2) kcal mol^{-1}).

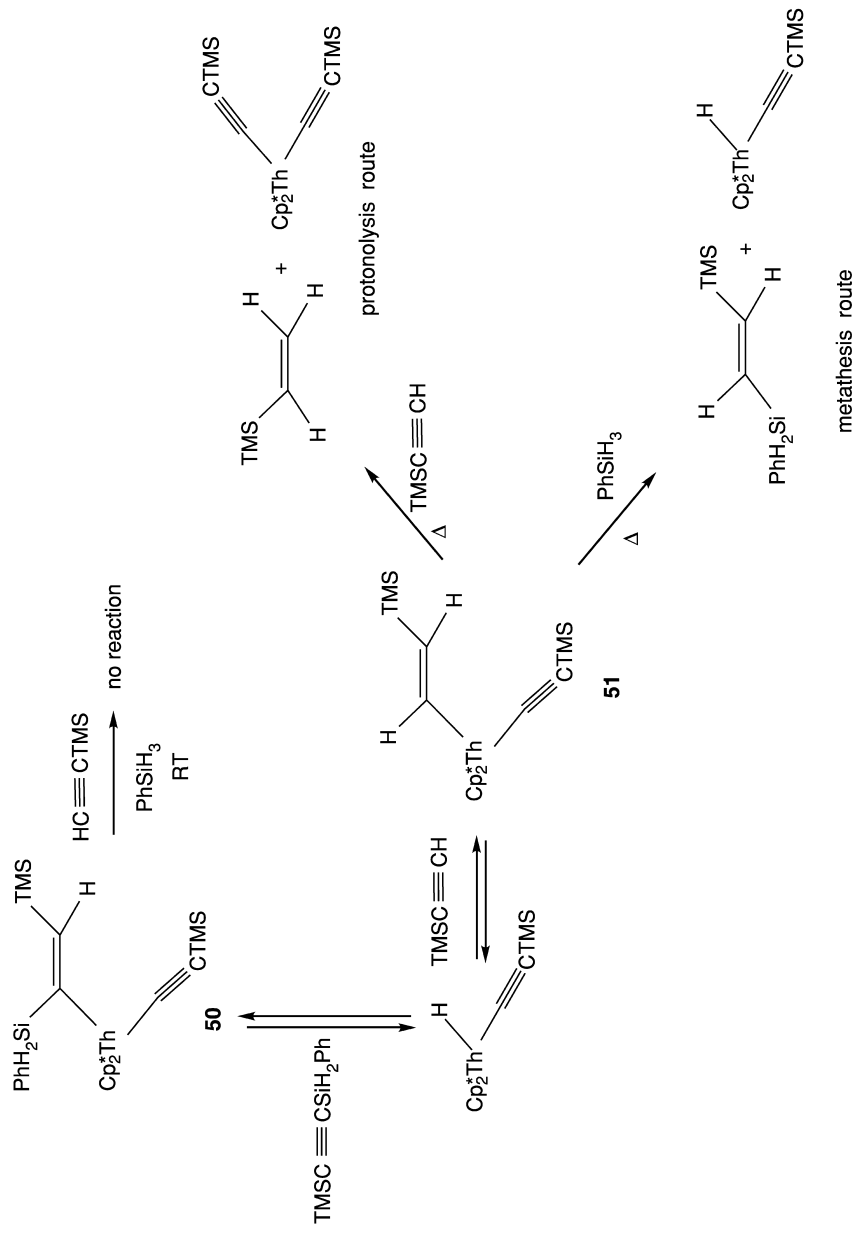
The most remarkable observation concerned the reaction products of complexes **18** or **19** with alkyne at either low or high temperatures. At elevated temperatures, the expected *cis*-hydrosilylated product was obtained, but at low temperatures, the unexpected *trans* isomer was achieved. These results have been explained through a competitive mechanism in which an equilibrium gives the different hydrosilylation products at different temperatures.



Different alkynes displayed different reactivities. $\text{TMSC}\equiv\text{CH}$ exhibited a total lack of reactivity with PhSiH_3 in the presence of $(\text{C}_5\text{Me}_5)_2\text{ThMe}_2$ at room temperature. However, at high temperature, the *trans* vinylsilane, the silylalkyne, and the alkene were obtained. This type of reactivity was explained, in general, as the result of a kinetic effect suggesting also an equilibrium between the organometallic complexes **50** and **51** (Scheme 26.15). Complex **51** was obtained by the insertion of the silylalkyne into a hydride complex. Complex **51** is able to react with another alkyne, yielding the alkene and the bis(acetylide) complex (protonolysis route) or react with a silane producing the organometallic hydride and the *trans*-product (σ -bond metathesis route). The low activity



Scheme 26.14 Expected organoacetylide intermediates in the stoichiometric hydrosilylation of terminal alkynes through a transient organoacetylide-silicon bond.



Scheme 26.15 Protonolysis and σ -bond metathesis routes for the high-temperature hydrosilylation of $\text{TMSC} \equiv \text{CH}$ with PhSiH_3 catalyzed by $(\text{C}_5\text{Me}_5)_2\text{ThMe}_2$.

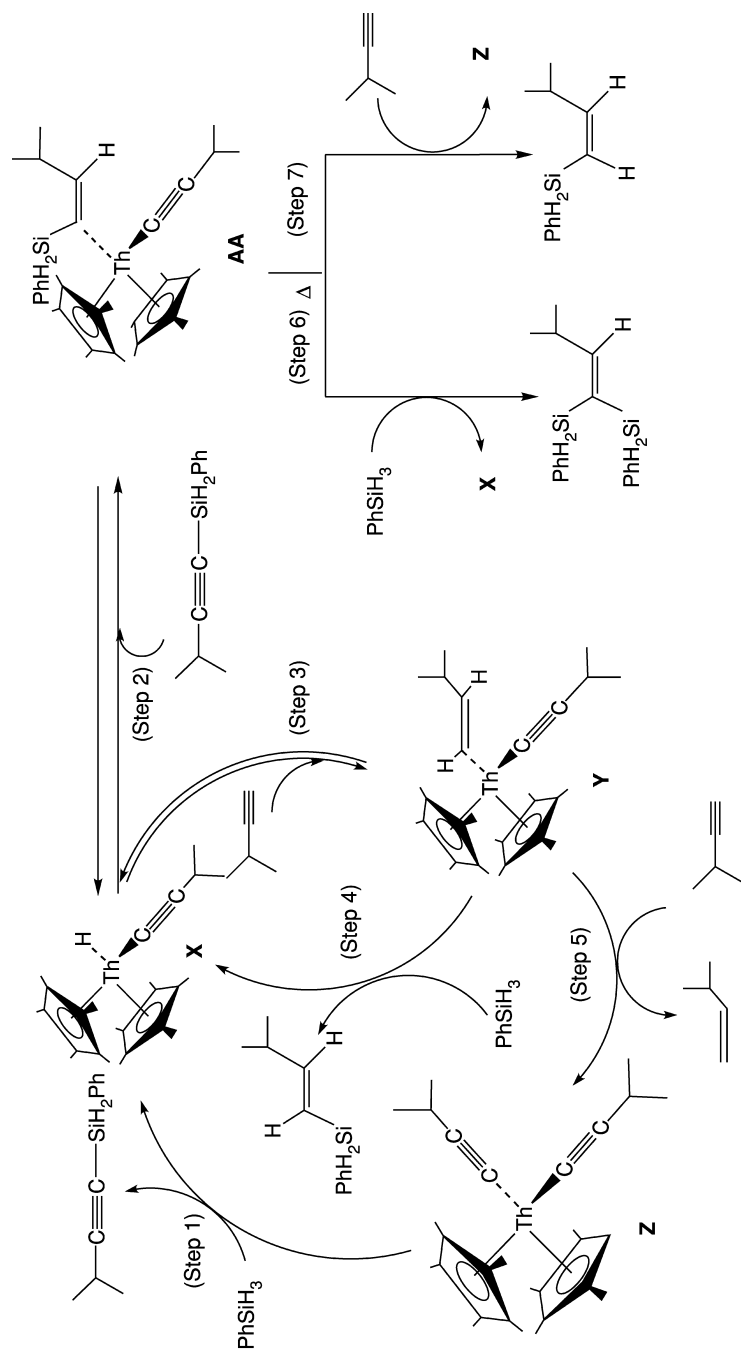
obtained for $\text{TMSC}\equiv\text{CH}$ was explained by an elevated activation energy to perform both the metathesis or protonolysis of complex **51**, as compared with other alkynes (Dash *et al.*, 1999).

The ratio between the silane and the alkyne were found to govern the kinetics leading to the different products. Thus, when the $\text{PhSiH}_3:\text{PrC}\equiv\text{CH}$ ratio was two, the *trans*- and the double-hydrosilylation products were the major products (metathesis route). Increasing the alkyne concentration routed the reaction towards the alkene and the bis(acetylide) complex (protonolysis route).

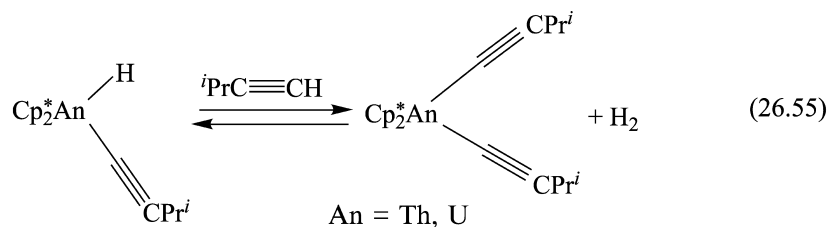
A likely mechanism for the hydrosilylation of terminal alkynes catalyzed by $\text{Cp}_2^*\text{ThMe}_2$ was proposed and described in Scheme 26.16.

The mechanism presented in Scheme 26.16 consists of insertion of acetylene into a metal-hydride σ -bond, σ -bond metathesis by a silane, and protonolysis by an acidic alkyne hydrogen. The precatalyst $(\text{C}_5\text{Me}_5)_2\text{ThMe}_2$ in the presence of alkyne was converted to the bis(acetylide) complex **Z**. Complex **Z** reacts with PhSiH_3 towards the silylalkyne and the organoactinide hydride **X** (step 1), which was found to be in equilibrium with the intermediate **AA** after reinsertion of the silylalkyne with the preferential stereochemistry (step 2). Complex **AA** was found to be the principal complex under silane and alkyne starvation. Complex **X** will react with an alkyne producing the alkenyl acetylide organothorium complex **Y** (step 3), which is presumably in equilibrium with complex **X** (first-order in alkyne). Complex **Y** was proposed to react with PhSiH_3 , as the rate-determining step, regenerating the hydride complex **X** and the *trans*-hydrosilylated product (step 4). Under the catalytic conditions, complex **Y** may also react with a second alkyne producing the alkene and the bis(acetylide) complex **Z** (step 5). A similar insertion of the alkene into complex **X** with the concomitant reaction with an additional alkyne produced the double hydrogenated product, as found for isopropylacetylene. At high temperature, complex **AA** may react with a silane (step 6), yielding complex **X** and the double hydrosilylation product or with an alkyne (step 7), yielding complex **Z** and the *cis*-isomer. Thus, the reaction rate law [equation (26.52)] was rationalized with rapid irreversible phenylsilane metathesis with complex **Z**, rapid pre-equilibrium involving the hydride, and alkenyl complexes **X** and **Y**, and a slow metathesis by the PhSiH_3 . For the thorium complex, step 6 was found to be much faster than step 7 since the amounts of the *cis*-product were obtained in trace amounts.

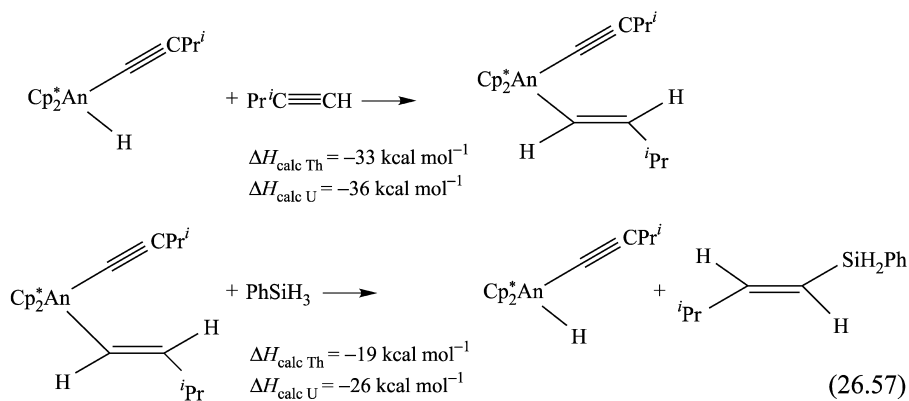
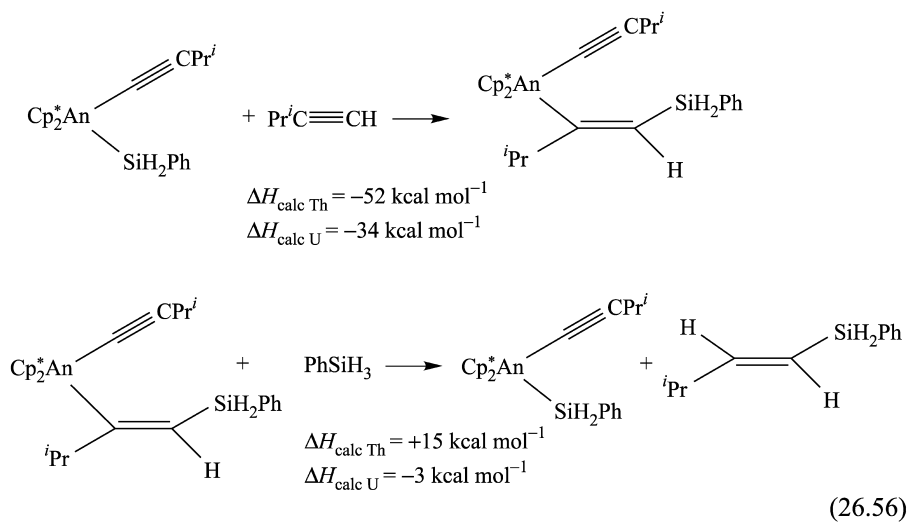
The mechanistic pathway as proposed, takes into the account comparable yields for the alkene and silylalkyne even when the alkyne concentration was in excess (the sum of the silylated products must equal the amount of the alkene). For the thorium or uranium complexes, the amount of the hydrosilylated product was always similar to or larger than that of the alkene, indicating that a competing equilibrium should be operative, responsible for the transformation of the hydride complex back to the bisacetylide complex, allowing the production of the silylalkyne without producing the alkene [equation (26.55)].



Scheme 26.16 Proposed mechanism for the room- and high-temperature hydroosilylation of isopropylacetylene with PhSiH_3 promoted by $(\text{C}_5\text{Me}_5)_2\text{ThMe}_2$.



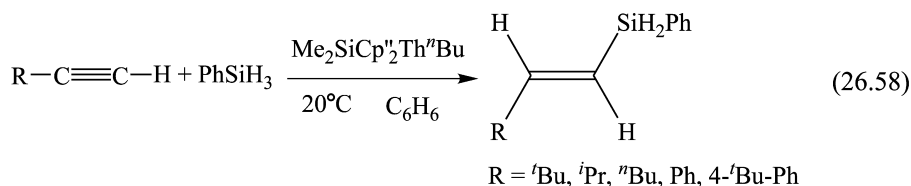
Thermodynamically, it is very interesting to compare the possible mechanistic silane and hydride intermediates towards the possible hydrosilylation *trans*-product as presented in equations (26.56) and (26.57), respectively.



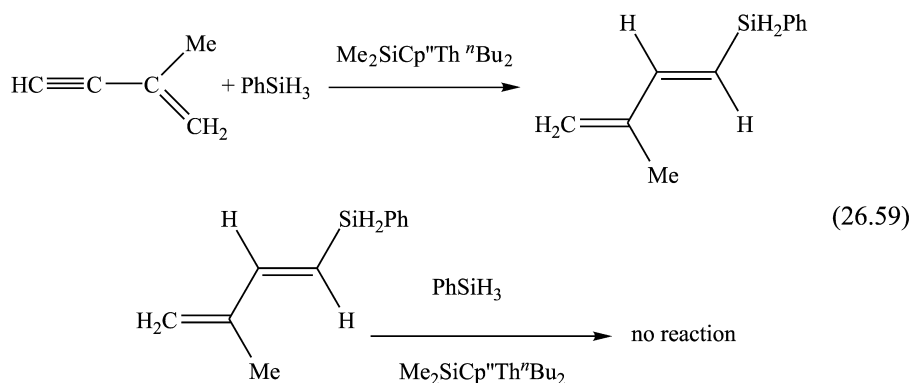
The calculated enthalpy of reaction for the insertion of an alkyne into an actinide–silane bond [equation (26.56)] ($\Delta H_{\text{Th}} = -52 \text{ kcal mol}^{-1}$, $\Delta H_{\text{U}} = -34 \text{ kcal mol}^{-1}$) or into an actinide hydride bond [equation (26.57)] ($\Delta H_{\text{Th}} = -33 \text{ kcal mol}^{-1}$, $\Delta H_{\text{U}} = -36 \text{ kcal mol}^{-1}$) was expected to be exothermic. However, the protonolysis by the silane yielding the An–Si bond and the *trans*-product [equation (26.56)] was for thorium an endothermic process ($\Delta H_{\text{Th}} = +15 \text{ kcal mol}^{-1}$), as compared to the exothermicity of the σ -bond metathesis [equation (26.57)] of the thorium alkenyl complex with the silane ($\Delta H_{\text{Th}} = -19 \text{ kcal mol}^{-1}$), yielding the corresponding Th–H bond and the *trans*-product. For the corresponding uranium complexes, the latter processes were calculated to be exothermic although the σ -bond metathesis route [equation (26.57)] was more exothermic ($\Delta H_{\text{U}} = -26 \text{ kcal mol}^{-1}$) than the protonolysis route [equation (26.56)] ($\Delta H_{\text{U}} = -3 \text{ kcal mol}^{-1}$).

26.6.2 Catalytic hydrosilylation of terminal alkynes promoted by the bridged complex $\text{Me}_2\text{SiCp}''\text{Th}''\text{Bu}_2$

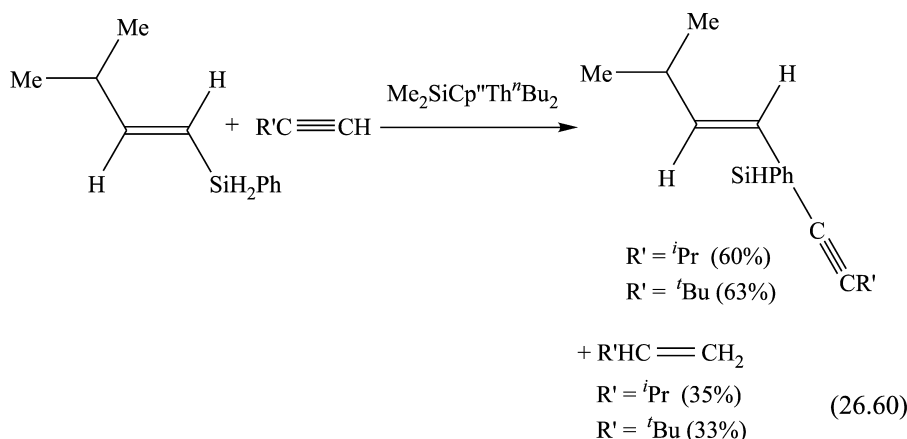
The hydrosilylation reaction of terminal alkynes and PhSiH_3 catalyzed by $\text{Me}_2\text{SiCp}''\text{Th}''\text{Bu}_2$ resulted in the speedy and regioselective formation of the hydrosilylated *trans*-vinylsilane as the unique product regardless of the alkyne substituent [equation (26.58)].



When an olefin-functionalized alkyne was used for the reaction with PhSiH_3 , the alkyne moiety was regioselectively hydrosilylated to yield the corresponding *trans*-diene [equation (26.59)]. Addition of an excess of PhSiH_3 did not induce any subsequent hydrosilylation.



The addition of an excess of PhSiH_3 to any of the vinylsilane products did not induce further hydrosilylation. However, addition of a second equivalent of an alkyne to a hydrosilylation product allowed the formation of the corresponding alkene and the dehydrogenative coupling of the alkyne with the *trans*-vinylsilane [equation (26.60)] (Forsyth *et al.*, 1991; Harrod, 1991; Corey *et al.*, 1993; Tilley, 1993).



(a) Kinetic and thermodynamic studies for the hydrosilylation of terminal alkynes with primary silanes promoted by the bridged complex $\text{Me}_2\text{Si}(\text{C}_5\text{Me}_4)_2\text{Th}''\text{Bu}_2$

Kinetic measurements on the hydrosilylation $i\text{PrC}\equiv\text{CH}$ with PhSiH_3 catalyzed by $\text{Me}_2\text{Si}(\text{C}_5\text{Me}_4)_2\text{Th}''\text{Bu}_2$ indicated that the reaction behaved with a first-order dependence in precatalyst and silane, and exhibited an inverse proportionality (inverse first-order) in alkyne [equation (26.61)]. The inverse proportionality was consistent with a rapid equilibrium before the turnover limiting-step, removing one of the key organoactinide intermediates from the catalytic cycle.

$$v = k[\text{Me}_2\text{Si}(\text{C}_5\text{Me}_4)_2\text{Th}''\text{Bu}_2][\text{silane}]^1[\text{alkyne}]^{-1} \quad (26.61)$$

The derived ΔH^\ddagger and ΔS^\ddagger parameter values from a thermal Eyring analysis were measured to be $10.07(5) \text{ kcal mol}^{-1}$ and $-22.06(5) \text{ eu}$, respectively (Dash *et al.*, 2001).

It is important to note the difference between the kinetic behavior of the alkyne in the hydrosilylation reaction and that in the dimerization process (*vide supra*). In the latter process, the alkyne was involved in two parallel routes, both sensitive to the alkyne concentration. In one route, the alkyne exhibited an inverse kinetic order (removing one of the active compounds from catalytic cycle), whereas in the second pathway the alkyne was involved in the rate-determining step. Thus, at high alkyne concentrations the overall dependence

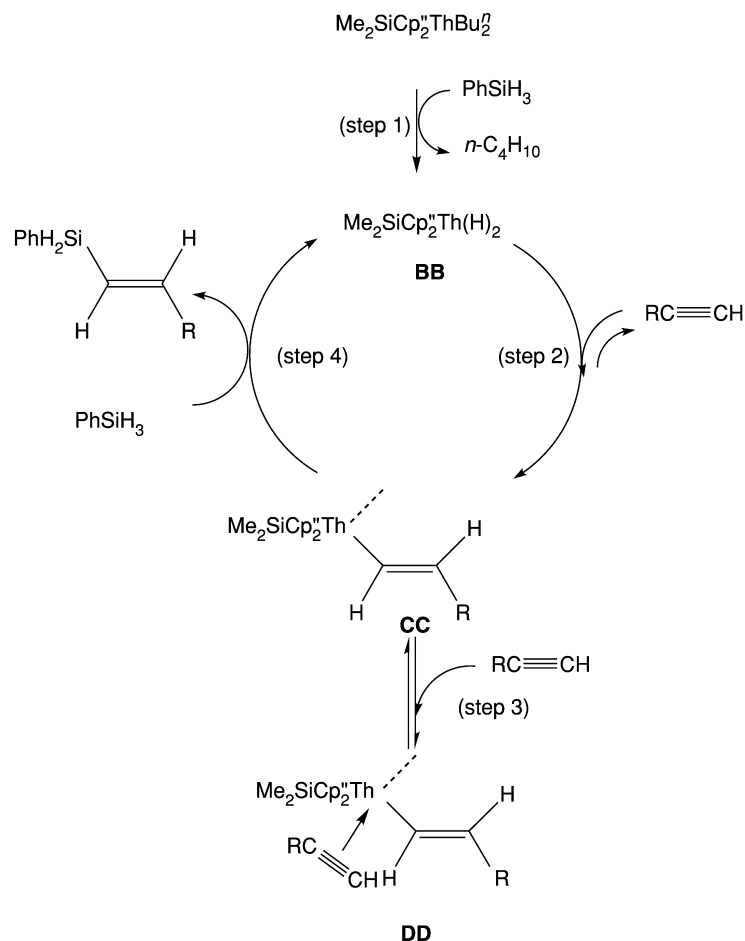
on alkyne is cancelled out. In the hydrosilylation process, the alkyne was proposed to be only involved in routing an active compound out of the catalytic cycle, with the silane presumably reacting in the rate-limiting step. Thus, modification of the alkyne order was observed.

In the hydrosilylation reactions of organo-f-element complexes, two Chalk–Harrod mechanisms have been proposed as plausible routes, differing in the inclusion of a σ -bond metathesis instead of the classical oxidative addition–reductive elimination processes. The two mechanisms differ in the reactive intermediates; the hydride (M–H) route and the silane (M–SiR₃) route (Chalk and Harrod, 1965; Harrod and Chalk, 1965; Ruiz *et al.*, 1987; Seitz and Wrighton, 1988; Tanke and Crabtree, 1991; Duckett and Perutz, 1992; Marciniak *et al.*, 1992; Takeuchi and Yasue, 1996; Bode *et al.*, 1998; Ojima *et al.*, 1998; Reichl and Berry, 1998; Sakaki *et al.*, 1998). The use of terminal alkynes with bridged organoactinides was an excellent probe to investigate which of the two routes was the major pathway followed. Thus, taking into account that the alkyne was expected to insert with the substituent group pointing away from the metal center (as observed in the dimerization) the following mechanistic insights were obtained. If the hydrosilylation reaction goes through a M–SiR₃ intermediate, the *gem*-hydrosilylated vinyl isomer will be formed, whereas only the *trans*-isomer will be obtained via the M–H route (if the insertion stereochemistry is not maintained, the *cis* product will be observed). The exclusive selectivity obtained for Me₂Si(C₅Me₄)₂ThⁿBu₂ towards the *trans* hydrosilylated isomer argued that the hydride route was acting as the major mechanistic pathway.

(b) Hydrosilylation of terminal alkynes with primary silanes promoted by the bridged complex Me₂Si(C₅Me₄)₂ThⁿBu₂: scope and mechanism

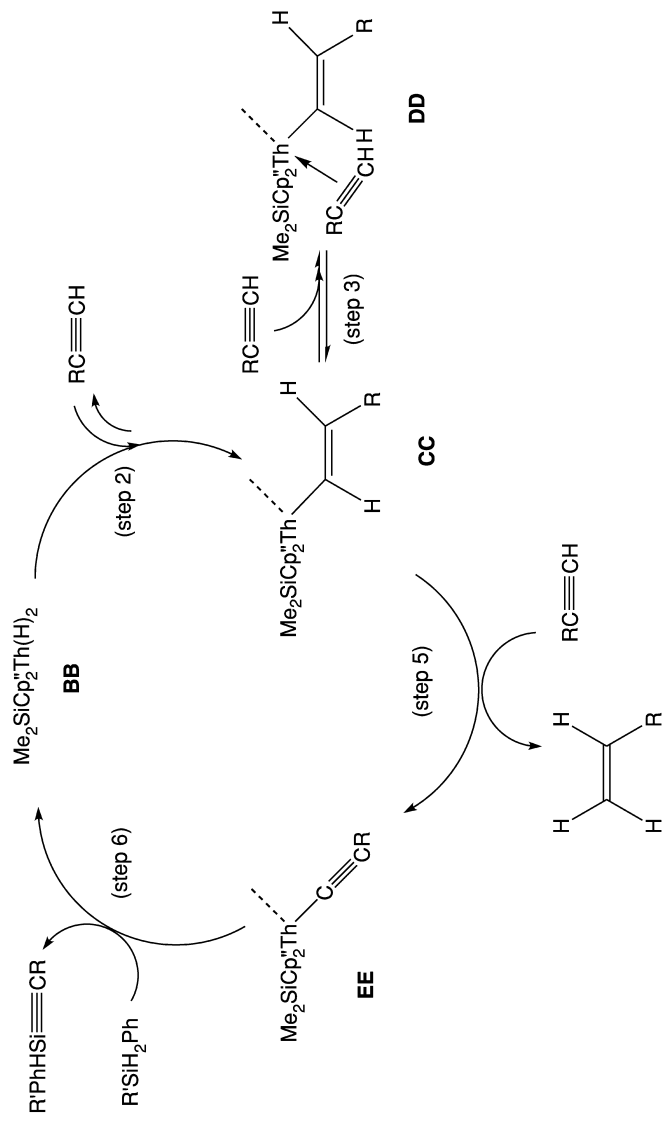
The hydrosilylation of terminal alkynes with PhSiH₃ promoted by the bridged complex Me₂Si(C₅Me₄)₂ThⁿBu₂ produced regioselectively and chemoselectively the *trans*-hydrosilylated vinylsilane without any other by-products. The lack of silylalkynes, the dehydrogenative silane coupling products, or any other geometrical isomer of the vinylsilane strongly indicated that the Th–H pathway was the major operative route in the hydrosilylation reaction. A plausible mechanism for the hydrosilylation of terminal alkynes towards *trans*-vinylsilanes was proposed and is presented in Scheme 26.17.

The precatalyst Me₂Si(C₅Me₄)₂ThⁿBu₂ in the presence of silane and alkyne was converted into the hydride complex **BB** (step 1), as observed by the stoichiometric formation of *n*-BuSiH₂Ph. Rapid insertion of an alkyne into complex **BB** allows the formation of the vinylic complex **CC** (step 2). Complex **CC** was found to be in rapid equilibrium with the proposed π -complex **DD** (step 3), responsible for the inverse order in alkyne, and undergoes a σ -bond metathesis with PhSiH₃, as the rate-determining step (step 4), producing selectively the *trans*-hydrosilylated vinyl product and regenerating complex **BB**. Since no



Scheme 26.17 Proposed mechanism for the hydrosilylation of terminal alkynes with PhSiH_3 promoted by the bridged complex $\text{Me}_2\text{Si}(\text{C}_5\text{Me}_4)_2\text{Th}^n\text{Bu}_2$.

geometrical isomers or different products were observed by adding an excess of PhSiH_3 to any of the vinylsilanes, neither the hydride complex **BB** nor the alkenyl complex **CC** were found to be the resting catalytic state, indicating complex **DD** is the resting state. However, the subsequent addition of a second equivalent of an alkyne to the reaction mixture formed the corresponding alkene and the silylalkyne. The formation of these two compounds was proposed to follow the mechanistic pathway as shown in Scheme 26.18. Complex **CC** reacts, in the absence of a primary silane, with another alkyne (step 5) producing the corresponding alkene and the acetylide complex **EE**. A σ -bond metathesis with the Si–H bond of the vinylsilane (step 6) formed the



Scheme 26.18 Proposed mechanism for the formation of alkene and silylalkyne in the presence of vinylsilanes and terminal alkynes promoted by $\text{Me}_2\text{Si}(\text{C}_5\text{Me}_4)_2\text{Th}^t\text{Bu}_2$. Only one of the equatorial ligations at the metal center is shown for clarity.

dehydrogenative coupling product and regenerated the hydride complex **BB** (Dash *et al.*, 2001).

The yield of the alkene was found to be lower than that of the silylalkyne product. Therefore, an additional equilibrium reaction was proposed to exist, responsible for the transformation of complex **BB** into the acetylide complex **EE**, allowing the formation of the silylalkyne without forming the alkene. This pathway was also observed for non-bridged organoactinides [equation (26.55)] (Dash *et al.*, 1999, 2001). Examination of the measured rates of the hydrosilylation process catalyzed by the bridged complex revealed larger turnover frequencies as compared to $(C_5Me_5)_2YCH_3 \cdot THF$ or other lanthanide complexes (Schumann *et al.*, 1999). The yttrium complex was found to induce the hydrosilylation reaction of internal alkynes preferentially towards the *E*-isomer, although in some case the *Z*-isomer was found in comparable amounts. Mechanistically, the active species for the yttrium hydrosilylation of internal alkynes was proposed to be the corresponding hydride (Molander and Knight, 1998). It is well known that the hydrosilylation of alkynes is induced either by radical initiators (Selin and West, 1962) or by transition metal catalysts (Weber, 1983; Hiyama and Kusumoto, 1991; Sudo *et al.*, 1999). The radical procedure often provides a mixture of *trans*- and *cis*-hydrosilylation products. In contrast, the transition metal catalyzed reaction proceeds with high stereoselectivity via a *cis*-hydrosilylation pathway usually producing a mixture of two regio-isomers (terminal and internal adducts). Thus, the organoactinide process seems to contain a unique chemical environment allowing the production of the *trans*-vinylsilane, complementing the chemistry of other transition metal complexes.

26.6.3 Catalytic hydrosilylation of alkenes promoted organoactinide complexes

The organoactinide complexes $(C_5Me_5)_2ThMe_2$ and $Me_2Si(C_5Me_4)_2Th^tBu_2$ were also found to be good precatalysts for the highly regio-selective hydrosilylation of alkenes. The chemoselectivity of the reactions was moderate since the hydrogenated alkane was always encountered as a concomitant product. The reactions of $(C_5Me_5)_2ThMe_2$ and $Me_2Si(C_5Me_4)_2Th^tBu_2$ with an excess of an alkene and $PhSiH_3$ resulted in the formation of the regioselective 1,2-addition hydrosilylated alkene and the alkane with no major differences between the two organoactinides [equation (26.62)] and Table 26.1 (Dash *et al.*, 2001).

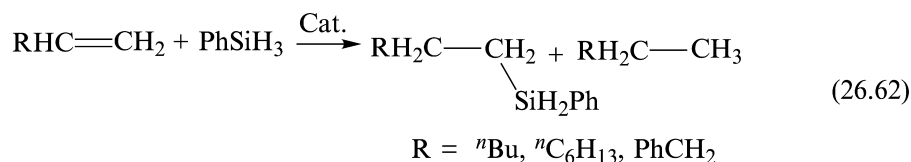


Table 26.1 Activity data for the hydrosilylation of alkenes promoted by $(C_5Me_5)_2ThMe_2$ and $Me_2Si(C_5Me_4)_2Th^iBu_2$.^a

Entry	Cat. ^b	R in RHC=CH	Temperature (°C)	Time (h)	Yield of 1-silylalkane (%)	Yield of alkane (%)	NT ^c (h ⁻¹)
1	NB	ⁿ Bu	20	12	54	44	1.5
2	B	ⁿ Bu	20	12	63	35	5.5
3	NB	ⁿ Bu	78	6	57	41	3.2
4	B	ⁿ Bu	78	1	62	36	64.5
5	NB	ⁿ C ₆ H ₁₃	20	12	68	30	1.9
6	B	ⁿ C ₆ H ₁₃	20	12	65	33	4.6
7	NB	PhCH ₂	78	6	61	38	4.8
8	B	PhCH ₂	78	1	71	29	83.1
9	NB	Ph	78	36	65(6) ^d	28	0.9
10	B	Ph	78	36	31(30) ^d	37	1.9

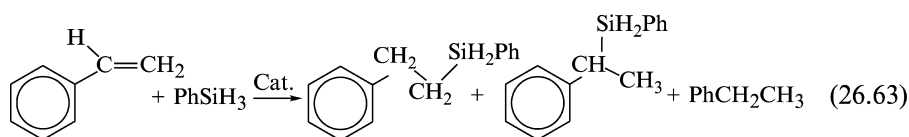
^a Solvent = benzene.

^b B = $Me_2Si(C_5Me_4)_2Th^iBu_2$, NB = $(C_5Me_5)_2ThMe_2$.

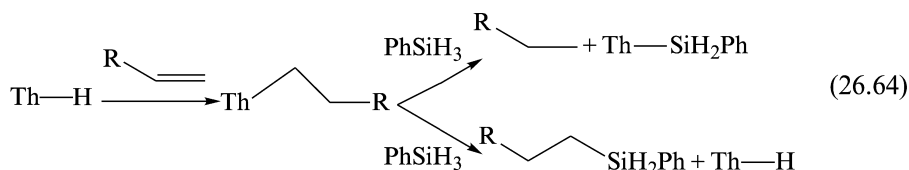
^c Turnover frequency for the hydrosilylation process.

^d The number in parentheses corresponds to the 2,1-addition hydrosilylation product, 2-(phenylsilyl)ethylbenzene.

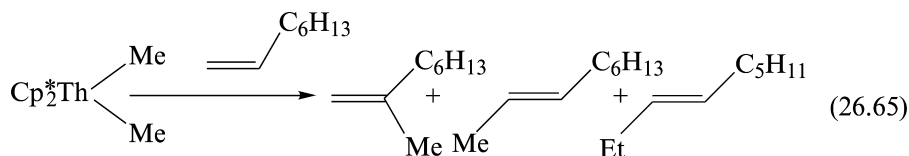
Since for the substrate allyl benzene only one hydrosilylated product was formed, a comparison of the effect of distance between the aromatic ring and the metal center was performed. In the hydrosilylation of styrene with each of the organoactinides [equation (26.63)], both 1,2- and 2,1-hydrosilylation products were obtained, in addition to ethylbenzene. For $(C_5Me_5)_2ThMe_2$, a small amount of the branched silane was obtained whereas for the coordinatively unsaturated complex $Me_2Si(C_5Me_4)_2Th^rBu_2$ equal amounts of both (linear and branched) isomers were found (entries 9,10 in Table 26.1).



The presence of the two major products (hydrosilylation and hydrogenation) indicated the existence of two parallel catalytic pathways. The formation of the hydrogenation products required considering the possibility that intermediates with Th–Si/Th–H bonds were formed [equation (26.64)]. Thus, the production of alkanes might be considered, to some extent, as indirect evidence of the existence of complexes containing an actinide–Si bond. Protonolysis of a Th–alkyl by the silane will yield the Th–Si bond and the hydrogenation product, whereas metathesis of the Th–alkyl by the silane will produce the hydrosilylated compound regenerating the hydride complex.



Another pathway to obtain a hydrogenation product from a Th–alkyl complex may be proposed, consisting of cutting the alkyl chain with an additional alkene, forming a transient vinyl complex. Therefore, the reaction between $(C_5Me_5)_2ThMe_2$ and an excess of 1-octene was studied. Although no hydrogenation product was observed, ruling out the protonolysis by an alkene, a stoichiometric reaction, resulting in the production of 2-methyl-1-octene, 2-nonene, and 3-nonene in almost equal amounts, and the additional slow catalytic isomerization of the starting 1-octene to *E*-4-octene (3.8%), *E*-3-octene (39.4%), *E*-2-octene (13.0%), and *Z*-2-octene (41.8%), was observed [equation (26.65)] (Dash *et al.*, 2001).



This result indicated that the Th–Me bond underwent insertion by the alkene moiety, forming a Th–alkyl complex, followed by a β -hydrogen elimination to the corresponding metal–hydride (Th–H) and equimolar amounts of all three isomeric nonenes. The hydride was proposed to be the active species in the isomerization of 1-octene. The same reaction with 2-octene showed a slower reaction and different product ratios (*E*-3-octene (11.2%), *E*-2-octene (82.2%), and *Z*-2-octene (6.6%)), indicating a non-equilibrium process between 1-octene and 2-octene. In order to study the resting state of the organoactinide catalyst given that only two complexes with either a thorium hydride (Th–H) or a thorium–alkyl (Th–R) were expected, the isomerization reaction was followed until full conversion of 1-octene (>98%) was obtained. All the volatiles were removed under vacuum and new solvent was reintroduced. The ratio between the products that remained in the reaction mixture was measured by gas chromatography, demonstrating the disappearance of 1-octene. Quenching of the reaction mixture with a slight excess of D₂O at low temperatures, and analysis of the solution showed the presence of a mono-deuterated 1-*d*-octane, indicating that the Th–alkyl moiety was the resting organoactinide. The most astounding result was the presence of equimolar amounts of 1-octene, based on the metal complex. This result indicated that a π -alkene thorium–alkyl complex (HH in Scheme 26.19) was the resting catalytic state of the organoactinide complex; addition of D₂O liberated the alkene and the alkane from the metal.

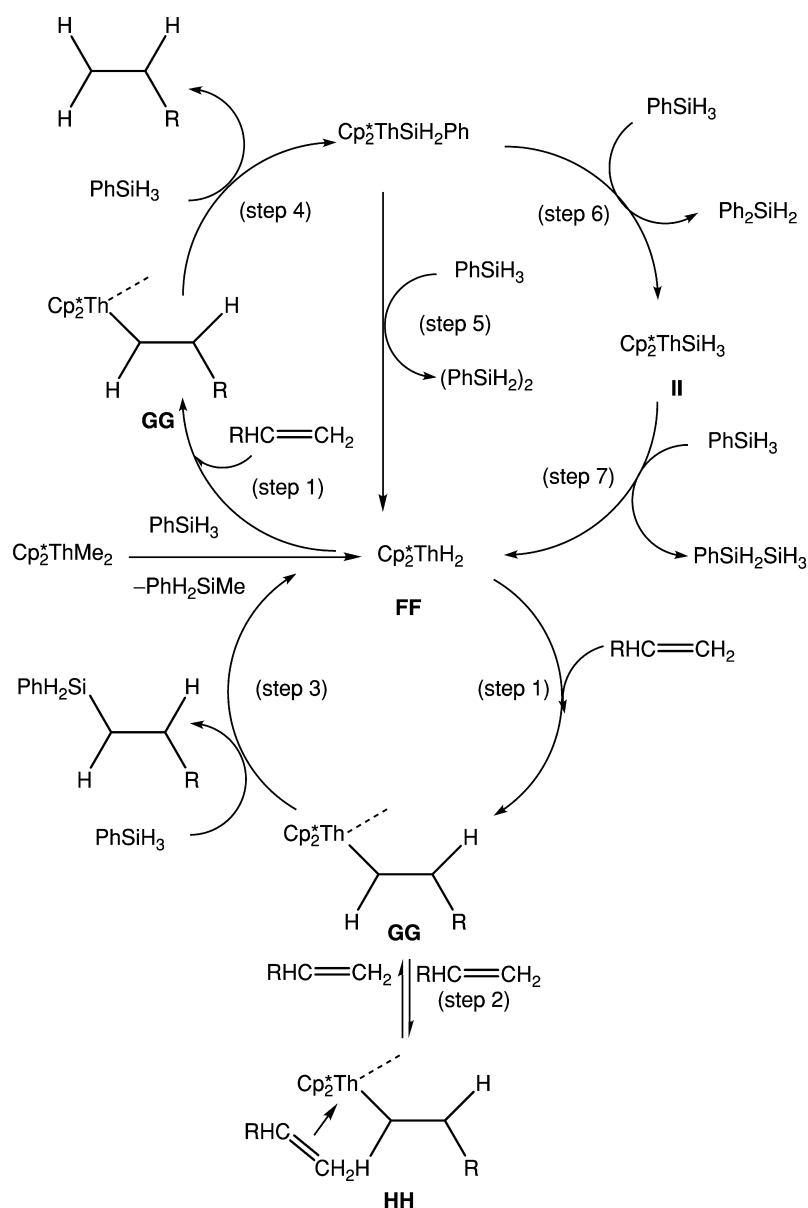
(a) Kinetic studies of the hydrosilylation of alkenes with PhSiH₃

Kinetic measurements of the hydrosilylation of allylbenzene with PhSiH₃ catalyzed by (C₅Me₅)₂ThMe₂ were performed. The reaction was found to follow a first-order dependence in precatalyst and silane, and exhibits an inverse first-order dependence in alkene. The inverse proportionality as described for alkynes is consistent with a rapid equilibrium before the rate-determining step, steering an intermediate out of the catalytic cycle. Thus, the rate law for the hydrosilylation of alkenes with PhSiH₃ promoted by (C₅Me₅)₂ThMe₂ can be expressed as presented in the following equation:

$$v = k[(C_5Me_5)_2ThMe_2][silane]^1[alkene]^{-1} \quad (26.66)$$

The derived E_a , ΔH^\ddagger , and ΔS^\ddagger parameter values from an Arrhenius and a thermal Eyring analysis were measured to be 11.0(4) kcal mol⁻¹, 10.3(4) kcal mol⁻¹, and –45 eu, respectively.

A comparison of the product distribution for both bridged and non-bridged organoactinides revealed that no special effects were introduced by increasing the coordinative unsaturation of the organothorium complex. The presence of double hydrosilylation products suggested the presence of two parallel interconnecting competing pathways. The formation of the alkane required the presence of the intermediate Th–H/Th–Si moieties (Eisen, 1997, 1998). The only evidence available so far for the formation of a Th–Si bond was obtained



Scheme 26.19 Proposed mechanism for the hydrosilylation of alkenes with PhSiH_3 promoted by $(\text{C}_5\text{Me}_5)_2\text{ThMe}_2$ or $\text{Me}_2\text{Si}(\text{C}_5\text{Me}_4)_2\text{Th}^n\text{Bu}_2$. The scheme depicts the mechanism for the unbridged metallocene. Only one of the equatorial ligations at the metal center is shown for clarity.

from the formation of a metalloxy ketene via the double insertion of carbon monoxide into a Th–Si bond (Radu *et al.*, 1995). The proposed mechanism for the hydrosilylation of alkenes promoted by organoactinides is described in Scheme 26.19.

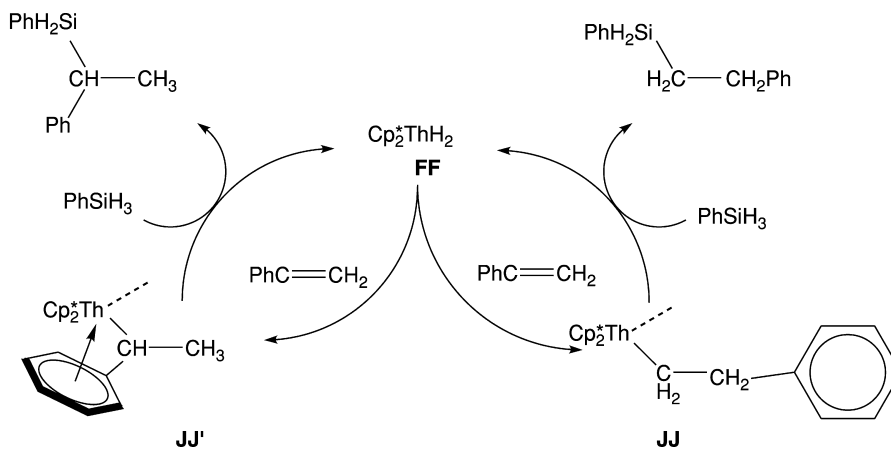
The first step in the proposed mechanism is the reaction of the precatalyst $(C_5Me_5)_2ThMe_2$ with $PhSiH_3$, yielding the hydride complex **FF** and $PhSiH_2Me$. Complex **FF** may react with an alkene producing the alkyl complex **GG** (step 1), which can undergo three parallel pathways. The first route is a reaction with an alkene, to produce a π -alkene complex **HH**, removing the complex **GG** from the catalytic cycle (step 2), and giving rise to the inverse order in alkene. The second and third paths are metathesis and protonolysis reactions between the Th–alkyl fragment and the Si–H moiety, yielding in the former case the substituted silane and regenerating complex **FF** (step 3), and yielding in the latter process the Th– SiH_2Ph complex and the alkane (step 4). The proposed scheme also takes into account the formation of materials in trace amounts.

For styrene, the formation of both hydrosilylation products in similar amounts indicates comparable activation energy for both processes, differing only in the disposition of the silane with respect to the thorium alkyl complex. The Th– SiH_2Ph bond can be activated by two different paths. The metathesis reaction with the Si–H bond in $PhSiH_3$ produces the dehydrogenative dimer and the hydride **FF** (step 5), whereas in the reaction with a Si–Ph bond, Ph_2SiH_2 , and a complex containing the Th– SiH_3 (**II**) moiety will be obtained (step 6), which will then rapidly react with an additional silane yielding the oligomeric dehydrogenative coupling of silanes (step 7). In the hydrosilylation of styrene, the formation of the branched isomer was rationalized by the stereochemistry of the insertion reaction of the styrene with the metal hydride complex (Scheme 26.20); the alkyl formed is presumably stabilized by the π -arene interaction (**JJ'**).

For alkenes, the hydrosilylation reaction promoted by organolanthanides of the type $(C_5Me_5)_2LnR$ ($Ln = Sm, La, Lu$) or $Me_2Si(C_5Me_4)_2SmR$ are much faster (by one order of magnitude) than those obtained with organoactinides. The major difference is found for linear α -alkenes, which lanthanides will hydrosilylate forming both isomers, whereas actinides will exclusively yield the 1,2-adduct product (Harrod, 1991; Ojima *et al.*, 1998; Schumann *et al.*, 1999). Mechanistically, the lanthanide hydrides have been proposed as the primary pathway towards the hydrosilylated products. Thus, organoactinides represent again complementary catalysts to organolanthanides and other transition metal complexes for the regioselective hydrosilylation of α -olefins.

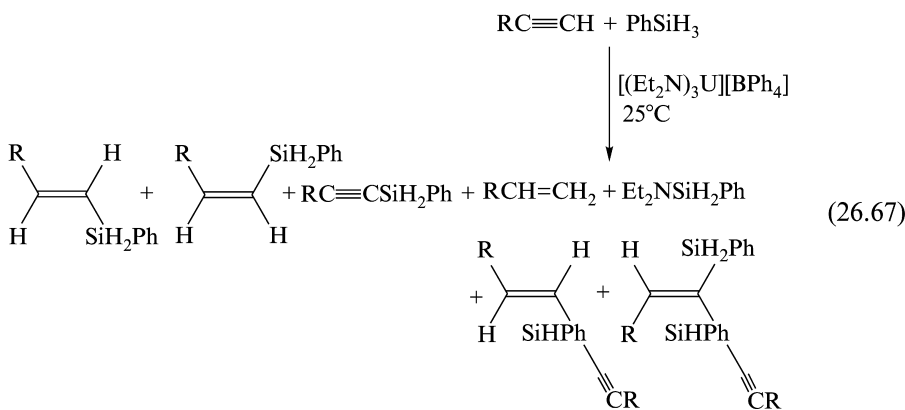
26.6.4 Catalytic hydrosilylation of alkynes promoted by the cationic complex $[(Et_2N)_3U][BPh_4]$

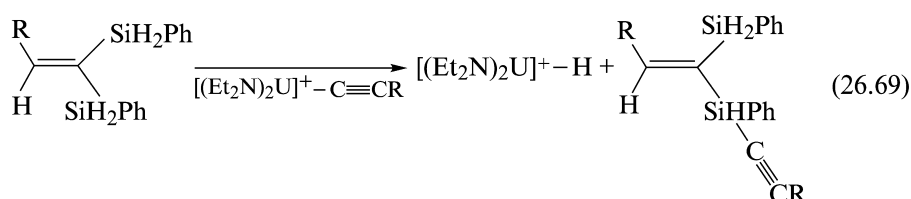
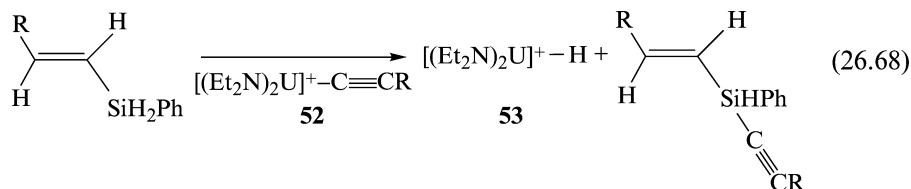
The hydrosilylation reactions of terminal alkynes promoted by neutral organoactinides has motivated similar studies whose goal is the formation of a cationic hydride complex as an intermediate in the catalytic hydrosilylation of



Scheme 26.20 Proposed mechanism for the hydrosilylation of styrene and PhSiH_3 promoted by $(\text{C}_5\text{Me}_5)_2\text{ThMe}_2$ or $\text{Me}_2\text{Si}(\text{C}_5\text{Me}_4)_2\text{Th}^n\text{Bu}_2$.

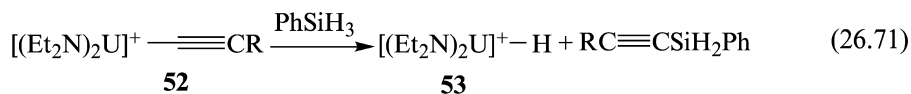
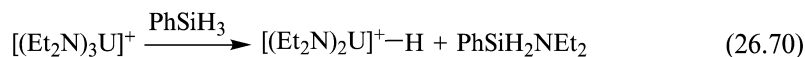
terminal alkynes. Reactions promoted by the cationic complex $[(\text{Et}_2\text{N})_3\text{U}][\text{BPh}_4]$ were studied (Dash *et al.*, 2000). The reaction of $[(\text{Et}_2\text{N})_3\text{U}][\text{BPh}_4]$ with terminal alkynes $\text{RC}\equiv\text{CH}$ ($\text{R} = \text{'}\text{Pr}, \text{'}\text{Bu}$) and PhSiH_3 resulted in the catalytic formation of a myriad of products. The observed products *cis*- and *trans*-vinylsilane ($\text{RCH}=\text{CHSiH}_2\text{Ph}$), the dehydrogenative silylalkyne ($\text{RC}\equiv\text{CSiH}_2\text{Ph}$), alkenes ($\text{RCH}=\text{CH}_2$) ($\text{R} = \text{'}\text{Pr}, \text{'}\text{Bu}$), and the aminosilane $\text{Et}_2\text{NSiH}_2\text{Ph}$ were found to account for 100% conversion with respect to the alkyne. For the bulky $\text{'}\text{BuC}\equiv\text{CH}$, the tertiary silanes *trans*- $\text{'}\text{BuCH}=\text{CHSi}(\text{HPh})(\text{C}\equiv\text{C}'\text{Bu})$, and $\text{'}\text{BuCH}=\text{C}(\text{SiH}_2\text{Ph})\text{Si}(\text{HPh})(\text{C}\equiv\text{C}'\text{Bu})$ were also observed [equation (26.67)]. Formation of the tertiary silanes can be accounted for by metathesis reactions of the *trans*-alkenylsilane and the double hydrosilylated compound with the metal acetylide complex **52**, respectively, as shown in equations (26.68) and (26.69).





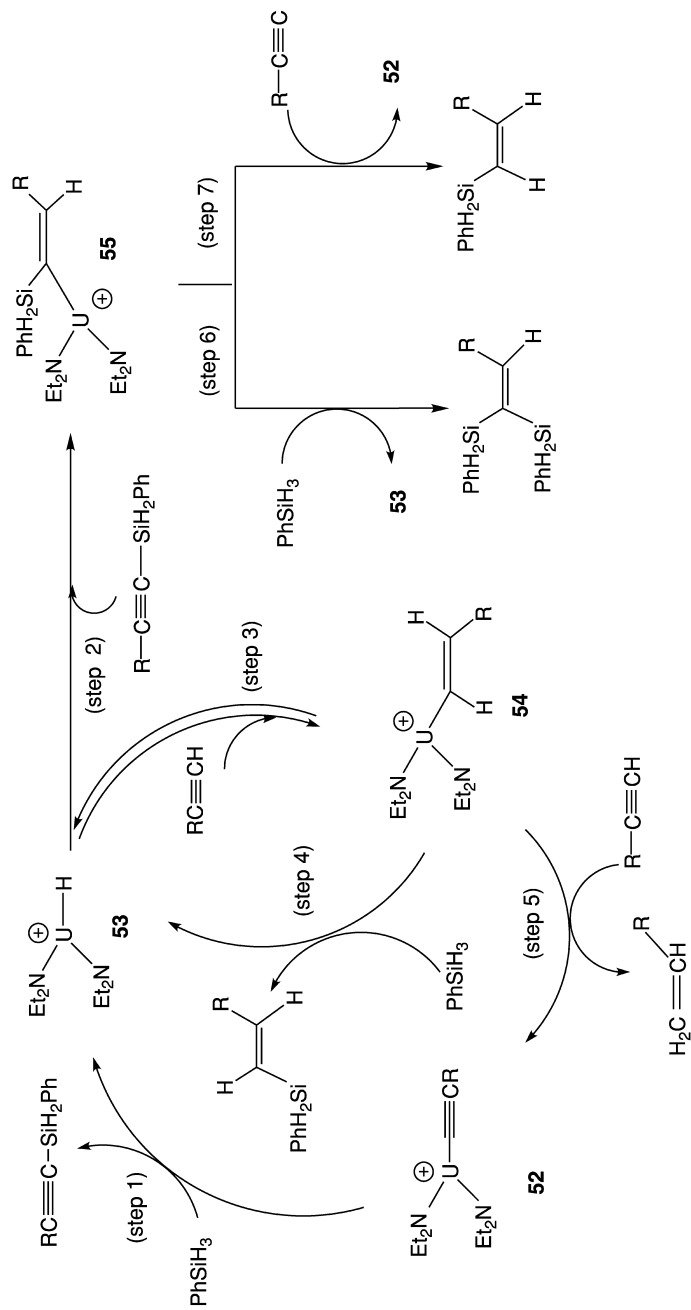
At high temperatures (65–78°C), the chemoselectivity and regioselectivity of the products formed in the cationic organouranium-catalyzed hydrosilylation of terminal alkynes with PhSiH₃ were found to be different in comparison to those obtained at room temperature. The hydrosilylation of RC≡CH (R = ⁿBu, ⁱPr, ^tBu) with PhSiH₃ catalyzed by [(Et₂N)₃U][BPh₄] produced, in addition to the hydrosilylation products at room temperature [equation (26.67)], the corresponding double hydrosilylated compounds: RCH=C(SiH₂Ph)₂ (R = ⁿBu, ⁱPr, ^tBu), and small amounts of the corresponding geminal dimers and trimers. A similar type of mechanism as observed for the neutral organoactinides was proposed, based on kinetic data and product distributions.

The formation of an active uranium hydride complex **53** was proposed to occur either by the reaction of the cationic complex with a silane molecule, giving the corresponding aminosilane, and/or by the reaction of the acetylide complex **52** with a silane, producing the corresponding silylalkyne [equations (26.70) and (26.71), respectively].



The proposed mechanism, which takes into account the formation of all products, is described in Scheme 26.21 (Dash *et al.*, 2000).

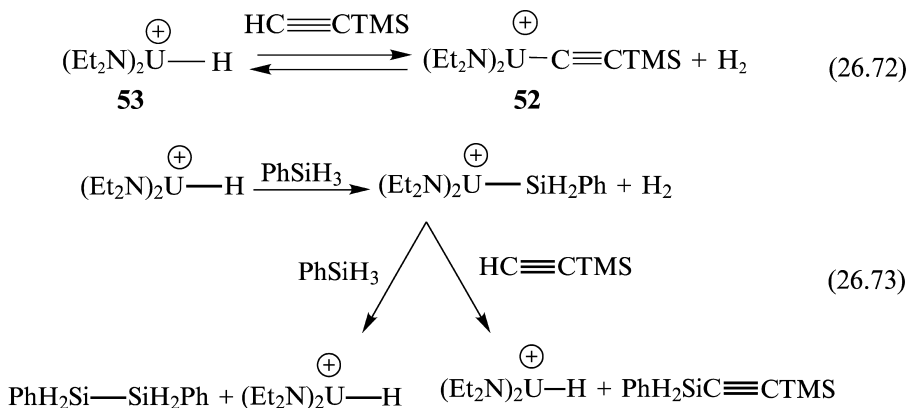
The precatalyst [(Et₂N)₃U][BPh₄] in the presence of alkyne was converted to the acetylide complex **52** by removal of one of the amido ligands. Complex **52** was proposed to react with PhSiH₃ to give the silylalkyne and the actinide hydride **53** (step 1). The hydride **53** may reinsert the silylalkyne forming complex **55** (step 2) or react with the alkyne to produce the alkenyl uranium complex **54** (step 3). Complex **54** is then proposed to react with PhSiH₃, regenerating the organouranium hydride complex **53** and the *trans*-hydrosilylated product



Scheme 26.21 Proposed mechanism for the room- and high-temperature hydroxylation of terminal alkynes promoted by $[(Et_2N)_3U][BPh_4]$. The transformation of the starting complex into the acetylide complex $[(Et_2N)_2U-C≡CR][BPh_4]$ (52) was described in Scheme 26.10, and is omitted here for clarity.

(step 4). Under catalytic conditions, complex **54** may also react with a second alkyne giving the alkene and the acetylide complex **52** (step 5). Complex **55** may react with a silane (step 6) yielding complex **53** and the double hydrosilylation product, or with an alkyne (step 7) yielding complex **52** and the *cis*-isomer.

This mechanistic scenario took into account the higher yields observed for the alkene compound as compared with those obtained for the silylalkyne. For $\text{TMSC}\equiv\text{CH}$ and ${}^t\text{PrC}\equiv\text{CH}$ at high temperature, the amount of the hydrosilylated products is larger than that of the alkenes, indicating that a competing equilibrium route was present. This would again involve the transformation of the hydride **53** back into the acetylide complex **52** by reaction with the alkyne [equation (26.72)], allowing the production of more silylalkyne without producing the alkene. The hydride **53** could alternatively react with PhSiH_3 to give the organometallic silyl compound $[(\text{Et}_2\text{N})_2\text{USiH}_2\text{Ph}][\text{BPh}_4]$ [equation (26.73)], which would further react with PhSiH_3 or $\text{RC}\equiv\text{CH}$ to regenerate the hydride **53** and $\text{PhH}_2\text{Si}-\text{SiH}_2\text{Ph}$ or $\text{PhH}_2\text{SiC}\equiv\text{CR}$, respectively.



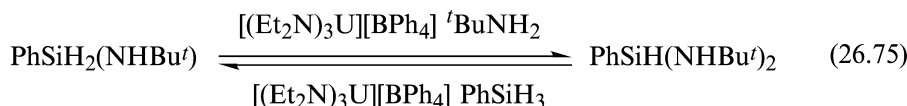
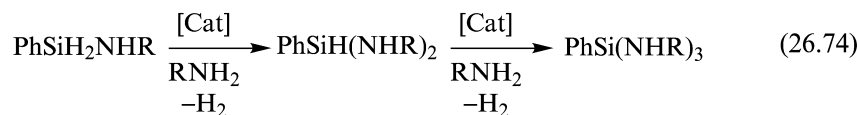
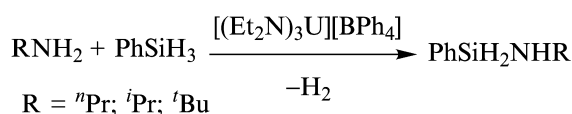
In the hydrosilylation reaction of ${}^t\text{BuC}\equiv\text{CH}$ at high temperature, a small amount of the dehydrogenative coupling of phenylsilane was observed. This product argued for the formation of a compound with an uranium-silicon bond, although not as a major intermediate. The compound $[(\text{Et}_2\text{N})_2\text{USiH}_2\text{Ph}][\text{BPh}_4]$ can be theoretically postulated instead of the hydride complex **53** either from steps 1, 4, or 6 in the catalytic cycle (Scheme 26.21). In these steps, the silane would act as the protonolytic source.

26.7 DEHYDROCOUPLING REACTIONS OF AMINES WITH SILANES CATALYZED BY $[(\text{Et}_2\text{N})_3\text{U}][\text{BPh}_4]$

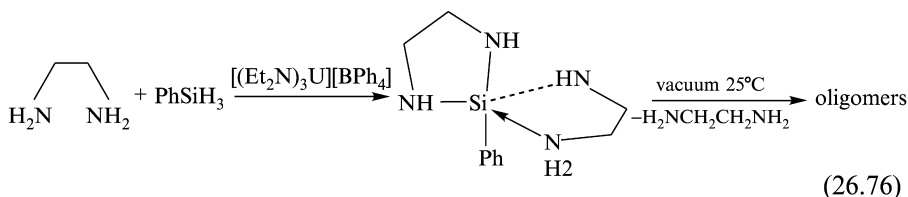
The catalytic processes involving the cationic uranium amide complex, $[(\text{Et}_2\text{N})_3\text{U}][\text{BPh}_4]$, have been found to be particularly efficient in the controlled dimerization of terminal alkynes and in the hydrosilylation reactions of terminal alkynes and alkenes with PhSiH_3 . These processes have been characterized

through the activation of the corresponding amido uranium–acetylide or the amido uranium–hydride species that were the active intermediates, respectively. A conceptual question that arose from those studies concerned the possibility of activating the amido ancillary ligands in $[(\text{Et}_2\text{N})_3\text{U}][\text{BPh}_4]$ with a silane molecule producing the corresponding aminosilane and an organometallic hydride complex. The ability to transform the hydride into the starting amido complex using another amine with the attendant elimination of dihydrogen would give a way to perform the catalytic dehydrogenative coupling of amines and silanes. Thermodynamic calculations have predicted this process as plausible (King and Marks, 1995). The dehydrogenative coupling of amines and silanes has been performed by either late transition metal catalysts (Blum and Laine, 1986; Biran *et al.*, 1988; Wang and Eisenberg, 1991) or early transition metal complexes (Liu and Harrod, 1992; He *et al.*, 1994; Lunzer *et al.*, 1998). These reactions are an alternate route to silazanes, which are precursors for the synthesis of silicon nitride materials. The reaction of ${}^n\text{PrNH}_2$ and PhSiH_3 promoted by the cationic complex $[(\text{Et}_2\text{N})_3\text{U}][\text{BPh}_4]$ produced dihydrogen and the aminosilanes $\text{PhSiH}(\text{NHPr}^n)_2$ and $\text{PhSi}(\text{NHPr}^n)_3$ [equation (26.74)]. The use of a large excess of amine allowed for full conversion of the silane into the di- and tri-aminosilanes. The monoaminosilane, $\text{PhSiH}_2(\text{NHPr}^n)$, was not detected, indicating that in this compound the Si–H hydride bonds were more reactive than those in the starting PhSiH_3 (Wang *et al.*, 2000).

The reaction of ${}^i\text{PrNH}_2$ and PhSiH_3 gave dihydrogen together with $\text{PhSiH}_2\text{NHPr}^i$ (33%) and $\text{PhSiH}(\text{NHPr}^i)_2$ (56%) with a total conversion of 89% for PhSiH_3 . The use of large amine excess promoted the reaction towards the bisaminosilane $\text{PhSiH}(\text{NHPr}^i)_2$. The bulky ${}^t\text{BuNH}_2$ reacted with PhSiH_3 producing $\text{PhSiH}_2\text{NHBu}^t$ quantitatively. This monoaminosilane reacted further with an excess of amine to produce an additional equivalent of dihydrogen and exclusively the bisaminosilane $\text{PhSiH}(\text{NHBu}^t)_2$. This latter compound was transformed back slowly into the mono aminosilane, $\text{PhSiH}_2\text{NHBu}^t$, after the addition of one equivalent of PhSiH_3 [equation (26.75)], which indicated that the production of aminosilanes promoted by the cationic complex $[(\text{Et}_2\text{N})_3\text{U}][\text{BPh}_4]$ was in equilibrium.



Ethylenediamine $\text{H}_2\text{NCH}_2\text{CH}_2\text{NH}_2$ reacted with PhSiH_3 in the presence of the catalyst, yielding dihydrogen and the spiro chelated complex $\text{PhSi}(\eta^2\text{-NHCH}_2\text{CH}_2\text{NH})(\eta^2\text{-NHCH}_2\text{CH}_2\text{NH}_2)$ quantitatively. When the spiro product was heated at 25°C under vacuum, ethylenediamine was removed and $\text{PhSi}(\eta^2\text{-NHCH}_2\text{CH}_2\text{NH})(\eta^2\text{-NHCH}_2\text{CH}_2\text{NH}_2)$ was transformed into a mixture of oligomers [equation (26.76)].

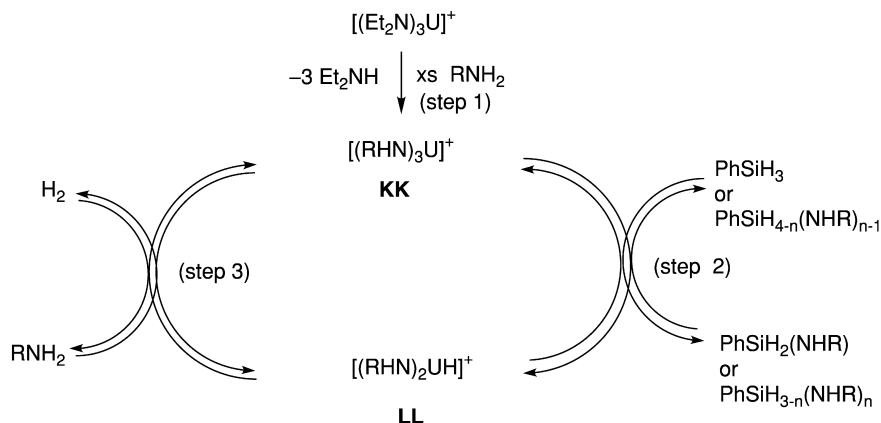


From these results it was concluded that the reactivity of primary amines RNH_2 in the formation of aminosilanes with PhSiH_3 catalyzed by the cationic uranium complex $[(\text{Et}_2\text{N})_3\text{U}][\text{BPh}_4]$ follows the order primary > secondary > tertiary.

Secondary amines and secondary silanes were found to be less reactive than the corresponding primary amine and silanes. The reaction of Et_2NH with PhSiH_3 produced H_2 and a mixture of $\text{PhSiH}(\text{NEt}_2)_2$ and $\text{PhSiH}_2\text{NEt}_2$. No reaction was observed between $(\text{Pr})_2\text{NH}$ and PhSiH_3 , presumably because of the steric hindrance of the amine. The bulk of the silane was also found to have an effect. ${}^n\text{PrNH}_2$ reacted with the secondary silane PhSiMeH_2 , generating H_2 , $\text{PhSiHMe}(\text{NHPr}^n)$ and $\text{PhSiMe}(\text{NHPr}^n)_2$.

$[(\text{Et}_2\text{N})_3\text{U}][\text{BPh}_4]$ reacted directly with stoichiometric or excess amounts of PhSiH_3 , creating in both cases one equivalent of the corresponding aminosilane $\text{PhSiH}_2\text{NEt}_2$ and $[(\text{Et}_2\text{N})\text{UH}][\text{BPh}_4]$; when an excess of silane was used, trace formation of the homodehydrogenative coupling product of the silane was observed. These results identified the monohydride complex as the active intermediate, since no other amido moieties were found to react with the phenylsilane. Therefore, the synthesis of a uranium hydride was accomplished by treatment of the corresponding amide with a silane, as has been reported in zirconium chemistry. Similar exchange reactions with boranes, alanes, and stannanes have been observed (Lappert *et al.*, 1980; Hays and Fu, 1997; Liu *et al.*, 1999).

A plausible mechanism for the dehydrocoupling of amines with silanes promoted by the cationic complex $[(\text{Et}_2\text{N})_3\text{U}][\text{BPh}_4]$ is described in Scheme 26.22. The first step of the mechanism was proposed to be the transamination reaction of $[(\text{Et}_2\text{N})_3\text{U}][\text{BPh}_4]$ with RNH_2 giving $[(\text{NHR})_3\text{U}][\text{BPh}_4]$ (**KK**) (step 1). Complex **KK** may react with PhSiH_3 to afford the monoaminosilane PhSiH_2NHR and the corresponding hydride $[(\text{NHR})_2\text{UH}][\text{BPh}_4]$ (**LL**) (step 2). The last step of the catalytic cycle (step 3) is the reaction of **LL** and the amine, regenerating **KK** with the concomitant elimination of dihydrogen.



Scheme 26.22 Proposed mechanism for the coupling of amine with silanes promoted by $[(Et_2N)_3U][BPh_4]$.

The different polyaminosilanes $PhSiH_{3-n}(NHR)_n$ are obtained by replacing $PhSiH_3$ with $PhSiH_{4-n}(NHR)_{n-1}$ ($n \geq 1$) in step 2.

Since in the presence of an excess of amine the reactive hydrogen atoms were found to be those of the silane, a study of the reactivity of the aminosilane products towards a silane was conducted. The reaction of $PhSi(NHPr^i)_3$ with an excess of $PhSiH_3$ in the absence of amine was considered in order to determine a possible equilibrium and/or a tailoring approach to specific products by activation of the amine hydrogen atoms of the aminosilane. $PhSi(NHPr^i)_3$ reacted with an excess of $PhSiH_3$ in the presence of $[(Et_2N)_3U][BPh_4]$ to give a mixture of four compounds (**MM**, **NN**, **OO**, **PP**) (Scheme 26.23).

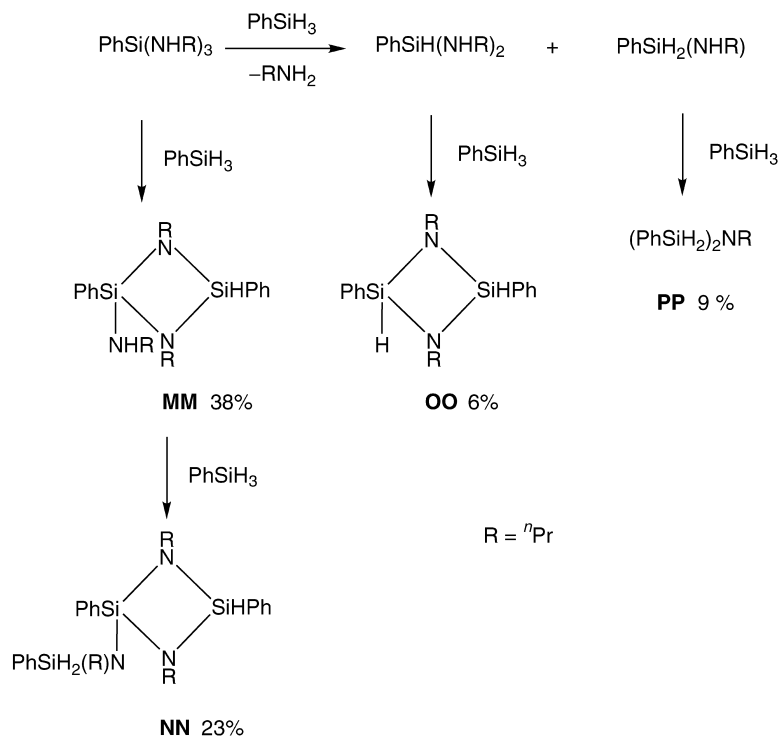
The explanation of how only four compounds were obtained may be found by consideration of the formation of all possible compounds as outlined in Scheme 26.24.

These results show how a cationic organoactinide complex offered an alternative route for the dehydrogenative coupling of amines with silanes by a mechanism consisting of activation of an amido ligand by a silane, producing the aminosilane and an organometallic hydride, which was recycled by addition of amine.

26.8 INTERMOLECULAR HYDROAMINATION OF TERMINAL ALKYNES

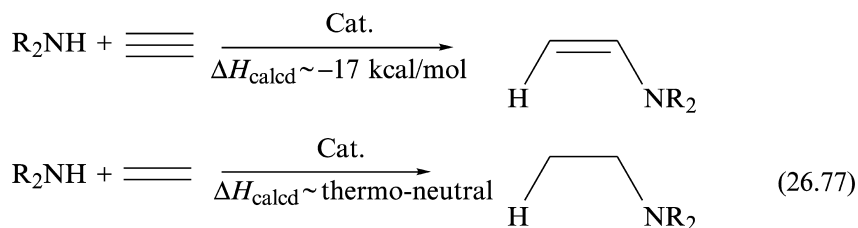
26.8.1 Intermolecular hydroamination of terminal alkynes catalyzed by neutral organoactinide complexes: scope and mechanistic studies

Catalytic C–N bond formation is a process of cardinal importance in organic chemistry, and the hydroamination of unsaturated substrates by the catalytic addition of a N–H moiety epitomizes a desirable atom-economic transformation

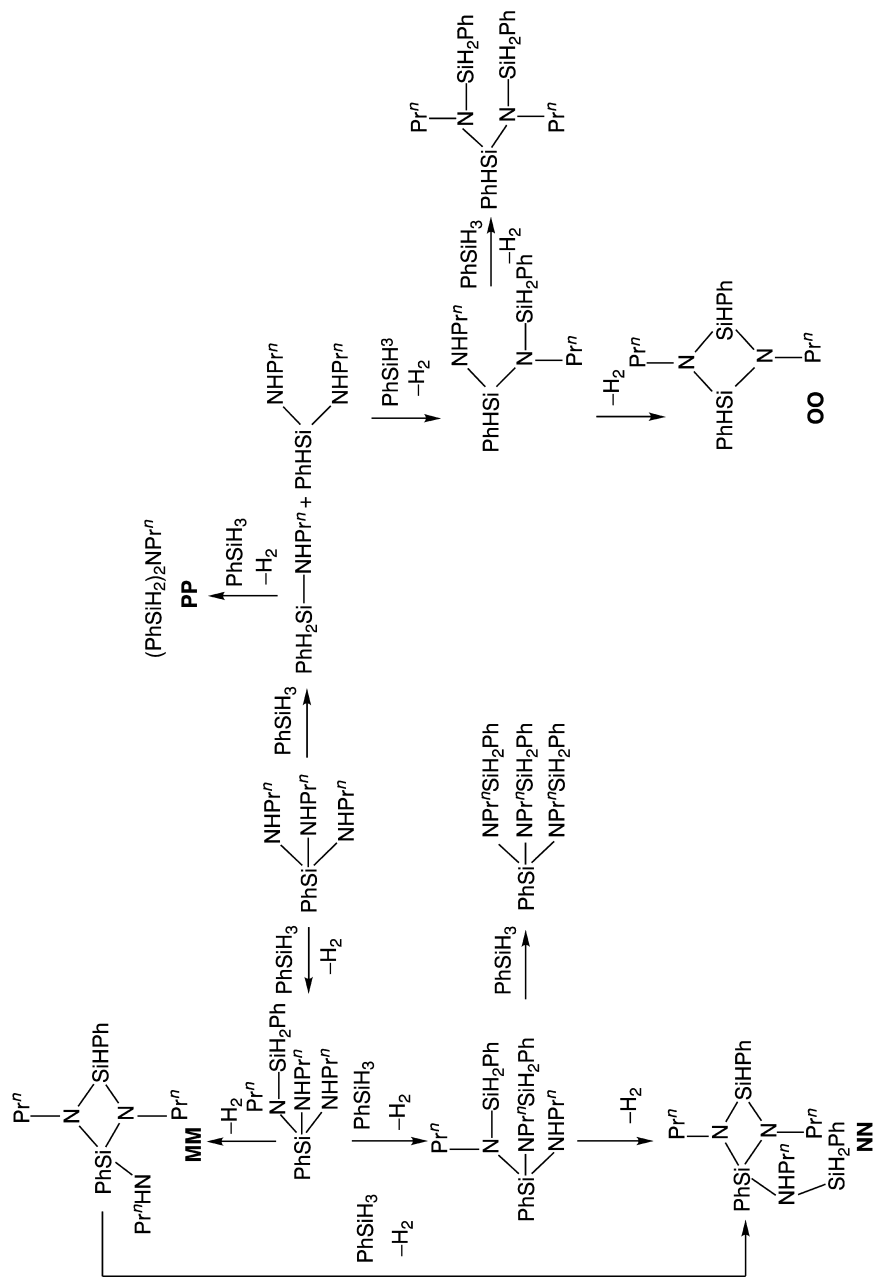


Scheme 26.23 Reactivity of $\text{PhSi(NHPr}^n)_3$ with an excess of PhSiH_3 in the presence of $[(\text{Et}_2\text{N})_3\text{U}][\text{BPh}_4]$.

with no by-products. This reaction remains a challenge [equation (26.77)] and current catalytic research activities in this area is widespread and spans to the entire periodic table (Nobis and Driessen-Hölscher, 2001; Molander and Romero, 2002; Pohlki and Doye, 2003; Seayad *et al.*, 2003; Trost and Tang, 2003; Utsunoyima *et al.*, 2003). The intermolecular functionalization of olefins and alkynes with amines has been mentioned as one of the ten most important challenges in catalysis (Haggin, 1993).



Thermodynamically, the addition process of amines to alkenes is close to thermoneutral whereas the addition to alkynes is more enthalpically favored.

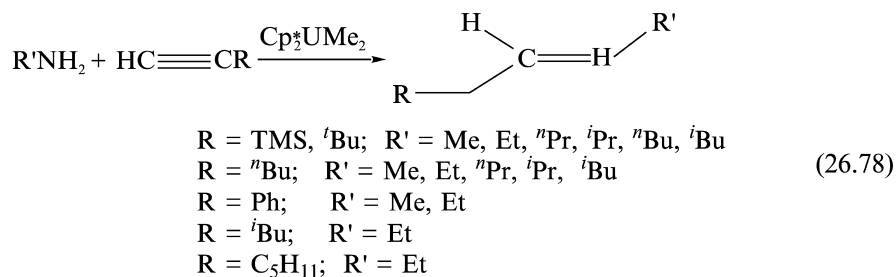


Scheme 26.24 Formation of compounds **MM**, **NN**, **OO**, and **PP** in the coupling of amine and silanes catalyzed by $[(Et_2N)_3U][BPh_4]$.

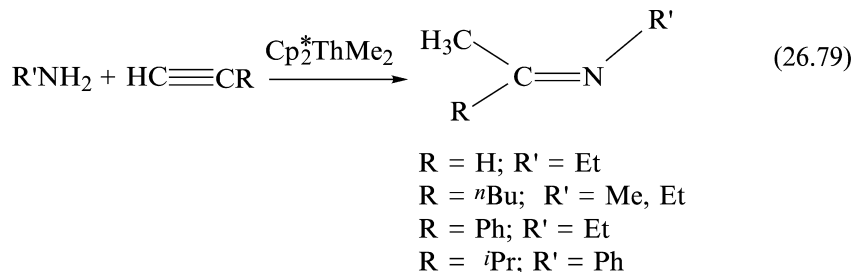
Because of the mode of activation of these organoactinides, the negative entropy of the reaction thwarts the use of high temperatures. Organolanthanide complexes have been found to be extremely good catalysts for the intramolecular hydroamination/cyclization of aminoalkenes, aminoalkynes, and aminoalkenes (Gagné *et al.*, 1992a,b; Li and Marks, 1996; Roesky *et al.*, 1997b; Buerstein *et al.*, 1998; Li and Marks, 1998; Arredondo *et al.*, 1999a,b; Molander and Dowdy, 1999; Tian *et al.*, 1999; Ryu *et al.*, 2001; Douglass *et al.*, 2002; Hong and Marks, 2002; O'Shaughnessy *et al.*, 2003), and enantioselective intramolecular amination reactions have been performed using chiral organolanthanide precatalysts (Gagné *et al.*, 1992a).

The organoactinide complexes $(C_5Me_5)_2AnR_2$ ($An = Th, U, R = Me, NHR', R' = \text{alkyl}$) were found to be excellent precatalysts for the intermolecular hydroamination of terminal aliphatic and aromatic alkynes in the presence of primary aliphatic amines yielding the corresponding imido compounds (Haskel *et al.*, 1996; Straub *et al.*, 2001). The reactivity exhibited for the uranium complexes was different, depending on the alkynes, when compared to organothorium complexes [equations (26.78) and (26.79)].

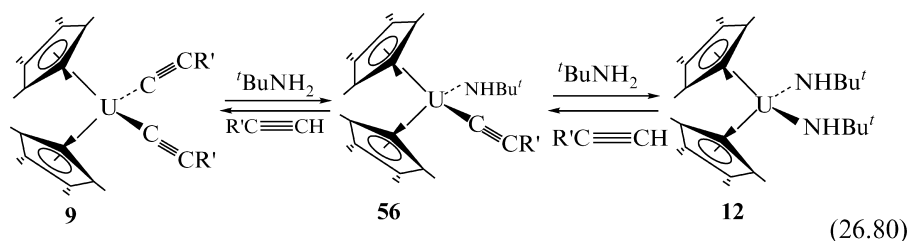
The intermolecular process [equations (26.78) and (26.79)] showed two hydroamination regioselectivities depending on the precatalyst. The intermolecular hydroamination catalyzed by the uranium compound exhibited large regioselectivity and chemoselectivity with the *E*-isomer of the imine usually formed. For the thorium catalyst, the methyl alkyl-substituted imines were obtained. In the latter case, the imines were produced in moderate yields with the concomitant formation of the alkyne *gem* dimer.



For $R = TMS$ the imines are obtained as mixtures of *E* and *Z* isomers.



When the alkyne reactions catalyzed by the uranium complexes were performed using the bulky $t\text{BuNH}_2$ as the primary amine, no hydroamination products were obtained. The products observed were only the selective *gem* dimers corresponding to the starting alkyne. This result has indicated that with $t\text{BuNH}_2$, the proposed active species responsible for the intermolecular hydroamination was not generated. Using this bulky amine, the observed organouranium complexes in solution were the corresponding uranium bis(acetylide) (**9**) and the uranium bis(amido) (**12**) complexes. These two compounds were found to be in rapid equilibrium with the monoamido acetylide complex (**56**), responsible for the oligomerization of alkynes in the presence of amines [equation (26.80)].

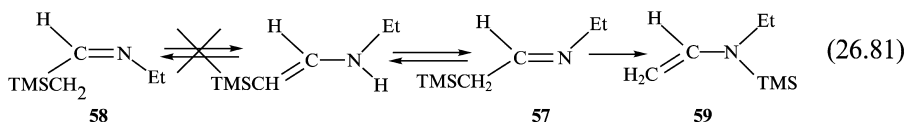


When comparing the hydroamination rates for a specific alkyne utilizing the various amines, the bulkier the amines, the lower the turnover frequency, and when comparing the hydroamination rates for a particular amine (MeNH_2) using various alkynes, similar turnover frequencies were observed. The lack of effect on the turnover frequency suggested no steric effect of the alkynes on the hydroamination process.

The intermolecular hydroamination catalyzed by the analogous organothorium complex (C_5Me_5) $_2\text{ThMe}_2$ exhibited similar reactivities with $\text{TMSC}\equiv\text{CH}$ and MeNH_2 or EtNH_2 [equation (26.78)]. However, in the intermolecular hydroamination with $t\text{BuC}\equiv\text{CH}$ or $\text{PhC}\equiv\text{CH}$ and MeNH_2 or EtNH_2 a dramatic change in the regioselectivity was obtained, generating the unexpected imines [equation (26.79)]. For all the organoactinides, no hydroamination products were formed by using either secondary amines or internal alkynes. With secondary amines, the chemoselective alkyne dimers and in some cases trimers were obtained.

The catalytic hydroamination of $t\text{BuC}\equiv\text{CH}$ or $\text{TMSC}\equiv\text{CH}$ with EtNH_2 with either the organothorium complexes **1** or **5** gave identical results (rate, yields, stereochemistry of the products, and kinetic curves) indicating that both reactions occurred through a common active species, in a similar manner to that observed for the uranium complexes. It is interesting to point out that when the mixture of imines **57** and **58** were obtained, **57** was found to undergo a non-catalyzed Brook silyl rearrangement to form the corresponding enamine **59** [equation (26.81)] (Brook and Bassindale, 1980). The rearrangement followed

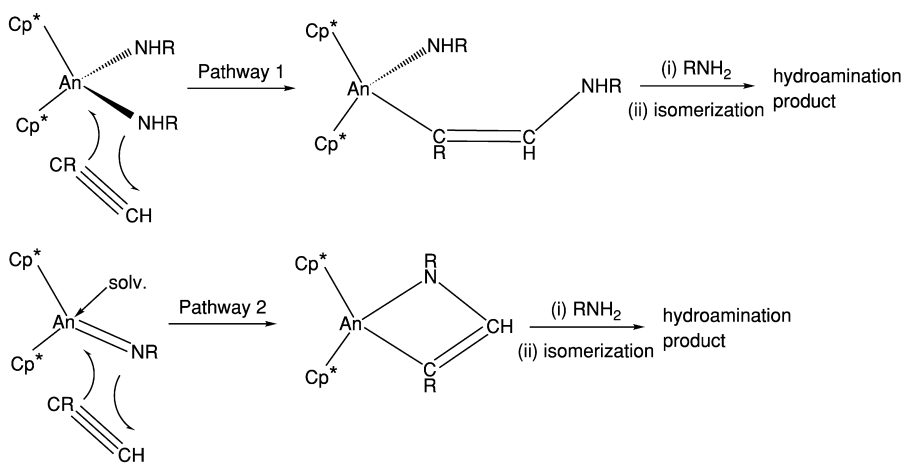
first-order kinetics with direct conversion of **57** to **59**, leaving the concentration of **58** unaffected:



The formation of the corresponding oligomers in the hydroamination reactions catalyzed by the thorium complexes indicated that two different complexes were active in solution, possibly interconverting, resulting in two parallel processes. It was possible to discriminate between the two most probable mechanistic pathways to find the key organometallic intermediate responsible for the hydroamination process (Scheme 26.25). The first route proposed involved the insertion of an alkyne into a metal–amido bond, as found in lanthanide chemistry (Gagné *et al.*, 1992a,b; Roesky *et al.*, 1997a,b; Tian *et al.*, 1999). The second route consisted of insertion of an alkyne into a metal–imido (M=N) bond, as observed for early transition metal complexes (Walsh *et al.*, 1992, 1993).

26.8.2 Kinetic studies of the hydroamination terminal alkynes with primary amines

Kinetic measurements of the hydroamination of $\text{TMSC}\equiv\text{CH}$ with EtNH_2 revealed that the reaction has a inverse first-order dependence in amine, first-order dependence in precatalyst, and zero-order dependence in alkyne



An = U;

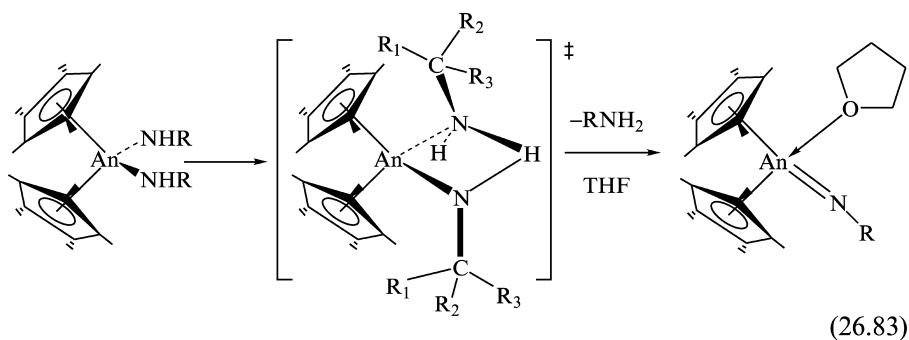
For An = Th, the stereochemistry approach for some alkynes was inverted before insertion

Scheme 26.25 Expected pathways for the organoactinide-catalyzed intermolecular hydroamination of primary amines with terminal alkynes.

concentration. Thus, the rate law for the hydroamination of terminal alkynes promoted by organoactinides can be formulated as presented in equation (26.82). The derived ΔH^\ddagger and ΔS^\ddagger parameter values (in the range 60–120°C) (error values are in parenthesis) from a thermal Eyring analysis were 11.7(3) kcal mol⁻¹ and -44.5(8) eu, respectively.

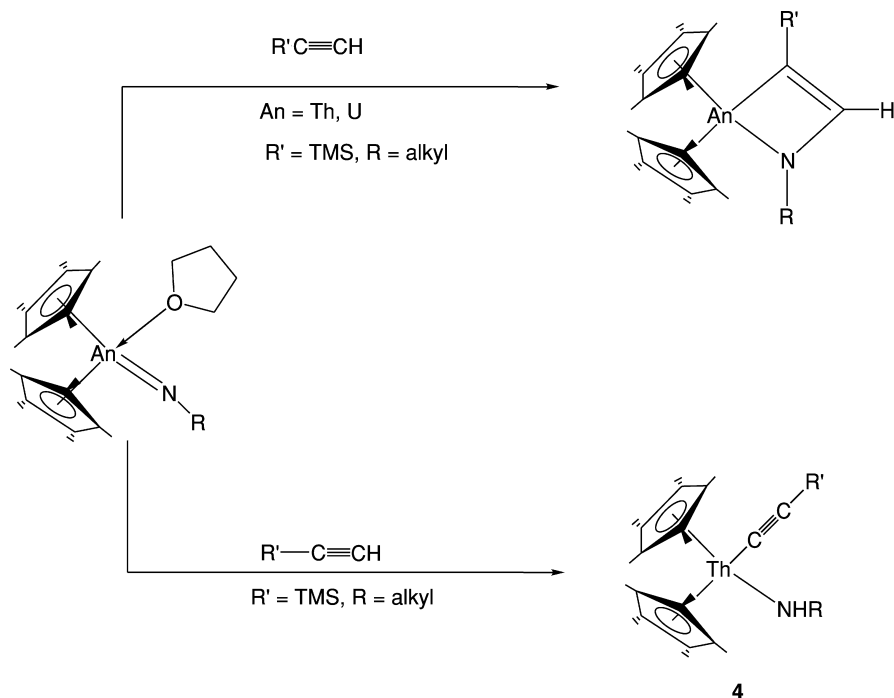
$$v = k[\text{An}][\text{amine}]^{-1}[\text{alkyne}]^0 \quad (26.82)$$

Since the approach of either alkyne or an amine to the organometallic catalyst is expected to occur in a side-on manner in the metallocene, the lack of alkyne concentration dependence in the kinetic hydroamination rate suggested that the proposed pathway 1 (Scheme 26.25) was not a major operative route. The zero kinetic order on alkyne suggests pathway 2 (Scheme 26.25) is consistent with the high coordinative unsaturation of the imido complexes that allows a fast insertion of the different alkynes with indistinguishable rates. When bulky amines were utilized, the formation of the corresponding imido complexes was hindered due to the encumbered transition state [equation (26.83)], reaching the highest steric hindrance with ^tBuNH₂.



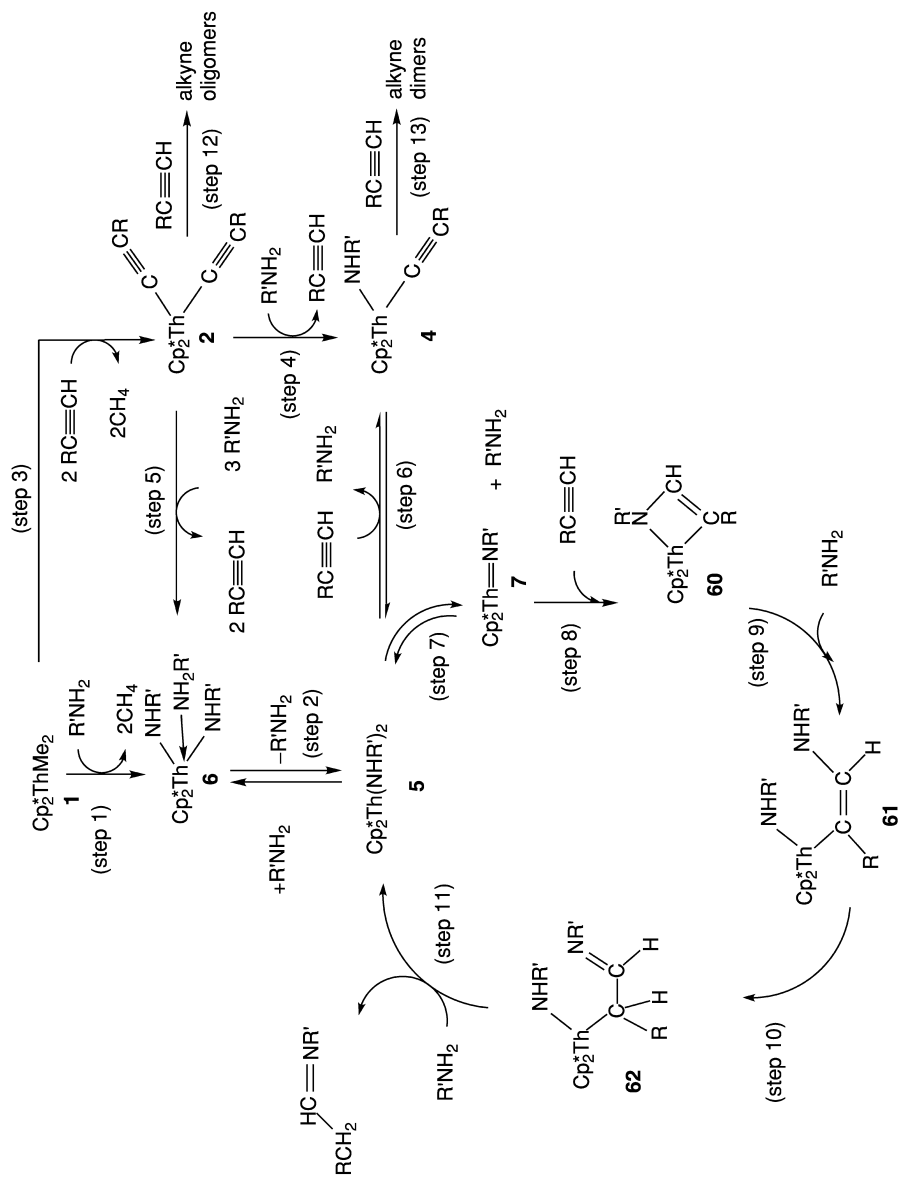
The different activation mode for the two organoactinides is very unusual. For both organoactinide–imido complexes, a selective metathesis with the π -bond of the alkyne was found to exist (demonstrated by the production of hydroamination products), whereas for the thorium complex a protonolysis reaction was observed as a competing reaction. The competing reaction was found to be responsible for the selective dimerization of the terminal alkynes (Scheme 26.26).

A likely scenario for the intermolecular hydroamination of terminal alkynes promoted by the organothorium complex is shown in Scheme 26.27. The first step in the catalytic cycle involved the N–H σ -bond activation of the primary amine by the starting organoactinide, yielding methane and the bisamido–amine complex (C₅Me₅)₂Ac(NHR')₂·H₂NR' **6** (step 1), which was found to be in rapid equilibrium with the corresponding bis(amido) complex **5** (step 2) (Straub *et al.*, 1996; Eisen *et al.*, 1998). An additional starting point



Scheme 26.26 Distinctive modes of activation for organoactinide-imido complexes in the presence of terminal alkynes.

involved a similar C–H activation of an alkyne with the organoactinide yielding methane and the bis(acetylide) complex **2** (step 3). This complex may react rapidly in the presence of amines either in equivalent amounts (step 4) or with an excess (step 5) yielding complexes **4** or **6**, respectively. Complex **5** followed two competitive equilibrium pathways. The σ -bond metathesis with a terminal alkyne yielded complex **4** (step 6), which induced the production of selective dimers (step 13). The second pathway (step 7), as the rate-limiting step, involves elimination of an amine molecule producing the corresponding imido complex **7**. The imido complex participated in a rapid π -bond metathesis with an incoming alkyne, yielding the metallacycle **60** (step 8). Rapid protonolytic ring opening of complex **60** by an amine yielded the actinide–enamine amido complex **61** (step 9). Complex **61** rapidly isomerized to the actinide–alkyl(imine) amido, **62**, by an intramolecular 1,3 sigmatropic hydrogen shift (step 10), which upon a subsequent protonolysis by an additional amine (step 11) produced the imine and regenerates the bis(amido) complex **5**.



Scheme 26.27 Proposed mechanism for the intermolecular hydroamination of terminal alkynes and primary amines promoted by neutral organoactinide complexes.

The preferential formation of the *E* imine isomer as compared to that of the *Z* isomer may be explained by the steric hindrance of the amine substituents in the isomerization pathway as described in Scheme 26.28.

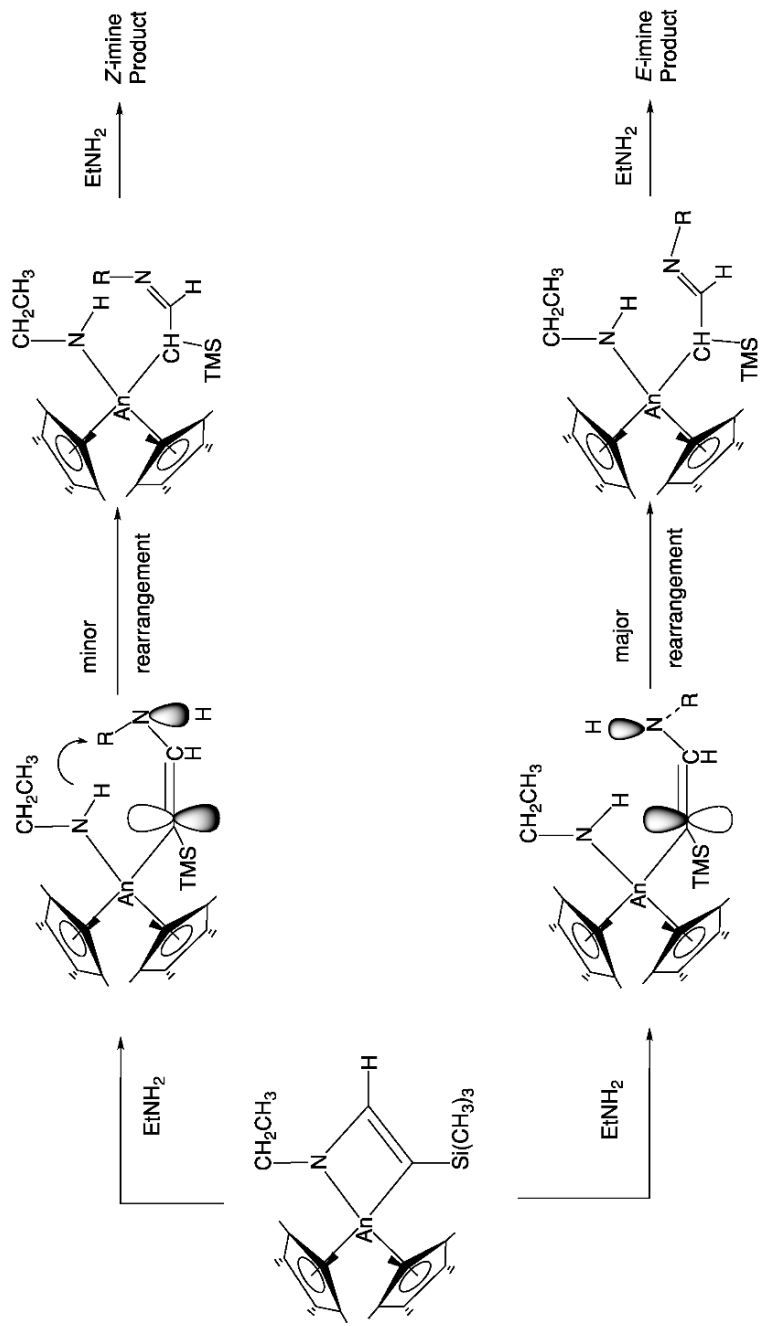
The distinct products formed by the two organoactinide catalysts in the hydroamination reaction are a result of a stereochemical difference in the approach of the alkyne to the imido complex (Scheme 26.29). It has been proposed that the regiochemistry of the intermolecular hydroamination between U and Th is driven by the differences in their electronic configurations, rather than the difference in their thermochemistry (potentially the f^2 electronic configuration of the uranium complex).

26.9 INTRAMOLECULAR HYDROAMINATION BY CONSTRAINED-GEOMETRY ORGANOACTINIDE COMPLEXES

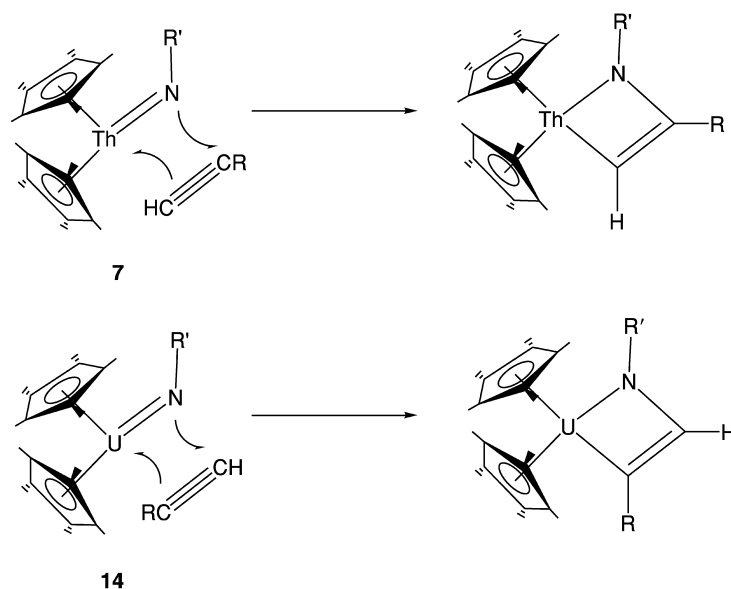
Recently novel types of constrained-geometry actinide complexes were synthesized by the amine elimination syntheses using a protic ligation and the corresponding homoleptic amido-actinide precursor (Scheme 26.30) (Stubbert *et al.*, 2003). The equilibrium position of the elimination reaction was controlled by the dialkylamine concentration, whereas the removal of this by-product was the key step to obtain good yields for both actinide metals (Th, U). A slight excess of the ancillary ligand was used to obtain the complexes under mild conditions in up to 77% yield.

All three uranium complexes were crystallized as well as the (CGC)Th(NMe₂)₂ (CGC=Me₂Si(η⁵-Me₄C₅)-(t-BuN)). The observed trends for the Cp(centroid)–metal–nitrogen angles for the actinide complexes and their respective comparison to lanthanides are Th > U > Sm > Yb, indicating a more open coordination for the 5f elements (Tian *et al.*, 1999; Stubbert, *et al.*, 2003). The *tert*-butylamido-metal bond length in all the complexes was found to be larger than the corresponding metal–NR₂ bond. The longer bonds are plausibly due to the lower basicity of the (Me₂Si *tert*-ButylN) as compared to that of the NR₂ moieties. Table 26.2 shows the turnover frequency for the hydroamination/cyclization of aminoalkenes and aminoalkynes. In addition, a nice comparison for the different abilities of the constrained geometry complexes with organoactinide metallocenes Cp₂*AnMe₂ (An = Th, U) in the hydroamination is illustrated.

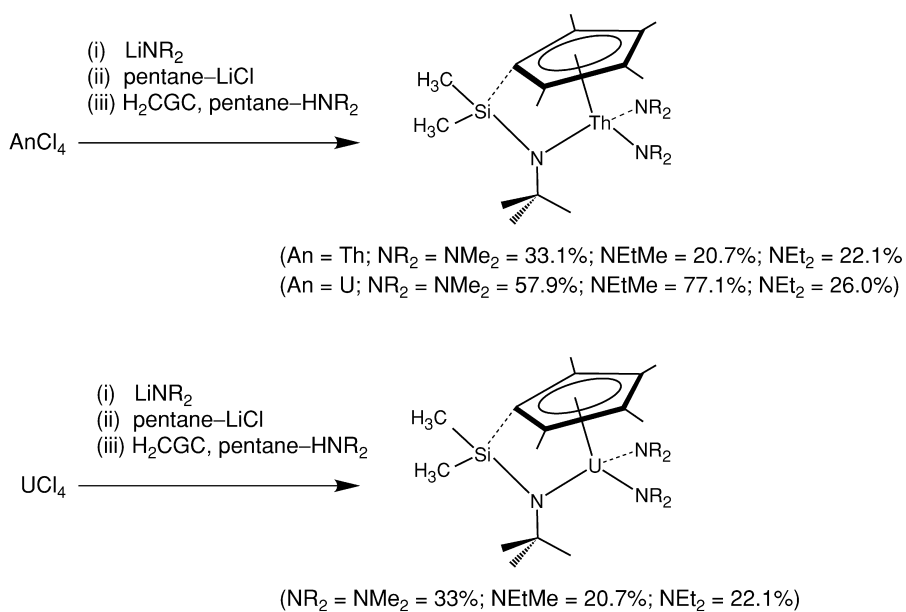
Kinetic studies on the hydroamination/cyclization reaction shows similar behavior as found for lanthanides. The kinetic rate law exhibits a first-order dependence on the precatalyst and zero order on the substrate i.e. rate \propto [precatalyst]¹[substrate]⁰. This result argues that the protonolysis of the precatalyst amido moieties by the substrate is rapid, and that the rate determining step of the reaction is the olefin (alkene or alkyne) insertion into the An–NHR bond. For aminoalkenes, faster reactions are observed for the organoactinide



Scheme 26.28 Formation of imines E and Z by a 1,3-sigmatropic hydrogen shift from the two possible organoactinide complexes. The curved arrow shows the steric interaction between the amine substituents present in the top route as compared to the bottom route.

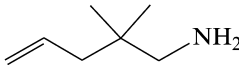
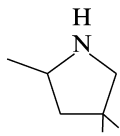
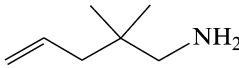
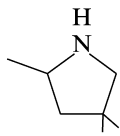
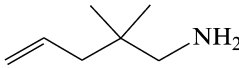
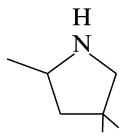
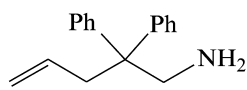
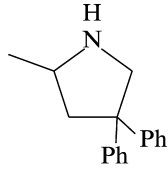
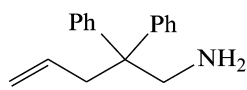
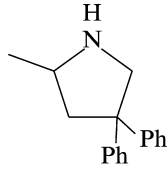
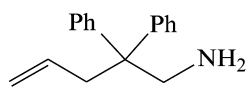
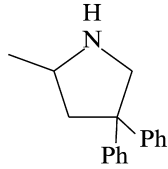
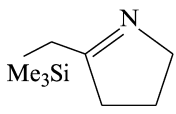
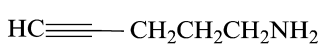
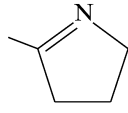
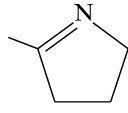
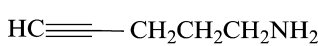
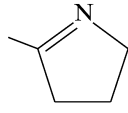
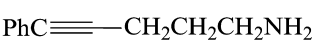
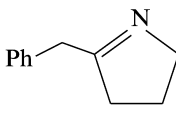
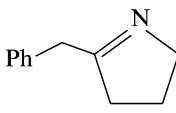
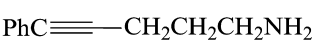
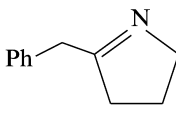


Scheme 26.29 Opposite reactivity exhibited in the reaction of organoactinide–imido complexes with terminal alkynes.



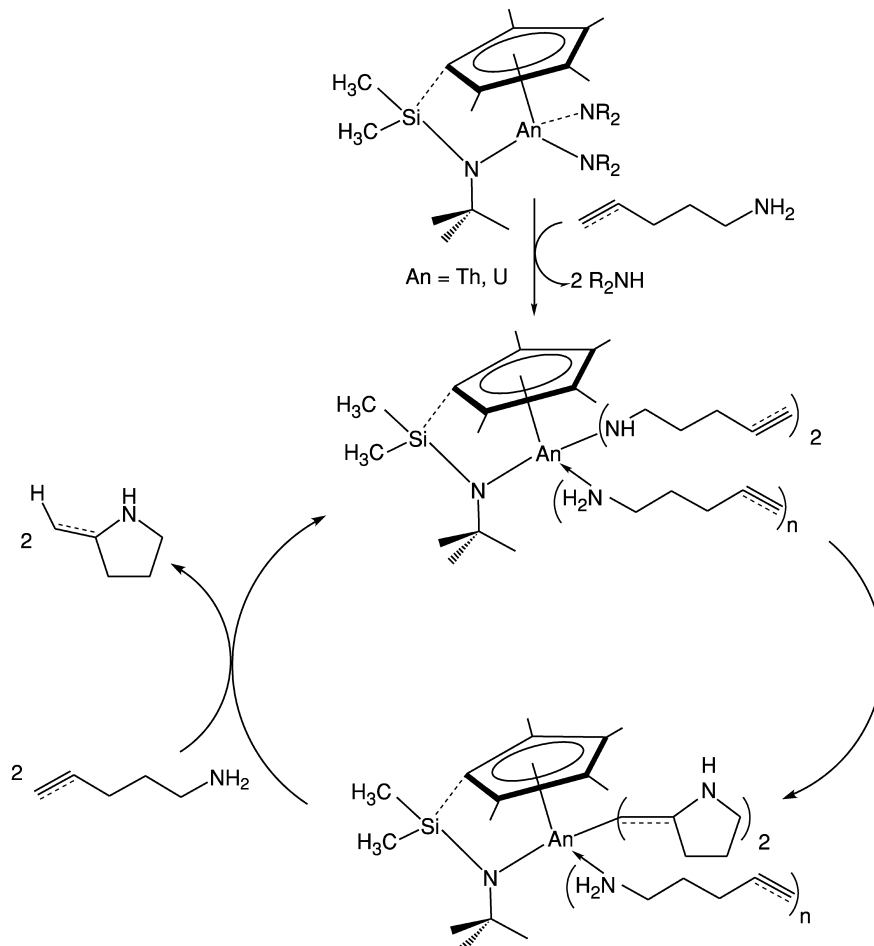
Scheme 26.30 Synthetic route towards constrained geometry organoactinides.

Table 26.2 Catalytic hydroamination/cyclization by various organoactinide complexes.

Entry	Precatalyst	Substrate	Product	N_t (h^{-1})
1	(CGC)Th(NR ₂) ₂			15
2	(CGC)U(NR ₂) ₂			2.5
3	Cp ₂ *ThMe ₂			0.4
4	(CGC)Th(NR ₂) ₂			1460
5	(CGC)U(NR ₂) ₂			430
6	(CGC)Th(NR ₂) ₂			82
7	(CGC)U(NR ₂) ₂	Me ₃ SiC≡—CH ₂ CH ₂ CH ₂ NH ₂		>1600
8	(CGC)Th(NR ₂) ₂			7.8
9	(CGC)Th(NR ₂) ₂	HC≡—CH ₂ CH ₂ CH ₂ NH ₂		1210
10	Cp ₂ *U Me ₂			26
11	(CGC)Th(NR ₂) ₂			4.3
12	(CGC)Th(NR ₂) ₂	PhC≡—CH ₂ CH ₂ CH ₂ NH ₂		51
13	Cp ₂ *ThMe ₂			0.8

with a larger ionic radius, while for aminoalkynes, the faster reactions are observed for the organoactinide with the smaller ionic radius. A plausible mechanism for the hydroamination/cyclization is presented in Scheme 26.31.

It can be seen that the more sterically open environment of the constrained geometry complexes induces to a greater turnover frequencies for the aminoalkene substrates by allowing a greater access to the metal center without interfering with the kinetics and the stability of the complexes. For both aminoalkene and aminoalkynes, the constrained geometry complexes react much faster than the corresponding organoactinide metallocenes.

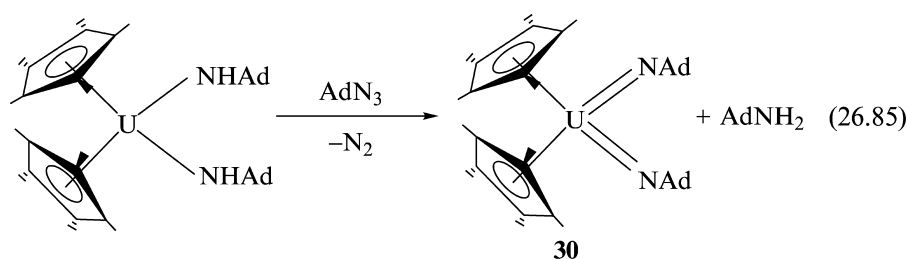
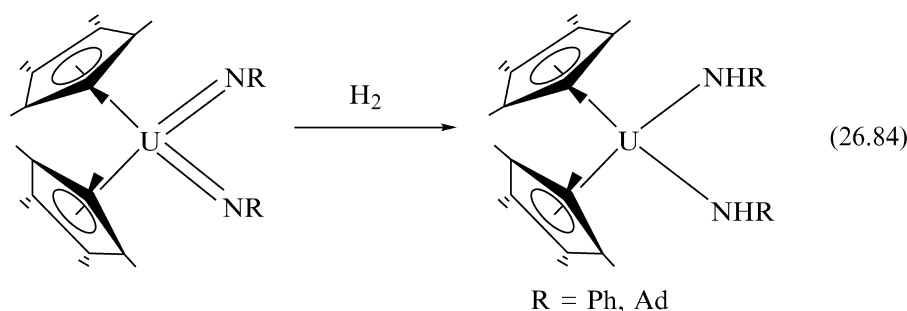


Scheme 26.31 Plausible mechanism for the intramolecular hydroamination/cyclization of aminoolefins promoted by constrained geometry organoactinide complexes.

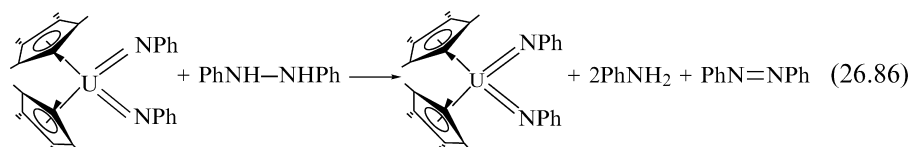
26.10 THE CATALYTIC REDUCTION OF AZIDES AND HYDRAZINES BY HIGH-VALENT ORGANOURANIUM COMPLEXES

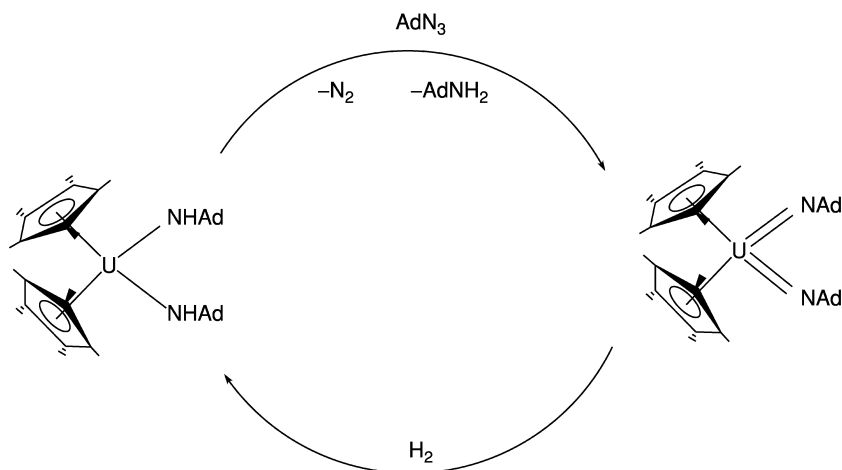
U(IV) metallocene compounds frequently show reactivities comparable to lanthanide and group IV transition metal metallocenes. Common types of processes among these metals (as demonstrated above) include olefin insertion, σ -bond metathesis, and protonolysis. In contrast to the lanthanides and group IV metals, however, uranium can also access the 6+ oxidation state, giving rise to the possibility of two-electron (4+/6+) redox processes. When the complexes (C₅Me₅)₂U(=NR)₂ (R = Ph, **29**; R = Ad = 1-adamantyl), **30**; are exposed to an

atmosphere of hydrogen, they are reduced to the corresponding bis(amide) complexes $(C_5Me_5)_2U(NHR)_2$ (**12**) (R = Ph, Ad,) [equation (26.84)]. The rate of hydrogenation of complex **30** was found to be much faster than that of complex **29**. When AdN_3 was added to a solution of the bis(amide) **12**, the bis(imido) **30** and $AdNH_2$ were formed [equation (26.85)]. Therefore, when complex **12** (R = Ad) was reacted with AdN_3 under an atmosphere of dihydrogen, catalytic hydrogenation of AdN_3 to $AdNH_2$ was observed (Scheme 26.32) (Peters *et al.*, 1999b).



N,N'-diphenylhydrazine was also used as the oxidant converting $(C_5Me_5)_2U(OMe)_2$ (**8**) to **29**. This reaction was shown to occur by the protonation of the methyl groups, liberating methane. When $(C_5Me_5)_2U(=NPh)_2$ was treated with an excess of *N,N'*-diphenylhydrazine in the absence of hydrogen, the substrate was entirely consumed, and aniline and azobenzene were observed to form in a 2:1 ratio [equation (26.86)]. This disproportionation indicated that the *N,N'*-diphenylhydrazine functioned as both oxidant and reductant. The formation of aniline during this reaction suggested that the $U(IV)$ bis(amide) **12** is formed and serves to reduce the hydrazine, although the only observed uranium species in solution throughout the reaction was $(C_5Me_5)_2U(=NPh)_2$, indicating that the oxidation from $U(IV)$ to $U(VI)$ is faster than the subsequent reduction (Peters *et al.*, 1999b).





Scheme 26.32 Catalytic reduction of azides by organouranium complexes.

This reaction is favored both enthalpically and entropically. The calculated ΔH_f for converting two molecules of *N,N'*-diphenylhydrazine to two molecules of aniline and one molecule of azobenzene is -14.6 kcal/mol. Entropy considerations also qualitatively favor product formation; two molecules of starting material are converted to three molecules of product.

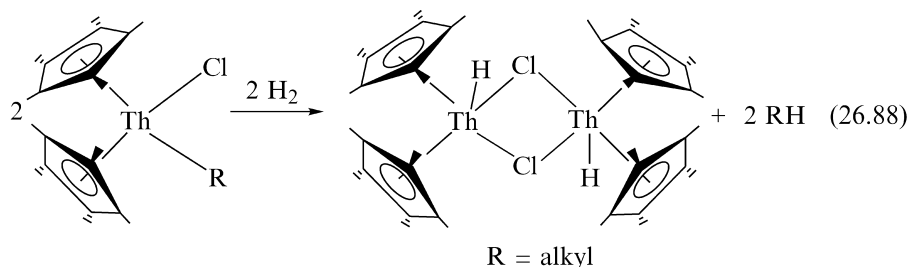
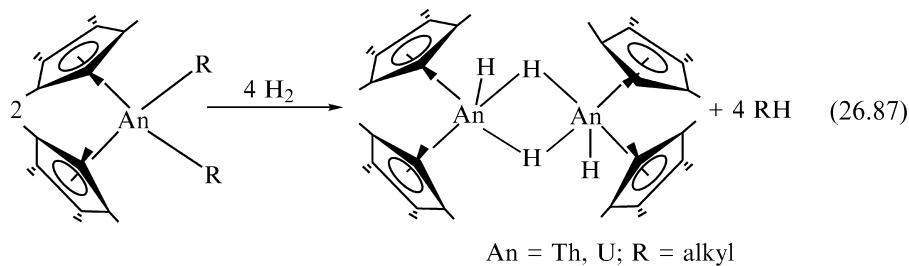
The catalytic activity of $(C_5Me_5)_2U(=NAd)_2$ (**30**) was also examined. The expectation was that if the mechanism of catalysis proceeds by protonation of the U(IV) bis(amide) by *N,N'*-diphenylhydrazine, similar to the reaction of *N,N'*-diphenylhydrazine with $(C_5Me_5)_2UMe_2$, initial product formation would include adamantylamine and azobenzene, with the concomitant formation of $(C_5Me_5)_2U(=NPh)_2$. However upon performing that reaction, $(C_5Me_5)_2U(=NAd)_2$, aniline and azobenzene were the only products observed, indicating that the imido ligands plausibly operated as sites for mediating H-atom transfer. No reaction was observed in the stoichiometric reaction of **29** with 1-adamantanamine ruling out the possibility of U–N bond rupture in which compound **29** is formed and undergoes subsequent rapid reaction with 1-adamantanamine regenerating **30** (Peters *et al.*, 1999a,b).

The catalytic transformations of substrates by two-electron processes are a novel type of reactivity for f-element complexes. The involvement of U(VI) species strongly argued for the requirement of f-orbital participation.

26.11 HYDROGENATION OF OLEFINS PROMOTED BY ORGANOACTINIDE COMPLEXES

The insertion of olefinic functionalities into metal–hydride bonds is an important step in various stoichiometric and homogeneous catalytic processes. A rich and versatile chemistry of organoactinide hydride complexes has been observed

for the complexes $(C_5Me_5)_2AnR_2$ ($An = Th, U; R = \text{alkyl}$). The formation of the hydride complexes has been obtained by hydrogenolysis of the corresponding organoactinide hydrocarbyl bonds [equations (26.87) and (26.88)] (Fagan *et al.*, 1981a,b; Marks, 1982, 1986a,b).

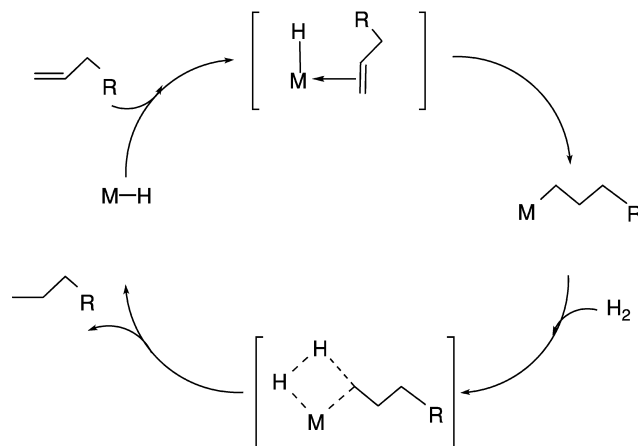


These reactions have been studied thoroughly, mechanistically following a four-center transition state. Kinetic studies show that the reaction displays a first-order dependence in both actinide complex and in dihydrogen (Lin and Marks, 1987, 1990).

The organoactinide hydrides of the type $[(C_5Me_5)_2AnH_2]_2$ react rapidly and quantitatively with olefins yielding the corresponding 1,2-addition product. For example, the hydride complex $[(C_5Me_5)_2UH_2]_2$ catalyzes the hydrogenation of 1-hexene at 25°C and 1 atm of H_2 in toluene with a turnover frequency of 63000 h^{-1} . Scheme 26.33 shows the proposed hydrogenation mechanism of alkenes. The mechanism was derived from kinetic investigations similar to the hydrogenations promoted by the organolanthanide hydride $[(C_5Me_5)_2Lu(\mu-H)]_2$.

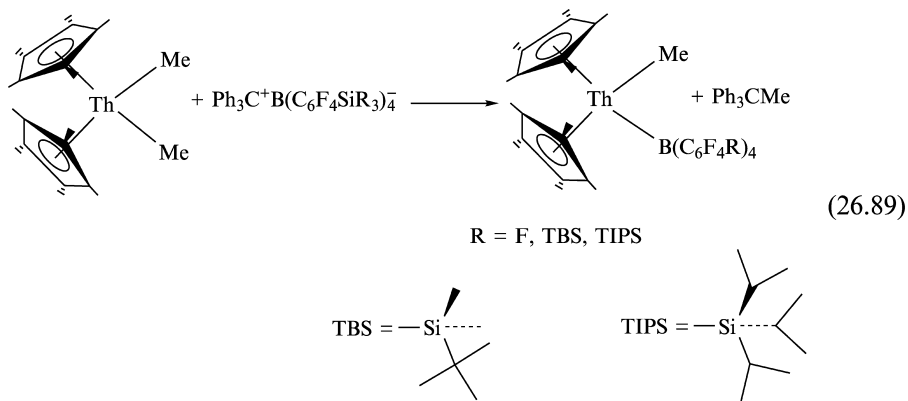
26.12 POLYMERIZATION OF α -OLEFINS BY CATIONIC ORGANOACTINIDE COMPLEXES

The synthesis of the cationic actinide complexes $[(C_5Me_5)_2ThMe][BPh_4]$ and $[(C_5Me_5)_2ThMe][B(C_6F_5)_4]$ has led to their study for the polymerization of ethylene and 1-hexene (Yang *et al.*, 1991). Mechanistically, the complexes $(C_5Me_5)_2AnMe_2$ ($An = Th, U$) react with a strong Lewis acid, like methylalumoxane (MAO), resulting in the formation of a cationic complex of the type $[(C_5Me_5)_2AnMe]^+[MAO-Me]^-$. These cationic complexes insert α -olefins many



Scheme 26.33 Proposed mechanism for the catalytic hydrogenation of alkenes promoted by $[(C_5Me_5)_2UH_2]_2$.

times before a β -hydrogen elimination or a β -methyl elimination occurs, producing polymers. For ethylene, high-density polyethylene has been obtained whereas for propylene, atactic polypropylene was the product. The search for different cocatalysts (instead of MAO) has brought the development of new and versatile perfluoroaromatic boron compounds. These highly coordinative unsaturated cationic organothorium complexes have been recently prepared and found active for the polymerization of olefins [equation (26.89)] (Jia *et al.*, 1994, 1997).



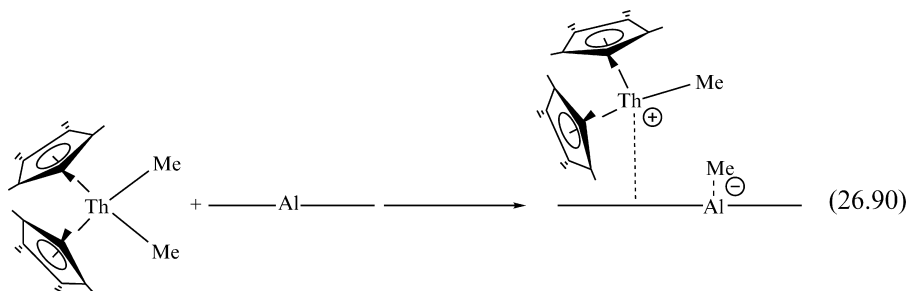
The reactivity of the organothorium complexes for the polymerization of ethylene follows the order: $[(C_5Me_5)_2ThMe][B(C_6F_5)_4] > [(C_5Me_5)_2ThMe]$

$[\text{B}(\text{C}_6\text{F}_4\text{TIPS})_4] > [(\text{C}_5\text{Me}_5)_2\text{ThMe}][\text{B}(\text{C}_6\text{F}_4\text{TBS})_4]$; however, their activity is an order of magnitude lower than that observed for the corresponding zirconium complexes.

26.13 HETEROGENEOUS SUPPORTED ORGANOACTINIDE COMPLEXES

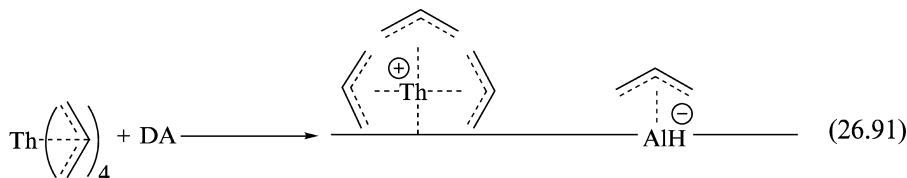
26.13.1 Hydrogenation of arenes by supported organoactinide complexes, kinetic, and mechanistic studies

Supporting homogeneous complexes on metal oxides creates a substantial alteration in their activity as compared to that observed in solutions (Iwasawa and Gates, 1989). For early transition metals (Yermakov *et al.*, 1981) and actinide alkyl complexes (Burwell and Marks, 1985; Finch *et al.*, 1990; Gillespie *et al.*, 1990; Marks, 1992) adsorbed upon metal oxide (e.g. alumina), large enhancements in the activities for catalytic hydrogenation were observed. The increase in coordinative unsaturation in metallocene organometallic-f-complexes generates a remarkable increase in the reactivity of these adsorbed complexes towards polymerization and hydrogenation of simple olefins, rivaling the activity of supported rhodium (He *et al.*, 1985; Marks, 1992), although these complexes are inefficient for the hydrogenation of arenes. Chemisorption of organoactinides involves the transfer of an alkyl group to the Al^{3+} (coordinatively unsaturated surfaces) sites and the formation of a 'cation-like' organothorium center as shown schematically in equation (26.90) (Jia *et al.*, 1997).



To address the question of how coordinatively unsaturated an organometallic-f-element complex was needed for the efficient reduction of arenes, a series of complexes of the type $\text{R}^1\text{R}_3^2\text{Th}$ ($\text{R}^1 = \eta^5 - (\text{CH}_3)_5\text{C}_5$; $\text{R}^2 = \text{CH}_2\text{C}_6\text{H}_5$; $\text{R}^1 = \text{R}^2 = 1, 3, 5 - (\text{CH}_3)_3\text{C}_6\text{H}_2$, $\text{R}^1 = \text{R}^2 = \eta^3 - \text{C}_3\text{H}_5$) chemisorbed on highly dehydroxylated γ -alumina (DA) were prepared (Eisen and Marks, 1992a). Presumably, the adsorption of these organometallic-f-complexes is similar as displayed in equation (26.90), transferring an allyl group from the

thorium coordination to the strong Lewis acid site at the surface [equation (26.91)].



The hydrogenation reactivity of the latter complexes towards the hydrogenation of arenes (Table 26.3) shows that faster rates of hydrogenation are observed for less sterically hindered substrates.

26.13.2 Assessment of the percentage of $\text{Th}(\eta^3\text{-C}_3\text{H}_5)_4/\text{DA}$ active sites

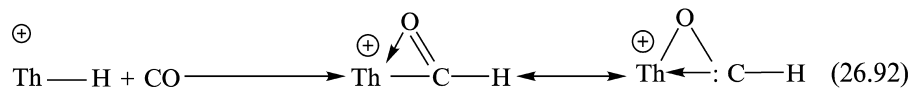
The percentage of supported organoactinide sites active in the olefin hydrogenation was estimated by dosing the catalyst with measured quantities of CO in a H_2 stream, measuring the amount of CO adsorbed by the catalyst, and determining the effect on subsequent catalytic activity. Similar results were found for $\text{H}_2\text{O}/\text{D}_2\text{O}$, and CH_3Cl poisoning experiments. The CO poisoning chemistry presumably involved migratory insertion equation (26.92) to produce surface η^2 -formyl, which may then undergo various possible subsequent reactions.

Table 26.3 Product and kinetic data for the $\text{Th}(\eta^3\text{-C}_3\text{H}_5)_4/\text{DA}$ catalyzed hydrogenation of various arenes^a

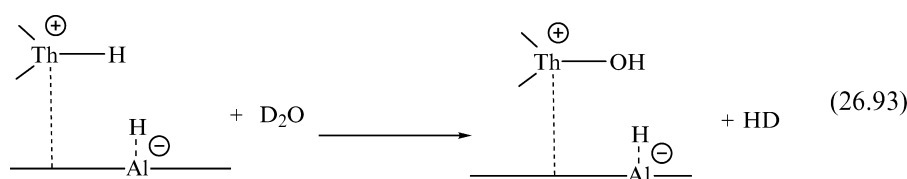
Substrate	Product	Turnover frequency (s^{-1})
C_6H_6	C_6H_{12}	6.80
C_6D_6	$\text{C}_6\text{H}_6\text{D}_6$	6.78
$\text{CH}_3\text{C}_6\text{H}_5$	$\text{CH}_3\text{C}_6\text{H}_{11}$	4.05 ^b
$\text{CD}_3\text{C}_6\text{D}_5$	$\text{CD}_{3-x}\text{H}_x\text{C}_6\text{H}_6\text{D}_5$	3.98 ^b
1,4- $(\text{CH}_3)_2\text{C}_6\text{H}_4$	 3 : 1	0.65 ^b
Naphthalene	 5 : 1	8.3×10^{-3}

^a $p\text{H}_2 = 190$ psi; [arene] = 10 mmol. Temp = 90°C .

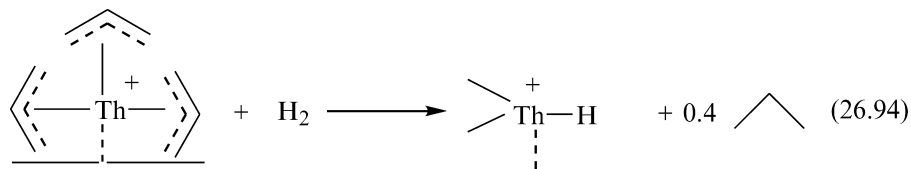
^b = values at 100% yield.



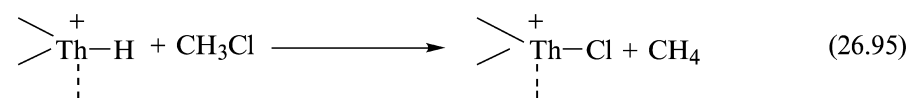
Additional confirmation of the estimated number of active sites was provided by measurement of the metal–hydride content by adding aliquots of D₂O, and studying the catalytic activity after each addition. This stepwise titration of active sites indicated that $8 \pm 1\%$ of the total Th($\eta^3\text{-C}_3\text{H}_5$)₄/DA sites present on the support were responsible for the majority of the catalysis [equation (26.93)].



Another additional complementary experiment for measuring the number of hydrides was undertaken by reacting the adsorbed Th($\eta^3\text{-C}_3\text{H}_5$)₄/DA with hydrogen and measuring the amount of organic gas recovery from the reaction. The amount of propane per thorium was found to be only 10% of the total amount expected [equation (26.94)]. No propylene was released from the reaction, indicating that the hydrogenation of propylene was extremely fast, and indeed, the turnover frequency for the hydrogenation of propylene was measured separately to be ($N_T(25^\circ\text{C}) = 25 \text{ s}^{-1}$).



The number of thorium hydride sites formed was confirmed to be the same by reaction with methyl chloride and measurement of the amount of methane per Th that was evolved from the reaction [equation (26.95)].

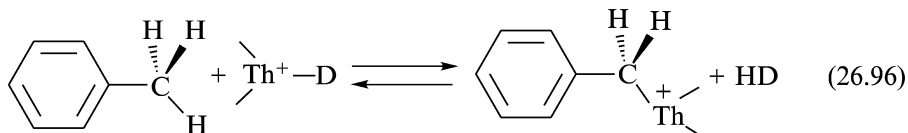


The importance of these poisoning experiments is that they indicate that only a very small fraction of the organothorium adsorbate sites on dehydroxylated alumina were responsible for the bulk of the catalytic reactivity. It is likely that one or more different structures of the suggested 'cation-like' organothorium moieties constitute the catalytic sites on alumina, but the exact structural characteristics defining these structures remain to be elucidated.

For arene hydrogenation, the kinetic data can be accommodated by three repetitions of a two-step sequence: (i) arene insertion (olefin insertion for the subsequent step) into a Th–H bond; (ii) hydrogenolysis of the resulting Th–alkyl bond. The kinetic data measured for benzene conforms to the rate law $N_t = k [\text{benzene}]^0 [\text{pH}_2]^1 [\text{Th}]^1$ (Th = tetraallyl complex). The kinetic isotope measurements for the hydrogenation of benzene indicated $N_t(\text{H}_2)/N_t(\text{D}_2) = 3.5 \pm 0.3$ at 90°C and 180 psi of H_2 . In the hydrogenation reaction of benzene with D_2 , the product $\text{C}_6\text{H}_6\text{D}_6$ was obtained as a mixture of two geometric isomers as refers to the disposition of the deuterium atoms: *all cis* and *cis, cis, trans, cis, trans* in a ratio of 1:3 respectively. The Arrhenius activation energies for the catalytic hydrogenation of benzene was measured to be $16.7 \pm 0.3 \text{ kcal mol}^{-1}$ and the corresponding thermodynamic activation parameters were $\Delta H^\ddagger = 16.0 \pm 0.3 \text{ kcal/mol}$ and $\Delta S^\ddagger = 32.3 \pm 0.6 \text{ eu}$ (Eisen and Marks, 1992).

The mechanism proposed for the hydrogenation of arenes is described in Scheme 26.34. The process takes into account the lack of facial selectivity by which the ratio 1:3 among the geometrical isomers were formed. As a function of substrate, the relative rates of $\text{Th}(\eta^3\text{-C}_3\text{H}_5)_4/\text{DA}$ -catalyzed hydrogenation of arenes was found to be in the order benzene > toluene > *p*-xylene > naphthalene.

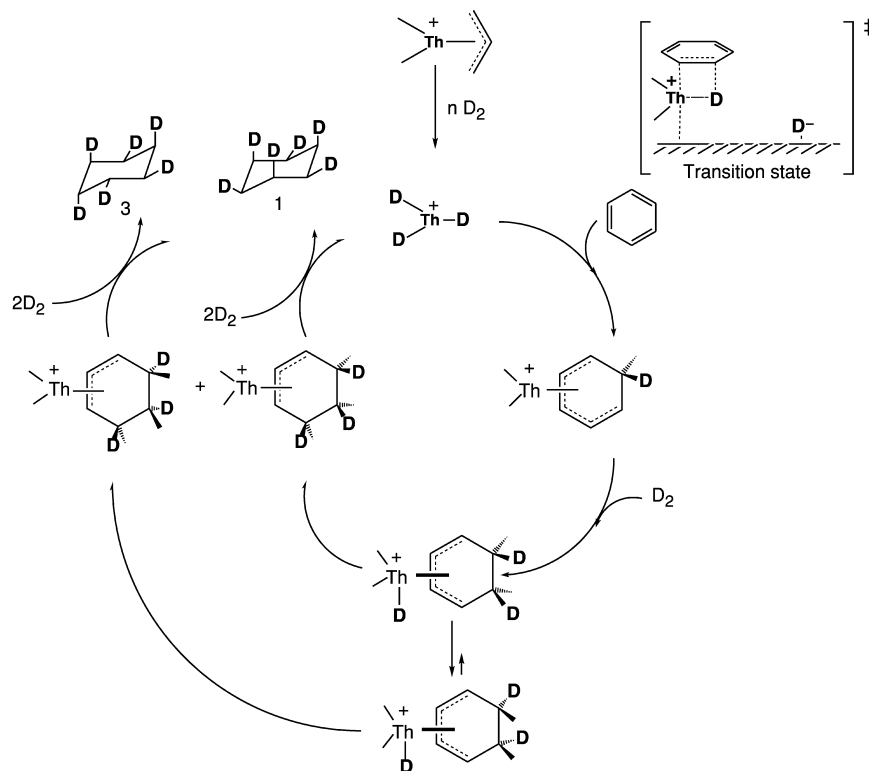
In the hydrogenation of benzene no H/D scrambling is observed during the process but H/D scrambling is observed after complete hydrogenation of the starting material. In the reaction between toluene- d_8 and H_2 or toluene and D_2 significant C–H/C–D exchange at the benzylic positions was observed during the hydrogenation. Significant incorporation of deuterium atoms into the starting toluene and subsequently into the cyclohexane product was observed at partial conversions. The C–H/C–D exchange was suggested to occur through a benzylic activation as shown in equation (26.96).



Competition experiments confirmed the large kinetic discrimination for the different arenes. The hydrogenation reaction of equimolar quantities of *p*-xylene and benzene yielded cyclohexane with almost complete selectivity (97%) and a mixture of 3:1 *cis:trans* 1,4-dimethylcyclohexane (3%).

26.13.3 Facile and selective alkane activation by supported tetraallylthorium

C–H activation processes involving alkanes are considered high-energy demanding transformations. Although significant advances have been made in the functionalization of C–H bonds by f- and early transition complexes (Shilov, 1984; Gillespie *et al.*, 1990; Ryabov, 1990; Watson, 1990; Basset *et al.*, 1998;

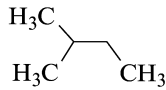
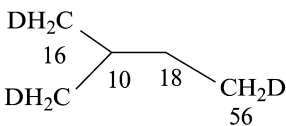
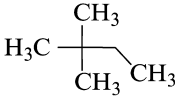
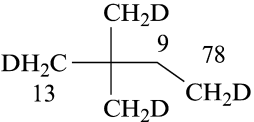
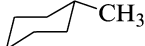
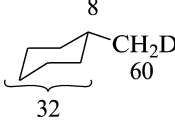
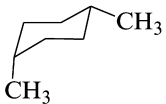
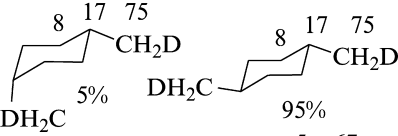
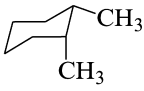
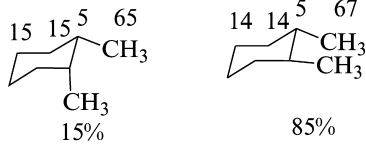


Scheme 26.34 Proposed mechanism for the hydrogenation of arenes by cationic supported organoactinide complexes.

Schneider *et al.*, 2001), the catalytic intermolecular activation of inert alkane molecules with favorable rates and selectivities is still a major challenge. As noted above, studies on benzene reduction with D_2 revealed C–H/C–D exchange in the cyclohexane product only after benzene conversion was complete. This observation prompted detailed studies of the activation of hydrocarbons. The results from slurry reaction studies of C–H/C–D exchange for a variety of alkanes catalyzed by thorium tetraallyl complex/DA under a D_2 atmosphere are summarized in Table 26.4 (Eisen and Marks, 1992b).

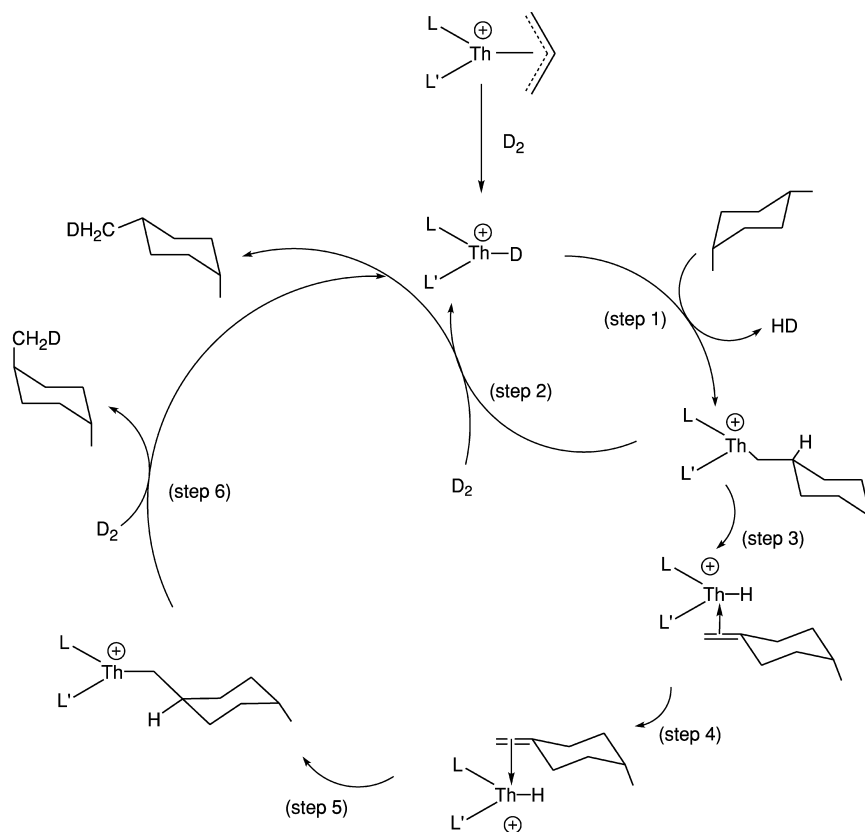
Rapid C–H/C–D exchange was promoted by the tetraallyl complex/DA, with turnover frequencies comparable to or exceeding those of conventional group 9 heterogeneous alkane activation catalysts (Butt and Burwell, 1992). C–H functionalization occurred with substantial selectivity and in an order which does not parallel the C–H bond dissociation energies: primary > secondary > tertiary,

Table 26.4 Kinetic and product structure/deuterium distribution data for $\text{Th}(\eta^3\text{-C}_3\text{H}_5)_4/\text{DA}$ catalyzed C–H/C–D functionalization.

Substrate	Deuterium distribution in product (%)	Turnover frequency (h^{-1})
$\text{CH}_3\text{CH}_2\text{CH}_2\text{CH}_2\text{CH}_3$	$\text{CH}_2\text{DCHDCHDCHDC}_2\text{H}_5$ 58 32 10	778
		879
		825
C_6H_{12}	$\text{C}_6\text{H}_{12-x}\text{D}_x$	1285
		1113
		884
		834

and sterically less hindered > sterically more hindered. NMR and GC-MS measurements as a function of conversion indicated single C–H exchanges, with no evidence for multiple exchange processes (e.g. non-statistical amounts of RD_2 species). Unexpectedly, the CH/CD exchange reaction of *cis*-dimethylcyclohexanes produced isomerization towards a *cis*–*trans* mixture. Based on the same two reasonable assumptions as for the arene hydrogenation, a plausible mechanistic scenario for the activation and isomerization of alkanes was proposed and summarized in Scheme 26.35. The mechanistic sequence invokes presumably endothermic Th–C bond formation and HD elimination via a ‘four-center’, heterolytic ‘ σ -bond metathesis’ (step 1), followed by deuterolysis

(step 2). Cycloalkane skeletal isomerization would then occur via a β -H elimination (step 3) and re-addition of the $\text{Th}^+\text{-H}$ to the opposite face of the double bond (step 4). This process would involve the rapid dissociation and re-addition of the alkene, although other mechanisms have been proposed as conceivable. Insertion (step 5) and deuterolysis (step 6) produced the isomerized cycloalkane. The isotopic labeling experiments revealed little D incorporation at the dimethylcyclohexane tertiary carbon centers and negligible differences in the D label distribution of the isomerized and un-isomerized hydrocarbons. These results indicated that the ancillary ligands L and L' in Scheme 26.35 are either non-D in identity (e.g. η^3 -allyl or oxide), or that such Th-D functionalities were chemically and stereochemically inequivalent to that formed in a β -H abstraction, since they do not compete for olefin addition.



Scheme 26.35 Proposed scenario for the $\text{Th}(\eta^3\text{-allyl})_4/\text{DA}$ -catalyzed C-H activation and isomerization of alkanes.

In summary, these results demonstrate that supported organo-f-complexes are extremely active catalysts for a number of high-energy organic chemistry transformations.

ACKNOWLEDGMENTS

C. J. B. gratefully acknowledges support at LANL by the U.S. Department of Energy, Office of Science, Office of Basic Energy Sciences, Division of Chemical Sciences, Geosciences, and Biosciences. M. S. E. thanks the Fund for the Promotion of Research at The Technion.

REFERENCES

- Aitken, C., Barry, J. P., Gauvin, F. G., Harrod, J. F., Malek, A., and Rousseau, D. (1989) *Organometallics*, **8**, 1732–6.
- Anwender, R. (1996) in *Applied Homogeneous Catalysis with Organometallic Compounds*, vol. 2 (eds. B. Cornils and W. A. Herrmann) VCH Publishers, New York.
- Anwender, R. and Herrman, W. A. (1996) *Top. Curr. Chem.*, **179**, 1–32.
- Apeloig, Y. (1989) in *The Chemistry of Organic Silicon Compounds* (eds. S. Patai and Z. Rappoport), Wiley-Interscience, New York, pp. 57–225.
- Arney, D. S. J., Burns, C. J., and Smith, D. C. (1992) *J. Am. Chem. Soc.*, **114**, 10068–9.
- Arney, D. S. J. and Burns, C. J. (1993) *J. Am. Chem. Soc.*, **115**, 9840–1.
- Arney, D. S. J. and Burns, C. J. (1995) *J. Am. Chem. Soc.*, **117**, 9448–60.
- Arredondo, V. M., Tian, S., McDonald, F. E., and Marks, T. J. (1999a) *J. Am. Chem. Soc.*, **121**, 3633–9.
- Arredondo, V. M., McDonald, F. E., and Marks, T. J. (1999b) *Organometallics*, **18**, 1949–60.
- Asao, N., Sudo, T., and Yamamoto, Y. (1996) *J. Org. Chem.*, **61**, 7654–5.
- Bajgur, C. S., Tikkanen, W. R., and Petersen, J. L. (1985) *Inorg. Chem.*, **24**, 2539–46.
- Baranger, A. M., Walsh, P. J., and Bergman, R. G. (1993) *J. Am. Chem. Soc.*, **115**, 2753–63.
- Basset, J. M., Lefebvre, F., and Santini, C. (1998) *Coord. Chem. Rev.*, **178–180**, 1703–23.
- Berthet, J. C., Boisson, C., Lance, M., Vigner, J., Nierlich, M., and Ephritikhine, M. (1995) *J. Chem. Soc., Dalton Trans.*, 3019–25.
- Berthet, J. C. and Ephritikhine, M. (1998) *Coord. Chem. Rev.*, **178–180**, 83–116.
- Biran, C., Blum, Y. D., Glaser, R., Tse, D. S., Youngdahl, K. A., and Laine, R. M. (1988) *J. Mol. Catal.*, **48**, 183–97.
- Blake, P. C., Edelman, M. A., Hitchcock, P. B., Hu, J., Lappert, M. F., Tian, S., Müller, G., Atwood, J. L., and Zhang, H. (1998) *J. Organomet. Chem.*, **551**, 261–70.
- Blum, Y. and Laine, R. M. (1986) *Organometallics*, **5**, 2081–6.
- Bode, B. M., Day, P. N., and Gordon, M. S. (1998) *J. Am. Chem. Soc.*, **120**, 1552–5.
- Brennan, J. G. and Andersen, R. A. (1985) *J. Am. Chem. Soc.*, **107**, 514–16.
- Brook, A. G. and Bassindale, A. R. (1980) in *Rearrangements in Ground and Excited States*, vol. 2, Academic Press, New York.

- Bruno, J. W., Marks, T. J., and Morss, L. R. (1983) *J. Am. Chem. Soc.*, **105**, 6824–32.
- Bruno, J. W., Smith, G. M., and Marks, T. J. (1986) *J. Am. Chem. Soc.*, **108**, 40–56.
- Buergestein, M. R., Berberich, H., and Roesky, P. W. (1998) *Organometallics*, **17**, 1452–4.
- Burns, C. J., Smith, W., Huffman, J. C., and Sattelberger, A. P. (1990) *J. Am. Chem. Soc.*, **112**, 3237–9.
- Bursten, B. E. and Strittmatter, R. J. (1991) *Angew. Chem. Int. Edn. Engl.*, **30**, 1069–85.
- Burwell, R. L. Jr and Marks, T. J. (1985) in *Catalysis of Organic Reactions* (ed. R. L. Augustine), Marcel Dekker, New York, pp. 207–24.
- Butt, J. B. and Burwell, R. L. Jr (1992) *Catal. Today*, **12**, 177–88.
- Chalk, A. J. and Harrod, J. F. (1965) *J. Am. Chem. Soc.*, **87**, 16–21.
- Chan, T. H. (1977) *Acc. Chem. Res.*, **10**, 442–8.
- Chen, Y.-X., Metz, M. V., Li, L., Stern, C. L., and Marks, T. J. (1998) *J. Am. Chem. Soc.*, **120**, 6287–305.
- Collman, J. P., Hegedus, L. S., Norton, J. R., and Finke, R. G. (1987) *Principles and Applications of Organotransition Metal Chemistry*, University Science, Mill Valley, CA, chs 6, 10, and 13.
- Colvin, E. W. (1988) *Silicon Reagents in Organic Synthesis*, Academic Press, London.
- Corey, J. Y., Huhmann, J. L., and Zhu, X.-H. (1993) *Organometallics*, **12**, 1121–30.
- Cramer, R. E., Roth, S., and Gilje, J. W. (1989a) *Organometallics*, **8**, 2327–30.
- Cramer, R. E., Roth, S., Edelmann, F., Bruck, M. A., Cohn, K. C., and Gilje, J. W. (1989b) *Organometallics*, **8**, 1192–9.
- Dash, A. K., Wang, J. Q., and Eisen, M. S. (1999) *Organometallics*, **18**, 4724–41.
- Dash, A. K., Wang, J. X., Berthet, J. C., Ephritikhine, M. and Eisen, M. S. (2000) *J. Organomet. Chem.*, **604**, 83–98.
- Dash, A. K., Gourevich, I., Wang, J. Q., Wang, J., Kapon, M., and Eisen, M. S. (2001) *J. Am. Chem. Soc.*, **20**, 5084–104.
- Den Haan, K. H., Wielstra, Y., and Teuben, J. H. (1987) *Organometallics*, **6**, 2053–60.
- Douglass, M. R., Ogasawara, M., Hong, S., Metz, M. V., and Marks, T. J. (2002) *Organometallics*, **21**, 283–92.
- Duckett, S. B. and Perutz, R. N. (1992) *Organometallics*, **11**, 90–98.
- Duttera, M. R., Day, V. W., and Marks, T. J. (1984) *J. Am. Chem. Soc.*, **106**, 2907–12.
- Edelman, M. A., Hitchcock, P. B., Hu, J., and Lappert, M. F. (1995) *New J. Chem.*, **19**, 481–9.
- Edelmann, F. T. (1995b) in *Comprehensive Organometallic Chemistry II* (eds. E. W. Abel, F. G. A. Stone, and G. Wilkinson), Pergamon Press, Oxford, ch. 4.
- Edelmann, F. T. (1996) *Top. Curr. Chem.*, **179**, 247–76.
- Edelmann, F. T. and Gun'ko, Y. (1997) *Coord. Chem. Rev.*, **165**, 163–237.
- Edelmann, F. T. and Lorenz, V. (2000) *Coord. Chem. Rev.*, **209**, 99–160.
- Eigenbrot, C. W. and Raymond, K. N. (1982) *Inorg. Chem.*, **21**, 2653–60.
- Eisen, M. S. and Marks, T. J. (1992a) *J. Am. Chem. Soc.*, **114**, 10358–68.
- Eisen, M. S. and Marks, T. J. (1992b) *Organometallics*, **11**, 3939–41.
- Eisen, M. S. (1997) *Rev. Inorg. Chem.*, **17**, 25–52.
- Eisen, M. S. (1998) in *The Chemistry of Organosilicon Compounds*, vol. 2 (eds. Y. Apeloig, and Z. Rappoport), John Wiley, Chichester, pp. 2038–122, part 3, ch. 35.
- Eisen, M. S., Straub, T., and Haskel, A. (1998) *J. Alloys Compd.*, **271–273**, 116–22.
- Elschenbroich, Ch. and Salzer, A. (1989) *Organometallics*, VCH, Weinheim, Germany, ch. 17.

- Ephritikhine, M. (1997) *Chem. Rev.*, **97**, 2193–242.
- Esteruelas, M. A., Nurnberg, O., Olivian, M., Oro, L. A. and Werner, H. (1993) *Organometallics*, **12**, 3264–72.
- Evans, W. J., Bloom, I., Hunter, W. E., and Atwood, J. L. (1983) *Organometallics*, **2**, 709–14.
- Evans, W. J., Drummond, D. K., Hanusa, T. P., and Olofson, J. M. (1989) *J. Organomet. Chem.*, **376**, 311–20.
- Fagan, P. J., Manriquez, J. M., Maata, E. A., Seyam, A. M., and Marks, T. J. (1981a) *J. Am. Chem. Soc.*, **103**, 6650–67.
- Fagan, P. J., Manriquez, J. H., Vollmer, S. H., Day, C. S., Day, V. W., and Marks, T. J. (1981b) *J. Am. Chem. Soc.*, **103**, 2206–20.
- Faller, J. W. and Rosan, A. M. (1977) *J. Am. Chem. Soc.*, **99**, 4858–9.
- Fendrick, C. M., Mintz, E. A., Schertz, L. D., Marks, T. J., and Day, V. W. (1984) *Organometallics*, **3**, 819–21.
- Fendrick, C. A., Schertz, L. D., Day, V. W., and Marks, T. J. (1988) *Organometallics*, **7**, 1828–38.
- Finch, W. C., Gillespie, R. D., Hedden, D., and Marks, T. J. (1990) *J. Am. Chem. Soc.*, **112**, 6221–32.
- Fleming, I., Dunogues, J., and Smithers, R. H. (1989) *Org. React.*, **37**, 57–575.
- Forsyth, C. M., Nolan, S. P., and Marks, T. J. (1991) *Organometallics*, **10**, 2543–5.
- Fu, P.-F. and Marks, T. J. (1995) *J. Am. Chem. Soc.*, **117**, 10747–8.
- Gagné, M. R. and Marks, T. J. (1989) *J. Am. Chem. Soc.*, **111**, 4108–9.
- Gagné, M. R., Stern, C. L., and Marks, T. J. (1992a) *J. Am. Chem. Soc.*, **114**, 275–94.
- Gagné, M. R., Brard, L., Conticello, V. P., Giardello, M. A., Stern, C. L., and Marks, T. J. (1992b) *Organometallics*, **11**, 2003–5.
- Giardello, M. A., King, W. A., Nolan, S. P., Porchia, M., Sishita, C., and Marks, T. J. (1992) in *Energetics of Organometallic Species* (ed. J. A. Martinho Simões), Kluwer Academic Press, Dordrecht, The Netherlands, pp. 35–51.
- Giardello, M. A., Conticello, V. P., Brard, L., Gagné, M. R., and Marks, T. J. (1994) *J. Am. Chem. Soc.*, **116**, 10241–54.
- Gillespie, R. D., Burwell, R. L. Jr, and Marks, T. J. (1990) *Langmuir*, **6**, 1465–77.
- Haar, C. M., Stern, C. L., and Marks, T. J. (1996) *Organometallics*, **15**, 1765–84.
- Haggin, J. (1993) *Chem. Eng. News*, **17(22)**, 23.
- Harrod, J. F. and Chalk, A. J. (1965) *J. Am. Chem. Soc.*, **87**, 1133–5.
- Harrod, J. F. (1991) in *Inorganic and Organometallic Polymers with Special Properties* (ed. R. M. Lain), Kluwer Academic Publishers, Amsterdam, ch. 14.
- Haskel, A., Straub, T., and Eisen, M. S. (1996) *Organometallics*, **15**, 3773–6.
- Haskel, A., Wang, J. Q., Straub, T., Gueta-Neyroud, T., and Eisen, M. S. (1999) *J. Am. Chem. Soc.*, **121**, 3025–34.
- Hays, D. S. and Fu, G. C. (1997) *J. Org. Chem.*, **62**, 7070–1.
- He, M.-Y., Xiong, G., Toscano, P. J., Burwell, R. L. Jr, and Marks, T. J. (1985) *J. Am. Chem. Soc.*, **107**, 641–52.
- He, J., Liu, H. Q., Harrod, J. F., and Hynes, R. (1994) *Organometallics*, **13**, 336–43.
- Heeres, H. J., Heeres, A., and Teuben, J. H. (1990) *Organometallics*, **9**, 1508–10.
- Heeres, H. J. and Teuben, J. H. (1991) *Organometallics*, **10**, 1980–6.
- Hegedus, L. S. (1995) in *Comprehensive Organometallic Chemistry II*, vol. 12 (eds. E. W. Abel, F. G. A. Stone, and G. Wilkinson), Pergamon Press, Oxford.

- Hitchcock, P. B., Hu, J., Lappert, M. F., and Tian, S. (1997) *J. Organomet. Chem.*, **536–537**, 473–80.
- Hiyama, T. and Kusumoto, T. (1991) in *Comprehensive Organic Synthesis*, vol 8 (eds. B. M. Trost and I. Fleming), Pergamon Press, Oxford.
- Hong, S. and Marks, T. J. (2002) *J. Am. Chem. Soc.*, **124**, 7886–7.
- Ihara, E., Nodono, M., Yasuda, H., Kanehisa, N., and Kai, Y. (1996) *Macromol. Chem. Phys.*, **197**, 1909–17.
- Iwasawa, Y. and Gates, B. C. (1989) *CHEMTEC*, **3**, 173–81.
- Jemine, X., Goffart, J., Berthet, J.-C., and Ephritikhine, M., Fuger, J. (1992) *J. Chem. Soc., Dalton Trans.*, 2439–44.
- Jemine, X., Goffart, J., Ephritikhine, M., and Fuger, J. (1993) *J. Organomet. Chem.*, **448**, 95–8.
- Jeske, C., Lauke, H., Mauermann, H., Schumann, H., and Marks, T. J. (1985a) *J. Am. Chem. Soc.*, **107**, 8111–18.
- Jeske, C., Schock, L. E., Mauermann, H., Swepston, P. N., Schumann, H., and Marks, T. J. (1985b) *J. Am. Chem. Soc.*, **107**, 8103–10.
- Jeske, G., Schock, L. E., Swepson, P. N., Schumann, H., and Marks, T. J. (1985c) *J. Am. Chem. Soc.*, **107**, 8091–103.
- Jia, J., Yang, X., Stern, C. L., and Marks, T. J. (1994) *Organometallics*, **13**, 3755–7.
- Jia, J., Yang, X., Stern, C. L., and Marks, T. J. (1997) *Organometallics*, **16**, 842–57.
- King, W. A., Marks, T. J., Anderson, D. M., Duncalf, D. J., and Cloke, F. G. N. (1992) *J. Am. Chem. Soc.*, **114**, 9221–3.
- King, W. and Marks, T. J. (1995) *Inorg. Chim. Acta.*, **229**, 343–54.
- Lappert, M. F., Power, P. P., Sanger, A. R., and Srivastava, R. C. (1980) in *Metal and Metalloid Amides: Synthesis, Structures, and Physical and Chemical Properties*, Ellis Horwood-Wiley, Chichester, New York, chs 12 and 13.
- Leal, J. P., Marquez, N., Pires de Matos, A., Caldhorda, M. J., Galvão, J. A., and Martinho Simões, J. A. (1992) *Organometallics*, **11**, 1632–7.
- Leal, J. P. and Martinho Simões, J. A. (1994) *J. Chem. Soc., Dalton Trans.*, 2687–91.
- Leal, J. P., Marquez, N., and Takats, J. (2001) *J. Organomet. Chem.*, **632**, 209–14.
- Li, Y. and Marks, T. J. (1996) *Organometallics*, **15**, 3770–3.
- Li, Y. and Marks, T. J. (1998) *J. Am. Chem. Soc.*, **120**, 1757–71.
- Lin, Z. and Marks, T. J. (1987) *J. Am. Chem. Soc.*, **109**, 7979–85.
- Lin, Z. and Marks, T. J. (1990) *J. Am. Chem. Soc.*, **112**, 5515–25.
- Liu, H. Q. and Harrod, J. F. (1992) *Organometallics*, **11**, 822–7.
- Liu, X., Wu, Z., Peng, Z., Wu, Y.-D., and Xue, Z. (1999) *J. Am. Chem. Soc.*, **121**, 5350–1.
- Lunzer, F., Marschner, C., and Landgraf, S. (1998) *J. Organomet. Chem.*, **568**, 253–5.
- Marçalo, J. and Pires de Matos, A. (1989) *Polyhedron*, **8**, 2431–7.
- Marciniec, B., Gulinsky, J., Urbaniak, W., and Kornetka, Z. W. (1992) *Comprehensive Handbook on Hydrosilylation* (ed. B. Marciniec), Pergamon, Oxford.
- Marks, T. J. (1982) *Science*, **217**, 989–97.
- Marks, T. J. and Day, V. W. (1985) in *Fundamental and Technological Aspects of Organo-f-Element Chemistry* (eds. T. J. Marks and I. L. Fragalà), Reidel, Dodrecht, ch 4.
- Marks, T. J. (1986a) in *The Chemistry of the Actinide Elements*, vol. 2 (eds. J. J. Katz, J. T. Seaborg, and L. R. Morss), Chapman & Hall, London; New York, ch. 22.

- Marks, T. J. (1986b) in *The Chemistry of the Actinide Elements*, vol. 2 (eds. J. J. Katz, J. T. Seaborg, and L. R. Morss), Chapman & Hall, London; New York, ch. 23.
- Marks, T. J., Gagné, M. R., Nolan, S. P., Schock, L. E., Seyam, A. M., and Stern, D. (1989) *Pure Appl. Chem.*, **61**, 1665–72.
- Marks, T. J. (1992) *Acc. Chem. Res.*, **25**, 57–65.
- Marthino Simões, J. A. and Beauchamp, J. L. (1990) *Chem. Rev.*, **90**, 629–88.
- Mitchell, J. P., Hajela, S., Brookhart, S. K., Hardcastle, K. I., Henling, L. M., and Bercaw, J. E. (1996) *J. Am. Chem. Soc.*, **118**, 1045–53.
- Molander, G. A. and Hoberg, J. O. (1992) *J. Am. Chem. Soc.*, **114**, 3123–5.
- Molander, G. A. and Winterfeld, J. (1996) *J. Organomet. Chem.*, **524**, 275–9.
- Molander, G. A. and Knight, E. E. (1998) *J. Org. Chem.*, **63**, 7009–12.
- Molander, G. A. (1998) *Chemtracs: Org. Chem.*, **11**, 237–63.
- Molander, G. A. and Dowdy, E. D. (1999) *J. Org. Chem.*, **64**, 6515–17.
- Molander, G. A. and Romero, J. A. C. (2002) *Chem. Rev.*, **102**, 2161–86.
- Nobis, M. and Driessen-Hölscher, B. (2001) *Angew. Chem., Int. Edn.*, **40**, 3983–5.
- Nolan, S. P., Stern, D., Hedden, D., and Marks, T. J. (1990) *ACS Symp. Ser.*, **428**, 159–74.
- Ohff, A., Burlakov, V. V., and Rosenthal, U. (1996) *J. Mol. Catal.*, **108**, 119–23.
- Ojima, I., Li, Z., and Zhu, J. (1998) in *The Chemistry of Organic Silicon Compounds* (eds. Z. Rappoport and Y. Apeloig), John Wiley, New York, ch. 29, and references therein.
- O'Shaughnessy, P. N., Knight, P. D., Morton, C., Gillespie, K. M., and Scott, P. (2003) *Chem. Commun.*, **14**, 1770–1.
- Pelletier, J.-F., Mortreux, A., Olonde, X., and Bujadoux, K. (1996) *Angew. Chem. Int. Edn. Engl.*, **35**, 1854–6.
- Peters, R. G., Warner, B. P., Scott, B. L., and Burns, C. J. (1999a) *Organometallics*, **18**, 2587–9.
- Peters, R. G., Warner, B. P., and Burns, C. J. (1999b) *J. Am. Chem. Soc.*, **121**, 5585–6.
- Pohlki, F. and Doye, S. (2003) *Chem. Soc. Rev.*, **32**, 104–14.
- Radu, N. S., Engeler, M. P., Gerlach, C. P., Tilley, T. D., and Rheingold, A. L. (1995) *J. Am. Chem. Soc.*, **117**, 3621–2.
- Reichl, J. and Berry, D. H. (1998) *Adv. Organomet. Chem.*, **43**, 197–265.
- Roesky, P. W., Denninger, U., Stern, C. L., and Marks, T. J. (1997a) *Organometallics*, **16**, 4486–92.
- Roesky, P. W., Stern, C. L., and Marks, T. J. (1997b) *Organometallics*, **16**, 4705–11.
- Ruiz, J., Bentz, P. O., Mann, B. E., Spencer, C. M., and Taylor, B. F., Maitlis, P. M. (1987) *J. Chem. Soc., Dalton Trans.*, 2709–13.
- Ryabov, A. D. (1990) *Chem. Rev.*, **90**, 403–24.
- Ryu, J. S., Marks, T. J., and McDonald, F. E. (2001) *Org. Lett.*, **3**, 3091–4.
- Sakaki, S., Mizoe, N., and Sugimoto, M. (1998) *Organometallics*, **17**, 2510–23.
- Samsel, E. G. (1993) Patent Application EP 574854.
- Schaverien, C. J. (1994) *Organometallics*, **13**, 69–82.
- Schnabel, R. C., Scott, B. L., Smith, W. H., and Burns, C. J. (1999) *J. Organomet. Chem.*, **591**, 14–23.
- Schneider, H., Puchta, G. T., Kaul, F. A. R., Raudaschl-Sieber, G., Lefebvre, F., Saggio, G., Mihalios, D., Hermann, W. A., and Basset, J. M. (2001) *J. Mol. Catal. A: Chem.*, **170**, 127–41.

- Schumann, H., Keitsch, M. R., Demtschuk, J., and Molander, G. A. (1999) *J. Organomet. Chem.*, **582**, 70–82.
- Seayad, A. M., Selvakumar, K., Ahmed, M., and Beller, M. (2003) *Tetrahedron Lett.*, **44**, 1679–83.
- Seitz, F. and Wrighton, M. S. (1988) *Angew. Chem., Int. Edn. Engl.*, **27**, 289–91.
- Selin, T. J. and West, R. (1962) *J. Am. Chem. Soc.*, **84**, 1860–3.
- Shannon, R. D. (1976) *Acta Crystallogr.*, **A32**, 751–67.
- Shen, Q., Zheng, D., Lin, L., and Lin, Y. (1990) *J. Organomet. Chem.*, **391**, 307–12.
- Shilov, A. E. (1984) *Activation of Saturated Hydrocarbons by Transition Metal Complexes*, Reidel, Hingham, MA.
- Smith, G. M., Carpenter, J. D., and Marks, T. J. (1986a) *J. Am. Chem. Soc.*, **108**, 6805–7.
- Smith, G. M., Susuki, H., Sonnenberg, D. C., Day, V. W., and Marks, T. J. (1986b) *Organometallics*, **5**, 549–61.
- Straub, T., Haskel, A., and Eisen, M. S. (1995) *J. Am. Chem. Soc.*, **117**, 6364–5.
- Straub, T. R. G., Frank, W., and Eisen, M. S. (1996) *J. Chem. Soc., Dalton Trans.*, 2541–6.
- Straub, T., Haskel, A., Dash, A. K., and Eisen, M. S. (1999) *J. Am. Chem. Soc.*, **121**, 3014–24.
- Straub, T., Haskel, A., Neyroud, T. G., Kapon, M., Botoshansky, M., and Eisen, M. S. (2001) *Organometallics*, **20**, 5017–35.
- Stubbert, B. D., and Stern, C. L., Marks, T. J. (2003) *Organometallics*, **22**, 4836–8.
- Sudo, T., Asao, N., Gevorgyan, V., and Yamamoto, Y. (1999) *J. Org. Chem.*, **64**, 2494–9.
- Takeuchi, R. and Tanouchi, N. (1994) *J. Chem. Soc., Perkin Trans. 1*, 2909–13.
- Takeuchi, R. and Yasue, H. (1996) *Organometallics*, **15**, 2098–102.
- Tanke, R. S. and Crabtree, R. H. (1991) *Organometallics*, **10**, 415–18.
- Tian, S., Arredondo, V. M., Stern, C. L., and Marks, T. J. (1999) *Organometallics*, **18**, 2568–70.
- Tilley, T. D. (1993) *Acc. Chem. Res.*, **26**, 22–9.
- Trost, B. M. and Tang, W. J. (2003) *J. Am. Chem. Soc.*, **125**, 8744–5.
- Utsonomiya, M., Kuwano, R., Kawatsura, M., and Hartwig, J. F. (2003) *J. Am. Chem. Soc.*, **125**, 5608–9.
- Walsh, P. J., Baranger, A. M., and Bergman, R. G. (1992) *J. Am. Chem. Soc.*, **114**, 1708–19.
- Walsh, P. J., Hollander, F. J., and Bergman, R. G. (1993) *Organometallics*, **12**, 3705–23.
- Wang, W. D. and Eisenberg, R. (1991) *Organometallics*, **10**, 2222–7.
- Wang, J. Q., Dash, A. K., Berthet, J. C., Ephritikhine, M., and Eisen, M. S. (1999) *Organometallics*, **18**, 2407–9.
- Wang, J. X., Dash, A. K., Berthet, J. C., Ephritikhine, M., and Eisen, M. S. (2000) *J. Organomet. Chem.*, **610**, 49–57.
- Wang, J., Dash, A. K., Kapon, M., Berthet, J. C., Ephritikhine, M., and Eisen, M. S. (2002a) *Chem. Eur. J.*, **8**, 5384–96.
- Wang, J., Kapon, M., Berthet, J. C., Ephritikhine, M., and Eisen, M. S. (2002b) *Inorg. Chim. Acta*, **344**, 183–92.
- Wang, J. Q. and Eisen, M. S. (2003) unpublished results.
- Warner, B. P., Scott, B. L., and Burns, C. J. (1998) *Angew. Chem., Int. Edn. Engl.*, **37**, 959–60.

- Watson, P. L. and Parshall, G. W. (1985) *Acc. Chem. Res.*, **18**, 51–6.
- Watson, P. L. (1990) in *Selective Hydrocarbon Activation* (eds. J. A. Davies, P. L. Watson, J. F. Liebman, and A. Greenberg), VCH, New York, ch. 4.
- Weber, W. P. (1983) *Silicon Reagents for Organic Synthesis*, Springer-Verlag, Berlin.
- Xing-Fu, L., Xi-Zhang, F., Ying-Ting, X., Hai-Tung, W., Jie, S., Li, L., and Peng-Nian, S. (1986a) *Inorg. Chim. Acta*, **116**, 85–93.
- Xing-Fu, L., Ying-Ting, X., Xi-Zhang, F., and Peng-Nian, S. (1986b) *Inorg. Chim. Acta*, **116**, 75–83.
- Xing-Fu, L. and Ao-Ling, G. (1987) *Inorg. Chim. Acta*, **134**, 143–53.
- Yang, X., Stern, C. L., and Marks, T. J. (1991) *Organometallics*, **10**, 840–2.
- Yermakov, Y. I., Kuznetsov, B. N., and Zakharov, V. A. (1981) *Catalysis by Supported Complexes*, Elsevier, Amsterdam.
- Zalkin, A., Edwards, P. G., Zhang, D., and Andersen, R. A. (1986) *Acta Crystallogr.*, **C42**, 1480–2.